**Independent University** **Bangladesh (IUB)**

**IUB Academic Repository**

Electrical and Electronics Engineering Senior Project

2026-08

# Design and simulation of a bidirectional underwater open-center micro tidal turbine for harvesting tidal energy

Afroz, Rajoana

Independent University, Bangladesh (IUB)

https://ar.iub.edu.bd/handle/11348/1546

*Downloaded from IUB Academic Repository*




**Independent University, Bangladesh**

# Design and Simulation of a Bidirectional Underwater Open-Center Micro Tidal Turbine for Harvesting Tidal Energy

An undergraduate Final Year Design Project submitted by

Tahmid Adityo (Student ID: 2031246)

Rajoana Afroz (Student ID: 2021413)

Sajid Zafry Ahsan (Student ID:2131227)

Md Parvez Sultan (Student ID: 2130503)

in consideration of the partial fulfillment of the requirements for the degree of

**BACHELOR OF SCIENCE**

**in**

**ELECTRICAL AND ELECTRONIC ENGINEERING**

Department of Electrical and Electronic Engineering

Spring 2026

# DECLARATION

I do hereby solemnly declare that the research work presented in this undergraduate thesis has been carried out by me and has not been previously submitted to any other University / Institute / Organization for an academic qualification / certificate / diploma or degree.

Tahmid Adityo
Student ID: 2031246
Date: July 18, 2026

Rajoana Afroz
Student ID: 2021413
Date: July 18, 2026

Sajid Zafry Ahsan
Student ID: 2131227
Date: July 18, 2026

MD. Parvez Sultan
Student ID: 2130503
Date: July 18, 2026

# Design and Simulation of a Bidirectional Underwater Open-Center Micro Tidal Turbine for Harvesting Tidal Energy

An undergraduate Final Year Design Project submitted by

Tahmid Adityo (Student ID: 2031246)
Rajoana Afroz (Student ID: 2021413)
Sajid Zafry Ahsan (Student ID:2131227)
Md Parvez Sultan (Student ID: 2130503)

has been approved on June, 2026.

_____

Dr. Khosru Mohammad Salim
Thesis Supervisor & Professor
Department of Electrical and Electronic Engineering
School of Engineering, Technology & Sciences
Independent University, Bangladesh

# ACKNOWLEDGEMENTS

I would like to express my sincere gratitude to Almighty for granting me the strength and patience to complete this thesis work. I am deeply thankful to my supervisor, Dr. Khosru Mohammad Salim, for his continuous guidance, valuable suggestions, and encouragement throughout the research.

I also extend my appreciation to the faculty members of the Department of Electrical and Electronic Engineering, IUB, for their support and for providing me with the academic foundation to carry out this study.

My heartfelt thanks go to my friends and classmates for their cooperation and motivation, which helped me overcome various challenges during this project. Finally, I owe my deepest gratitude to my parents and family members for their unconditional love, prayers, and constant encouragement, without which this achievement would not have been possible.

The Authors
June 2026
Dhaka, Bangladesh

# ABSTRACT

Costal and Island regions of Bangladesh require reliable, predictable, and locally adaptable renewable energy solutions. Sandwip and similar coastal locations experience repeated tidal motion, which makes tidal Stream Energy a promising option for decentralized electricity generation. This thesis presents the design, hydrodynamic simulation, and electrical output evaluation of a bidirectional micro tidal stream turbine intended for low-to-moderate tidal current applications. The proposed turbine uses a ducted, open-centered annular geometry with a six-blade rotor. The open-centered rotor allows flow to pass through the central region while the blades extract energy from the surrounding annular flow region. A curved ducted housing is used to guide the incoming tidal current and support the practical turbine assembly. The turbine was first designed in SolidWorks. Two CAD representations were considered: a practical assembly including support base, stator housing, coil slots, rotor-magnet concept, and duct structure; and a simplified no-base geometry used for ANSYS Fluent simulation. The CFD model was analyzed for tidal velocities from 0.4 m/s to 2.4 m/s at a fixed tip-speed ratio of 3. The CFD dataset produced turbine efficiency values mostly between approximately 50% and 56%, The mechanical outputs were then used in a simplified MATLAB/Simulink electrical model. In the third term, the turbine torque and angular speed are applied to a permanent magnet synchronous machine (PMSM) generator, which is directly connected to a balanced 15 ohm three-phase resistive load. Phase RMS voltage, phase RMS current, three-phase load power, load energy, electrical frequency, and mechanical-to-load efficiency were calculated for each operating point. At 2.1 m/s, the system produced about 3362.83W mechanical shaft power and delivered about 528.7W load power. A 21-point power-velocity lookup table was also used with a 24.84-hour tidal velocity profile to estimate energy output over one lunar tidal day. The integrated energy output was approximately 6.675 kWh per lunar tidal day, 193.48 kWh per 30 days, and 2.354 MWh per year.

# TABLE OF CONTENTS


**DECLARATION** ii

**ACKNOWLEDEMENT** iv

**ABSTRACT** v

**LIST OF FIGURES** x

**LIST OF TABLES** xiii

**CHAPTER 1 INTRODUCTION**

1.1 Overview 1

1.2 Background and motivation 2

1.3 Objectives 4

1.4 Research methodology 5

1.5 Project Planning 6

1.5.1 Work Plan – RACI Matrix 6

1.5.2 Work Plan – Gantt Chart 7

1.6 Project Budget 7

1.6.1 Overall Budget 8

1.6.2 Component/Software Budget 9

1.7 Organization of the report 10

**CHAPTER 2 LITERATURE REVIEW AND METHODOLOGY**

2.1 Tidal Turbine Working Principle 12

2.2 Current Tidal Stream Turbine Technologies 12

2.3 Open Duct, Open-Center and Bidirectional Turbine Concept 13

2.3.1 Horizontal Axis Tidal Turbine (HATT) 14

2.3.2 Vertical Axis Tidal Turbine (VATT) 14

2.3.3 Ducted (Shrouded) Turbines 15

2.3.4 Bidirectional Tidal Turbine 15

2.4 Blade & Rotor Design for Bidirectional Turbines 15

2.5 PMSM/PMSG Generator for Tidal Energy system 17

2.6 CFD and Simulation-Based Performance Evaluation 17
2.7 Summary of Literature Review and Research Gap 18

**CHAPTER 3 DESIGN AND MATHEMATICAL MODELLING**

3.1 Design Concept 20
3.2 Proposed System Concept 20
3.3 Practical Design and Simulation Design 21
3.4 Turbine Geometry and Design Parameters 22
3.5 Annular Swept Area Calculation 27
3.6 Tip to speed Ratio, Rotor Speed and Angular Speed 27
3.7 Available Hydraulic Power 28
3.8 Torque and Mechanical Shaft Power 29
3.9 Hydraulic to Mechanical Turbine Efficiency 30
3.10 PMSM Generator and Electrical Frequency 31
3.11 Permanent Magnet Flux Linkage Calculation for 0.218Wb 32
3.12 Three-Phase Resistive Load Power Calculation 34
3.13 Mechanical to Load Efficiency 35
3.14 Load Energy and Long-Term Energy Estimation 36

**CHAPTER 4 PROJECT IMPLEMENTATION**

4.1 Overall Methodology 38
4.2 SolidWorks Modelling 39
4.3 ANSYS Fluent Geometry and Mesh 39
4.4 Mesh Generation and Mesh Settings 41
4.5 Fluid Properties and Material Selection 43
4.6 Boundary Conductions 45
4.6.1 Velocity Inlet 45
4.6.2 Pressure Outlet 46
4.6.3 Rotor and Stator Cell Zones 47
4.6.4 Moving Wall Surface 47
4.7 Solution Methods and Transient Simulation Setting 48
4.8 Representative ANSYS Case at 2.1 m/s 49

4.9 Torque Extraction Method 51
4.10 Hydraulic performance Calculation Method 51
4.10.1 Mechanical Shaft Power Calculation 52
4.10.2 Available Hydraulic Power Calculation 52
4.10.3 Turbine Efficiency Calculation 52
4.11 Torque Extraction Method 52
4.12 MATLAB/SIMULINK Electrical Model 53
4.13 Data Processing Workflow 56

**CHAPTER 5 INVESTIGATIONS, RESULT AND DISCUSSION**
5.1 Overview of Result Structure 57
5.2 Turbine Operating Conditions and Hydraulic-Mechanical Performance 57
5.2.1 Mechanical Shaft Power vs Tidal Velocity 59
5.2.2 Mechanical Shaft Power and Available Hydraulic Power vs Tidal Velocity 60
5.2.3 Turbine Efficiency vs Tidal Velocity 61
5.3 Tidal Cycle Representation and Turbine Operating Variation 62
5.3.1 Tidal height Variation Over One Lunar Tidal Day 62
5.3.2 Tidal Current Velocity Variation Over One Lunar Tidal Day 63
5.3.3 Relationship between Tide height and Water Current Velocity 64
5.3.4 Turbine RPM Variation Over One Lunar Tidal Day 65
5.4 Electrical Output Characteristics of the PMSM Generator 66
5.4.1 Three-Phase Load Power vs Water Velocity 68
5.4.2 Load Energy (J) vs Water Velocity 69
5.4.3 Load Energy (kWh) vs Water Velocity 70

5.4.4 Phase RMS Voltage vs Water Velocity 71
5.4.5 Phase RMS Current vs Water Velocity 72
5.4.6 Mechanical to Load Efficiency 73
5.4.7 Electrical Frequency 74
5.5 Three Representative Operating Points 75
5.5.1 Load Power Comparison 76
5.5.2 Mechanical to Load Efficiency 77
5.5.3 Estimated Seasonal Variation of Monthly Delivered Load Energy 78
5.6 Simulated Scope Waveform Results 79
5.6.1 Phase-A Voltage Waveform from Scope 80
5.6.2 Phase-A Current Waveform from Scope 81
5.6.3 Three-Phase Load Power Waveform 82
5.7 Simulated Scope Waveform Results for Load resistance on Three-Phase 84
5.7.1 Efficiency vs Load Resistance 85
5.7.2 Three-Phase Load Power vs Load Resistance 86
5.8 Tidal Velocity Profile and Daily Energy Estimation 87
5.8.1 Cumulative Energy Graph 88
5.9 Estimated Energy Output 89
5.10 Energy Calculation 90
5.11 Discussion of Accuracy and Defensibility 90

**CHAPTER 6 SOCIO-ECONOMIC IMPACT AND SUSTAINABILITY**
6.1 Impact of the project on societal, health, safety, legal and cultural issues 92
6.2 Impact of project on the environment and sustainability 94

**CHAPTER 7 ADDRESSING COMPLEX ENGINEERING PROBLEMS AND ACTIVITES**
7.1 Addressing Complex Engineering Problems 100

7.2 Addressing Complex Engineering Activities 101

**CHAPTER 8 CONCLUSION, LIMITATIONS AND FUTURE WORKS**

8.1 Conclusions 103

8.2 Limitations 104

8.3 Future Works 104

**REFERENCES** 106

# LIST OF FIGURES


| Figure | | Page |
|---|---|---|
| 1.1 | Design and Simulation of a Bidirectional Underwater Open-Center Micro Tidal Turbne for Harvesting tidal energy | 3 |
| 1.2 | Research Methodology | 5 |
| 2.1 | Open-duct bidirectional tidal stream turbine concept with curved rotor blade and base structure | 14 |
| 2.2 | SolidWorks Design of six-blade turbine | 16 |
| 3.1 | Simplified PMSM-load architecture Simulink Electrical model | 20 |
| 3.2 | Practical SolidWorks assembly concept with support structure | 21 |
| 3.3 | Six-blade CFD without base structure for simulation | 22 |
| 3.4 | Assembly of Six-blade CFD Turbine Components | 22 |
| 3.5 | Six-blade rotor and ducted open-centered turbine geometry | 24 |
| 3.6 | Sator with embeded coils | 24 |
| 3.7 | Stator and coil-slot arrangment | 25 |
| 4.1 | Six-blade design with Rotor angle 13 degree | 39 |
| 4.2 | ANSYS mesh of the Cylindrical Computational fluid domain used of CFD simulation | 41 |
| 4.3 | Mesh details for Six-blade design with Rotor angle 13 degree | 42 |
| 4.4 | Fluid properties | 43 |
| 4.5 | Velocity Inlet boundary condition applied at the upstream boundary of the computational domain | 45 |
| 4.6 | Pressure Outlet boundary condition setup in ANSYS Fluent | 46 |
| 4.7 | Rotor and Stator Cell Zones settings in ANSYS Fluent | 47 |
| 4.8 | Moving wall boundary condition applied to rotor blade and hub surface | 47 |
| 4.9 | Transient simulation settings for one rotor revolution ANSYS Fluent | 48 |
| 4.10 | Example residual convergence plot from ANSYS Fluent | 50 |
| 4.11 | Example force monitor plot from ANSYS Fluent | 50 |
| 4.12 | Example moment/torque monitor plot from ANSYS Fluent | 51 |
| 4.13 | MATLAB/Simulink model for electrical power generation | 53 |

| | | |
|---|---|---|
| 4.14 | MATLAB/Simulink electrical architecture for the PMSM turbine generator system | 55 |
| 5.1 | Mechanical shaft power output of the turbine at different tidal current velocities | 59 |
| 5.2 | Comparison between available hydraulic power and extracted mechanical shaft power at different tidal velocity | 60 |
| 5.3 | Variation of hydraulic-to-mechanical turbine efficiency with tidal current velocity for the proposed open-center tidal turbine | 61 |
| 5.4 | Tidal height variation over one lunar tidal day showing two high tides and two low tides | 62 |
| 5.5 | Tidal current velocity magnitude over one lunar tidal day showing maximum flow and slack points | 63 |
| 5.6 | Turbine rotational speed variation over one lunar tidal day based on tidal current velocity profile | 65 |
| 5.7 | Three-Phase load power vs water velocity for PMSM Generator system | 68 |
| 5.8 | Three-phase load energy in kilojoules vs water velocity for the PMSM generator system | 69 |
| 5.9 | Three-Phase load energy in kilowatt-hours vs water velocity for the PMSM generator system | 70 |
| 5.10 | Phase RMS voltage vs water velocity for the PMSM generator connected to a balanced 15Ω load | 71 |
| 5.11 | Phase RMS current vs water velocity for the PMSM generator connected to a balanced 15Ω load | 72 |
| 5.12 | Mechanical-to-load efficiency vs water velocity for the PMSM generator-load system | 73 |
| 5.13 | Electrical frequency vs water velocity for the PMSM generator | 74 |
| 5.14 | Three-Phase load power comparison at selected operating points | 76 |
| 5.15 | Mechanical-to-load efficiency comparison at selected operating points | 77 |
| 5.16 | Estimated Seasonal monthly delivered load energy output from the PMSM tidal turbine generator system | 78 |
| 5.17 | Phase-A RMS voltage Waveform at 1.4 m/s tidal velocity 74.29 rpm rotor speed | 80 |

| | | |
|---|---|---|
| 5.18 | Phase-A RMS current Waveform at 1.4 m/s tidal velocity 74.29 rpm rotor speed | 81 |
| 5.19 | Three-Phase load power Waveform at 1.4 m/s tidal velocity and 74.29 rpm rotor speed | 82 |
| 5.20 | Three-Phase power calculation in MATLAB/Simulink | 83 |
| 5.21 | Mechanical-to-load efficiency vs load resistance at 1.9 m/s tidal velocity | 85 |
| 5.22 | Mechanical-to-load load power vs load resistance at 1.9 m/s tidal velocity | 86 |
| 5.23 | Mechanical-to-load load power vs load resistance at 1.9 m/s tidal velocity for over one lunar day | 88 |
| 5.24 | Cumulative three-phase load energy over one lunar tidal day | 88 |
| 5.25 | Estimated electrical energy output for one lunar tidal day, 30 days and One year | 89 |
| 6.1 | Current (2019) and planned (2041) composition of fuel type for energy generation in Bangladesh | 94 |

# LIST OF TABLES


| Table | | Page |
|---|---|---|
| 1.1 | RACI matrix for project task distribution | 6 |
| 1.2 | Project work plan represented using a Gantt Chart | 7 |
| 1.3 | Overall Budget distribution and its Justification | 8 |
| 1.4 | Budget distribution for software implementation | 9 |
| 1.5 | Budget distribution for Site visit and Computer | 10 |
| 2.1 | Short review of recent literature relevant of the Thesis model | 18 |
| 3.1 | The main turbine dimensions used in the project are summarized below | 26 |
| 4.1 | Water-liquid Properties | 44 |
| 4.2 | Summary of ANSYS Fluent setup and data extraction method | 44 |
| 4.3 | Simulations time step size, Number of time steps and Maximum iterations per time step | 48 |
| 4.4 | Representative ANSYS case documentation for V = 2.1 m/s | 49 |
| 4.5 | MATLAB/Simulink PMSM-load model parameter summary | 55 |
| 5.1 | Turbine operating conditions and hydraulic-mechanical performance | 58 |
| 5.2 | Simulated Electrical output Characteristics of the PMSM generator Connected to a balanced 15Ω Three-Phase resistive load | 67 |
| 5.3 | Simulated Comparison of PMSM-load performance at selected operating points | 75 |
| 5.4 | Seasonal summary of estimated delivered load energy point | 76 |
| 5.5 | Effect of load resistance on three-phase Electrical output at a fixed turbine Operating point | 84 |
| 5.6 | Estimated energy outputs using 21-point interpolation and tidal-cycle integration | 90 |
| 7.1 | Complex engineering problems associated with the current project | 100 |
| 7.2 | Complex engineering activities associated with the current project | 102 |

# CHAPTER 1
# INTRODUCTION

## 1.1 Overview

Bangladesh has recently emerged as a country from with a thriving economy with one of the highest GDP growths in 2022[1]. It is expected that this growth will continue and with this phenomenal growth, the demand for power will increase exponentially. Unfortunately, Bangladesh is still predominantly dependent on fossil fuels to produce electricity [2]. This dependency will create major problems as the fossil fuel reserve of natural gas is estimated to dry out within a decade and the severe impact on environment of fossil fuels will make the situation even more difficult [3].

Tidal energy has the potential to address the problem as it provides a greener alternative to the traditional fossil fuel. Tidal energy is one of the cleanest renewable energy sources. Tides are among the most predictable and renewable natural forces on Earth [4]. They are driven by the gravitational pull of the Moon and the Sun on the oceans, combined with the planet's rotation and the shape of its coastlines and sea basins [5]. These rhythmic oscillations give rise to two primary forms of energy: potential energy, associated with changes in sea level, and kinetic energy, derived from the horizontal movement of tidal currents. The second one, kinetic form of energy—often referred to as tidal current or tidal Stream Energy—has increasingly attracted global attention as a reliable and sustainable source of electricity [6]. This energy can be harnessed using underwater devices called tidal stream turbines which can be installed in tidal channels or coastal straits [7]. Tidal stream turbines work in the same way wind turbines harvest power from moving air, wind turbines capture the wind, on the other hand tidal stream turbines capture the tidal currents that pass through them and generate electricity as the turbine blades rotate [8]. Since seawater is more than 800 times denser than air [9], even moderate tidal flows can produce substantial energy. This high density, together with the precise predictability of tidal cycles, makes tidal energy one of the most reliable and continuous renewable energy resources are available.

However, there are some major challenges of current Tidal Turbine technology, first is the relatively high cost of production [10], secondly the high cost of maintenance and operation [11]. Some recent studies have suggested that coastal Bangladesh is ideal for harnessing tidal electricity [12] from the existing embankments and sluice gates by utilizing small-scale appropriate tidal energy technology. Bangladesh can take tidal power generation as a challenge and can easily overcome at least some of the power crisis existing in the coastal islands [13] off the main coast of Bangladesh since our independence 54 years ago. Together with its shallow waters and proximity to coastal infrastructure, these characteristics give Bangladesh a natural advantage for developing tidal current energy potentially serving for both off grid and on grid power generation [14].

Bangladesh is a country of 1,47,570 sq. km land area and 1,18,813 sq km of sea area attached to our coastline in the Bay of Bengal just south of Bangladesh [15]. Out of this area 18,000 sq km is our Internal water as per UNCLOS 1982 where we exercise total sovereignty and most of our coastal islands are situated in this area. Bangladesh has about 170 million people located in South Asia at 24° N latitude and 90° E longitude [16].

Bangladesh's unique coastal geography offers exceptional potential for harnessing tidal power as it has a long coastline stretching about 710 km with 2 to 8 m tidal range along the northern rim of the Bay of Bengal—one of the world's most hydrodynamically energetic regions—the country's coastline provides naturally favorable conditions for tidal energy development [17]. The periodic variation of the height of sea water level corresponding to this tidal range can be used for power generation.

## 1.2 Background and Motivation

The majority of the electricity generated in Bangladesh is through the use of non-renewable energy sources like natural gas and other fossil fuels [18]. With the rising energy requirement than ever before, as Bangladesh strives towards development goals by opening new industries in different sectors, providing a reliable electrical energy supply is of the utmost priority. It is of utmost importance to highlight, analyze, and predict the current trends of electrical energy generation in Bangladesh. Figure (1.1) highlights the current electric energy generation capacity sorted using different types of resources. From Figure

(1), it can be clearly observed that the overwhelming generation of electricity depends on the use of non-renewable energy sources (92.51%) and renewable energy generation makes up a very small percentage (1.6%) in the total generation capacity. For the year of 2019, electrical generation capacity using gas as the fuel accounted for 57.36% (10877 MW) of the total installed generation capacity followed by oil (furnace oil and diesel) with a percentage of 32.239% (6140 MW), imported power with 6.12% (1160 MW), coal with 2.76% (524 MW), hydro with 1.21%(230 MW) and lastly solar PV which only accounted for 0.16% (30 MW) of total generation capacity. The current annual production of gas is at 0.97 Tcf (trillion cubic feet) (2018) and 11.47 Tcf of reserves remaining [19]. Considering the yearly growth and production rate, natural gas reserves in Bangladesh will last up to 2026. In order to tackle this problem, coal generation power plants are expected to play a key role for power generation. This can bring about adverse effects on the environment and decrease the already low air quality in the country. In 2024, Dhaka city has repeatedly been ranked as the city with the worst air quality, with an air quality index (AQI) score ranging from 242 to 252 [20]. Hence, to mitigate the negative environmental impact of fossil fuels (diesel, furnace oil, gas, coal) and decrease the reliance on fossil fuels for energy generation, special attention should be given in increasing the renewable energy sector.

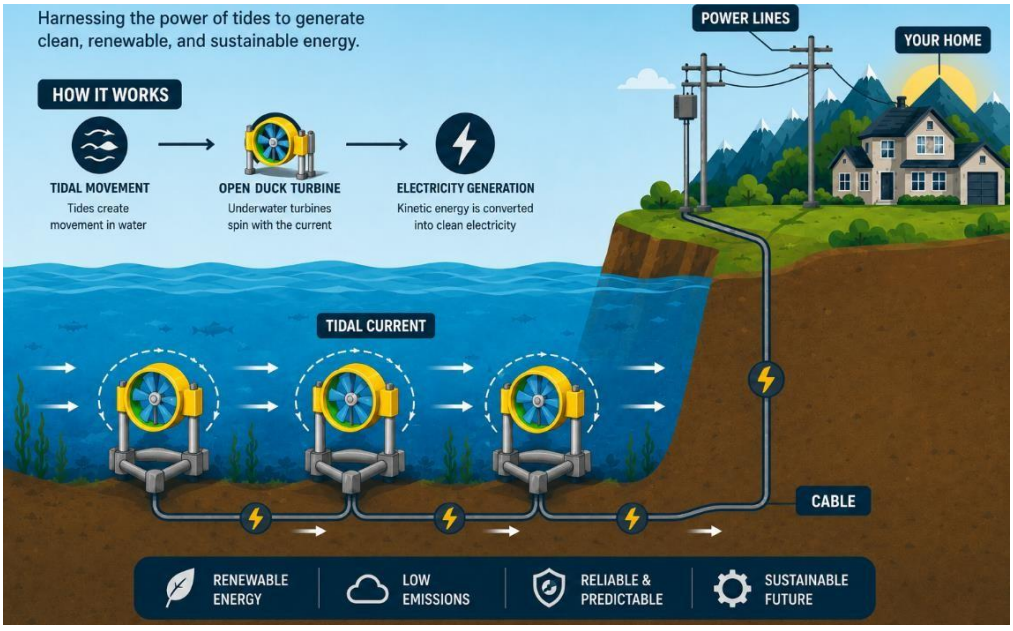



Fig. 1.1. Design and Simulation of a Bidirectional Underwater Open-Center Micro Tidal Turbne for Hrvesting tidal energy

Bangladesh's unique coastal geography offers exceptional potential for harnessing tidal power as it has a long coastline stretching about 710 km with 2 to 8 m tidal range along the northern rim of the Bay of Bengal—one of the world's most hydrodynamically energetic regions—the country's coastline provides naturally favorable conditions for tidal energy development. The periodic variation of the height of sea water level corresponding to this tidal range can be used for power generation.

Moreover, the geographical location of Bangladesh gives it a distinctive advantage for tidal energy extraction. The Bay of Bengal's broad, funnel-like shape intensifies tidal ranges and current speeds as seawater moves toward the shore [21]. As the tidal currents move along narrow estuaries, river mouths, and islands, the speed of the tidal current increases, generating alternating flood and ebb flows that are ideal for tidal energy extraction. Field measurements and numerical modelling indicate that average tidal velocities in the northern Bay of Bengal reach about 0.9 m/s, rising to 1.5–1.7 m/s during spring tides [22]. In constricted passages such as the Sandwip Channel and Hatiya Channel, flow speeds may reach 2–3.5 m/s—well within the operational range of commercial tidal turbines [23]. Therefore, the installation and implementation of Tidal Stream turbines to generate tidal energy can be more lucrative and efficient than the existing renewable energy sources like wind, solar and biogas [24].

## 1.3 Objectives

- To study the feasibility of extracting clean tidal power in the channels and canals of Bangladesh by conducting research about installation of suitable tidal stream turbines.
- Analyze the current state of the power generation in Bangladesh and the state of renewable energy power generation globally
- Design an open-center bidirectional micro tidal stream turbine for coastal tidal flow conditions and evaluate hydrodynamic performance using ANSYS Fluent over tidal velocities from 0.4m/s to 2.4m/s.
- Develop a MATLAB/Simulink PMSM generator model connected to a balanced three-phase resistive load.
- To estimate electrical load power and energy production from a single turbine for possible rural/coastal application.

## 1.4 Research Methodology

The methodology presented in this thesis was designed to assess the design, hydrodynamic performance and electrical output of a bidirectional underwater open-center micro tidal turbine. First, a literature review was carried out to gain an understanding of the potential of tidal energy, the current tidal stream turbine technology, the ducted/open center turbine concept, the advantages of a bidirectional operation and the use of PMSM/PMSG generators for low-speed renewable energy systems. Once the project requirements were determined, a turbine geometry was created in SolidWorks. The principal design characteristics were an open-center ducted machine, and a six-blade rotor with an underwater support system.

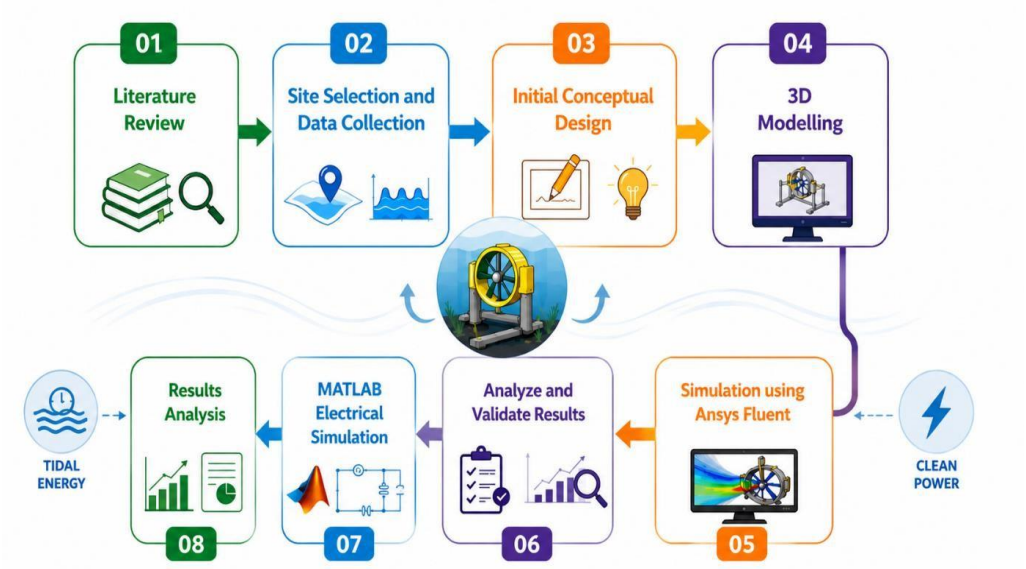



Fig. 1.2. Research Methodology.

Once the turbine 3D-model was created, it was exported to ANSYS Fluent for the CFD simulation. A cylindrical fluid domain was developed around the turbine, and the inlet boundary was subjected to four different tide current velocities, ranging from 0.4 m/s to 2.4 m/s. Using the CFD simulation, the flow behavior around the turbine was analyzed, and the important parameters of mechanical output including torque, angular speed, mass flow rate and mechanical shaft power were extracted and analyzed. These values were then used as mechanical input values to the MATLAB/Simulink electrical model. [Fig. shown as 1.2]

## 1.5 Project Planning

The Project planning of the project was done to schedule the work of the thesis into smaller tasks to be accomplished during the entire life of the project. The project was split into several stages, literature review, problem identification, conceptual design, 3D modelling, ANSYS fluent simulation, electrical modelling using MATLAB/Simulink, result analysis, report writing and final presentation. A RACI matrix was created to clearly outline the responsibilities of each group member, and a Gantt chart was created to illustrate the timeline of the major activities as planned. Using these planning tools, the group were able to divide up the work, track progress and finish on time within the academic calendar.

### 1.5.1 Work Plan – RACI Matrix

The matrix was created to define roles and responsibilities of the project members and project supervisor. So, in this matrix table, the letter "R" is the person who is tasked to do the work, the letter "A" is someone who is accountable to do work, while the letter "C" is the person who is someone who provides guidance to everyone, lastly the letter "I" is the person who is informed about the overall progress. The project has a good number of organized steps. [Table shown as 1.1]

**Table 1.1** RACI matrix for project task distribution.

| Period | Assignments | Responsible (R), Accountable (A), Consulted (C) & Informed (I) - RACI Matrix | | | | | Start | End | Days | Status |
|---|---|---|---|---|---|---|---|---|---|---|
| | | Prof. Dr. Khosru Mohammad Salim (Supervisor) | Rajoana Afroz | Sajid Zafry Ahsan | Tahmid Adityo | Md. Pravez Sultan | | | | |
| 1st Term | ▪ Prepare Plan | C | R | R | R | R | 20.10.2024 | 17.11.2024 | 27 | |
| | ▪ Review Literature | I | R | R | A | A | 19.11.2024 | 22.12.2024 | 33 | |
| | ▪ Problem Identification | I | A | R | R | A | 23.12.2024 | 08.01.2025 | 16 | |
| | ▪ Prepare Draft Budget | I | R | A | R | R | 09.01.2024 | 12.01.2025 | 3 | |
| | ▪ Prepare, Submit & Present (Proposal, Progress Presentation & Progress Report) | C | R | R | R | R | 13.01.2025 | 25.01.2025 | 12 | ✓ |
| 2nd Term | ▪ 3D modelling SolidWorks Designing | C | R | R | R | A | 07.03.2025 | 29.03.2025 | 22 | |
| | ▪ ANSYS Fluent Simulation of Tidal Turbine | C | R | R | R | A | 06.04.2025 | 06.05.2025 | 30 | ✓ |
| | ▪ Prepare, Submit & Present (Presentation & Progress Report) | I | R | R | R | R | 09.05.2025 | 18.05.2025 | 9 | |
| 3rd Term | ▪ Result & Analysis | C | R | R | R | R | 19.04.2025 | 23.04.2025 | 10 | |
| | ▪ Prepare, Submit & Present (Final Report & Presentation) | I | A | A | A | A | 01.05.2026 | 12.05.2026 | 12 | ✓ |
| | ▪ Prepare Poster & Present Group Demonstration | I | A | A | A | A | 12.05.2026 | 13.05.2026 | 1 | |

The steps are Project plan preparation, literature survey, problem identification, budget preparation, SolidWorks modelling, ANSYS Fluent simulation, result analysis, report preparation and presentation of the poster. This matrix provided clarity on the roles

of each and minimized confusion during project work. It also helped to ensure that there was a member of the group responsible for each major task and that the supervisor was consulted and reviewed.

### 1.5.2 Work Plan – Gantt Chart

The Gantt chart represents the planned time for the different project activities from the initial project proposal until the final demonstration and presentation. The primary activities in the first term involved the submission of the project proposal and project planning, literature review and problem identification and draft budget preparation. In the second term, the emphasis was placed on 3D modelling, design using SolidWorks and simulation using ANSYS Fluent for the tidal turbine. During the last term, the main tasks involved were the preparation of the final report, electrical modelling in MATLAB/Simulink analysis of results and final presentation and poster demonstration. The project progress was monitored using the Gantt chart and the design, simulation, analysis and documentation work progressed in an orderly fashion. [Table shown as 1.2]

**Table 1.2** Project work plan represented using a Gantt Chart.

| Task Name | 1st Term | | | | 2nd Term | | | | 3rd Term | | | |
|---|---|---|---|---|---|---|---|---|---|---|---|---|
| | Oct-20 | Nov-21 | Dec-19 | Jan-25 | Feb-16 | Mar-24 | Apr-22 | May-16 | July-21 | Oct-22 | Dec-20 | May-10 |
| Prepare Plan | | | | | | | | | | | | |
| Research Literature | | | | | | | | | | | | |
| Problem Finding | | | | | | | | | | | | |
| Prepare Draft Budget | | | | | | | | | | | | |
| Prepare & Submit Project Proposal | | | | | | | | | | | | |
| Prepare & Submit 1st Term Progress Report | | | | | | | | | | | | |
| Prepare & Present 1st Term Progress | | | | | | | | | | | | |
| System Design | | | | | | | | | | | | |
| 3D modeling (Simulation) | | | | | | | | | | | | |
| Prepare & Submit 2nd Term Progress Report | | | | | | | | | | | | |
| Prepare & Present 2nd Term Progress | | | | | | | | | | | | |
| Prototyping (3D) | | | | | | | | | | | | |
| Testing & Evaluation | | | | | | | | | | | | |
| Final Report | | | | | | | | | | | | |
| Final Presentation | | | | | | | | | | | | |
| Project Demonstration | | | | | | | | | | | | |

## 1.6 Project Budget

The project budget summarizes the estimated resources required to complete this simulation-based research. The budget includes the computational resources, software tools, and field survey expenses necessary for the design, modeling, analysis, and evaluation of the proposed tidal turbine. ANSYS Fluent was used for computational fluid dynamics (CFD)

analysis, including fluid flow, pressure distribution, torque extraction, and turbine performance evaluation. MATLAB was utilized for data processing, graphical analysis, electrical system modeling, and energy yield calculations. SolidWorks was employed to develop a three-dimensional model of the turbine, including the duct, rotor, blades, and support structure. Site data collection and survey expenses were included to obtain information on tidal current velocity, water conditions, and potential installation locations. As this research was conducted entirely through computer-aided design and simulation, no physical prototype was fabricated. Therefore, the proposed budget represents the estimated resources required to complete the design, simulation, and feasibility assessment of the project.

### 1.6.1 Overall Budget

**Table 1.3** Overall Budget distribution and its Justification.

| Sl | Item | Specifications | Justification | Qty | Unit Price (BDT) | Price (BDT) |
|---|---|---|---|---|---|---|
| 1. | ANSYS Fluent Student Version | CFD Simulation Software | Used for fluid flow analysis, pressure distribution, and turbine performance simulation. | 1 | Free (Student Version) | 0 |
| 2. | PC | AMD Ryzen 5 3500X 6-core, 12GB RAM, GTX 1650 | Purchased necessary for project development | 1 | 60000 | 60000 |
| 3. | MATLAB | Data Analysis & Visualization Tool | Used for data processing, graphical analysis, sensor data visualization, and performance calculation. | 1 | Free (IUB EEE Dept Authorized) | 0 |
| 4. | Site Data Collection & Survey | River flow and environmental data collection | Used for collecting site information such as water velocity, depth, flow rate, and turbine installation analysis. | 1 | 10000 | 10000 |
| 5. | SolidWorks | 3D Design & Modeling Software | Used for 3D modeling, turbine blade design, assembly, and mechanical structure development. | 1 | Free (IUB EEE Dept Authorized) | 0 |
| Total (BDT) | | | | | | 70000 |
| In words: Seventy Thousand Taka Only. | | | | | | |

The overall budget represents the estimated resources required to complete the project using simulation-based design and analysis. Since the proposed tidal turbine was designed and evaluated entirely through software tools without fabricating a physical prototype, no hardware manufacturing costs were incurred. The budget primarily includes the computational resources used for modeling and simulation, software tools provided through educational licenses, and site survey expenses for collecting field data and evaluating the feasibility of the proposed installation locations shown Table 1.3. The total estimated project budget is BDT 70,000.

### 1.6.2 Component/Software Budget

The software tools used in this project were provided through educational licenses and university-authorized resources. Therefore, there was no specific direct software cost involved in this project for the software part only. [Table shown as 1.4]

**Table 1.4** Budget distribution for software implementation

| Sl. | Software | Specifications | Purpose | Qty | Unit Price (BDT) | Price (BDT) |
|---|---|---|---|---|---|---|
| **1** | ANSYS Fluent Student Version | CFD Simulation Software | Used for fluid flow analysis, pressure distribution, and turbine performance simulation. | 1 | Free (Student Version) | 0 |
| **2** | MATLAB | Data Analysis & Visualization Tool | Used for data processing, performance calculation, and graphical analysis of simulation results. | 1 | Free (IUB EEE Department Authorized) | 0 |
| **3** | SolidWorks | 3D Design & Modeling Software | Used for 3D modeling, turbine blade design, assembly, and mechanical structure development. | 1 | Free (IUB EEE Department Authorized) | 0 |
| | **Total** | | | | | **0 BDT** |

In our project, no physical prototype was actually fabricated, a personal computer had been used for running all the simulation activities as well as for designing the turbine structure and its intricate well measured components. The site visits were conducted to

collect tidal and also environmental data which was essential and necessarily needed for the project to be validated for accurate as well as for precise results.

**Table 1.5** Budget distribution for Site visit and Computer.

| Sl. | Item | Specifications | Justification | Qty | Unit Price (BDT) | Price (BDT) |
|---|---|---|---|---|---|---|
| 1 | Personal Computer | AMD Ryzen 5 3500X (6-Core), 12 GB RAM, NVIDIA GTX 1650 | Used for SolidWorks modelling, ANSYS Fluent CFD simulation, MATLAB analysis, and report preparation. | 1 | 60,000 | 60,000 |
| 2 | Site Data Collection & Survey | River flow and environmental data collection | Used for collecting tidal current velocity, water depth, flow characteristics, and installation feasibility data during field visits. | 1 | 10,000 | 10,000 |
| | Total | | | | | 70,000 BDT |

This project was completed entirely through software-based design, CFD simulation, MATLAB analysis, and field data collection. No physical prototype was fabricated; therefore, no hardware fabrication or manufacturing costs were incurred. This budget reflects only the resources required to conduct research and simulation activities. Table 1.5 present down the cost for site data collection, it took us 10,000 BDT on average which included bus fares, hotel rooms, food and average pocket allowance

## 1.7 Organization of the Project

The thesis comprises

- **Chapter 1**

  Introduces the background, motivation, objectives, methodology, project planning and budget of the study.

- **Chapter 2**

  This part represents the literature review related to tidal energy, tidal stream turbine technologies, bidirectional turbine operation, ducted/open-center turbine concepts, PMSM/PMSG generators and the research gap addressed by this thesis.

- **Chapter 3**

  This section details the proposed turbine design, including the open center ducted geometry, blade and rotor arrangement, main design parameters and the SolidWorks modelling process.

- **Chapter 4**

  Explain the simulation modelling and implementation, including ANSYS Fluent CFD setup, boundary conditions, mesh generation, torque extraction and the MATLAB/Simulink PMSM generator-load model.

- **Chapter 5**

  The section represents the results and discussion, including hydraulic-mechanical performance, electrical output characteristics, load resistance study, waveform analysis and energy estimation over a lunar tidal day.

- **Chapter 6**

  Discusses the impact of the project on society, culture and health, and address concerns regarding the environment and sustainability.

- **Chapter 7**

  Outlines the engineering activities undertaken to address the complex engineering problems associated with the current project.

- **Chapter 8**

  Provides the conclusion, limitations of the study and recommendations for future work.

# CHAPTER 2
# LITERATURE REVIEW AND METHODOLOGY

## 2.1 Tidal Turbine Working Principle

When rise and fall and horizontal movement of seawater due to the gravitational pull of the Moon and the Sun is a predictable form of marine renewable energy, unlike solar and wind power. The principle is similar to that of wind turbines, with the kinetic energy of the water currents being converted into electrical energy, however, due to the high density of water compared to air, moderate currents can provide adequate mechanical torque on the rotor for useful electrical energy generation [24], [25].

When Tidal & Coastal current resource is significant for Bangladesh as many coastal and island communities are in need of a reliable local energy source. Past research on Bangladesh mentions the tidal energy potential and shows that Sandwip and the surrounding coastal channels are areas where tidal power is feasible [26], [27], [28]. The current project is based on this context and aims at developing a small open-center bidirectional tidal stream turbine concept capable of operation at low-to-moderate tidal current velocities and bidirectional flow regime [29].

## 2.2 Current Tidal Stram Turbine Technologies

Tidal There are a number of different technology categories for tidal stream turbines: horizontal axis turbines; vertical axis turbines; and ducted/turbines with shrouds [25], [26]. Horizontal axis tidal turbines have a rotor axis that is approximately parallel to the tidal flow [25]. Many conventional designs are primarily optimized for a specific flow direction, and they are extensively studied and can achieve relatively high-power coefficients [25], [28]. In a reversing tidal environment, the turbines may need to be yawned, or blades pitch adjusted, or flow aligned, to ensure efficient operation during the flood or ebb tide [25].

Vertical axis tidal turbine's rotor axis runs across the flow [27]. They have the advantage of being able to take flow from various directions which is beneficial in reversing tidal streams [27]. They might have reduced efficiency, start-up problems at low velocity, torque fluctuation and dynamic stall, however, depending on the blade shape and operating condition. Ducted or shrouded turbines add a duct around the rotor to guide and speed up the flow, increase the effective flow velocity at the rotor plane and power extraction [29]. Ducted turbines can enhance the flow behavior around the rotor and increase the mass flow passing through the turbine that is effective to the rotor. For both ducted and open-center tidal turbines research indicates that the duct shape, arrangement of the rotors, the turbine blade design and the effects of blockage impact strongly on the hydrodynamic performance of the turbine.

## 2.3 Open Duct, Open-Center and Bidirectional Turbine Concept

Open-center or open-duct tidal turbine concepts are relevant to this thesis because the proposed turbine uses an annular flow path with an open central region [29]. In this type of concept, the turbine is designed so that water can pass through and around the rotor region while the duct helps guide the flow [29]. Open-center tidal turbine studies have shown that ducted arrangements can be analyzed using hydrodynamic modelling and CFD-based approaches, and that the shape of the duct and rotor has a direct influence on torque and power output [29].

Bidirectional operation is important because tidal currents reverse direction between flood tide and ebb tide [24]. A unidirectional turbine may require yawing or blade-pitch reversal, which increases mechanical complexity. A bidirectional turbine reduces this requirement by allowing operation under flow from either side of the duct [29]. In the present project, the turbine is treated as bidirectional, and the tidal current velocity magnitude is used in the energy-estimation method so that both flood and ebb flow periods contribute positive power generation. Previous studies on bidirectional tidal turbine performance support the importance of blade symmetry, duct arrangement and flow-reversal capability in such systems [29].

Tidal flow changes direction between flood tide and ebb tide [24]. In a unidirectional turbine, this may require yawing or blade-pitch adjustment so that the rotor faces the flow

direction. A bidirectional turbine aims to reduce the need for yawing or active pitch reversal. The present design is described as bidirectional because the turbine is intended to operate under flow from either side of the duct. In the energy-estimation method, tidal velocity magnitude was used so that both flood and ebb directions contribute positive power [29] [Fig. shown as 2.1].

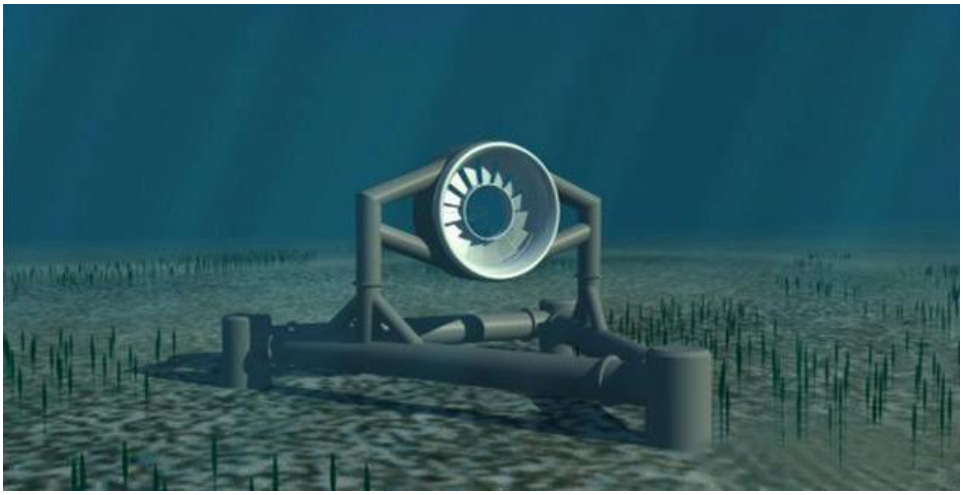


Fig. 2.1. Open-duct bidirectional turbine concept [27]

### 2.3.1 Horizontal Axis Tidal Turbine (HATT)

The most widely researched and commercially advanced design is the Horizontal Axis Tidal Turbine (HATT), where the rotor shaft is aligned parallel to the incoming flow direction [25], [27]. These turbines typically employ two or three-bladed rotors and are capable of achieving high power coefficients (Cp), approaching the Betz limit of 0.593. Notable commercial examples include the Atlantis Resources AR1500 and the ANDRITZ HYDRO Hammerfest HS1000, both of which have been deployed in real tidal environments. However, a critical limitation of conventional HATTs is their unidirectional operation — they require a yaw mechanism or physical reorientation to maintain efficiency during tidal flow reversal, adding mechanical complexity and increasing maintenance costs.

### 2.3.2 Vertical Axis Tidal Turbine (VATT)

Vertical Axis Tidal Turbines (VATTs) feature a rotor shaft oriented perpendicular to the flow [25], [27]. The most common configurations include the Darrieus and Gorlov helical turbine designs [25]. A key advantage of VATTs is their inherent omni-directionality — they can accept flow from multiple directions without requiring reorientation, making

them naturally suitable for reversing tidal environments [27]. However, they generally exhibit lower efficiency compared to HATTs and suffer from issues such as dynamic stall, torque fluctuation, and self-starting difficulties at low flow velocities.

### 2.3.3 Ducted (Shrouded) Turbine

Ducted turbines incorporate a shroud or duct around the rotor to accelerate incoming flow, thereby increasing the effective velocity at the rotor plane and improving power output [29]. The Open Hydro and Clean Current turbines are examples of this configuration. The duct design can also be adapted for bi-directional operation using symmetric duct profiles, though structural loading and biofouling remain engineering challenges [29].

### 2.3.4 Bidirectional Tidal Turbines

Conventional tidal turbines are predominantly designed for unidirectional flow, making them inefficient in reversing tidal streams where the flow alternates between ebb and flood cycles approximately every 6 hours [24]. Bidirectional tidal turbines address this limitation through design strategies such as:

- **Symmetric hydrofoil blade profiles (e.g., NACA 0015, NACA 0018)** that generate lift in both flow directions [29].
- **Variable pitch mechanisms** that adjust blade angles during flow reversal [24]
- **Contra-rotating rotor arrangements** for enhanced torque generation
- **Double-rotor configurations** positioned back-to-back

However, recent studies have shown that bi-directional turbines designed for this specific purpose can be competitive in both ebb and flood tide with capacity factor and energy yield over the tidal cycle without mechanical yawning [29].

## 2.4 Blade & Rotor Design for Bidirectional Turbines

The parameters to consider for the hydrodynamic performance of a tidal turbine are rotor diameter, number of blades, blade profile, tip-speed ratio, hub size, duct geometry and duct operating velocity. Blade geometry should be designed to provide adequate torque at low tidal velocities and to prevent excessive rotor speeds and mechanical loading. For the micro tidal turbine, a simple and compact design which can be fabricated should also be

considered. For this project, a six-bladed open center rotor was chosen to achieve practically the right compromise between torque production, simplicity of structure and low speed operation.

The area swept by the proposed open center turbine is not a whole circular area due to its open center. Hence, the flow area available is considered as annular flow area between the outer rotor and inner hub or open-center radius. A fixed tip-speed ratio was applied to convert the tidal velocity to the rotor angular speed, and this angular speed was then combined with ANSYS Fluent torque results to determine the mechanical shaft power. The geometric model, the hydrodynamic simulation and the electrical generator model are all linked in a coherent workflow through these design choices.

This is the optimal design structure and foundation we were able to come up with which produced the best results of the efficiency and the torque as well as the mass flow rate of the turbine. The design has 13 degrees of blade twist which is also the optimal value as later found while running the electrical simulation in MATLAB/Simulink. There, the model with 13 degrees of twist produced the greater electrical load output as compared to other twist angles [Fig. shown as 2.2].

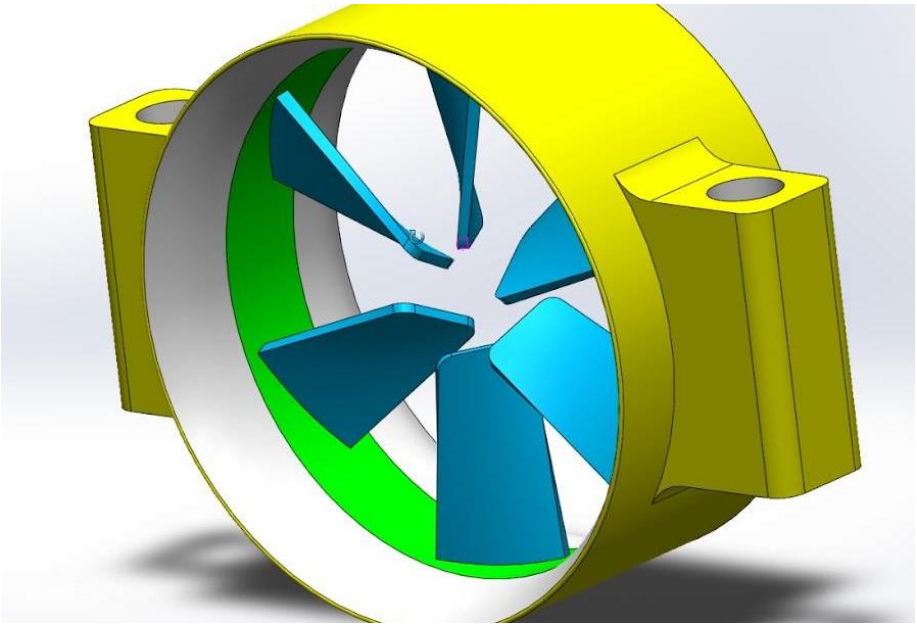


Fig. 2.2. SolidWorks Design of six-bladed turbine.

## 2.5 PMSM/PMSG Generator for Tidal Energy system

Permanent magnet synchronous machines are commonly used in renewable energy systems because they can provide good efficiency, high torque density and direct-drive capability. In tidal turbines, direct-drive operation is attractive because gearboxes can increase losses, maintenance requirements and underwater mechanical complexity. A high-pole permanent magnet generator is especially useful for low-speed turbines because it can produce a useful electrical frequency even when the mechanical rotational speed is low.

Several tidal energy studies have used PMSG or PMSM-based generator systems to convert turbine shaft rotation into three-phase electrical output. In this thesis, the PMSM block is used as a generator model in MATLAB/Simulink. The torque and angular speed obtained from ANSYS Fluent are applied to the mechanical side of the PMSM, and the electrical terminals are connected to a balanced three-phase resistive load. This allows the phase RMS voltage, phase RMS current, electrical frequency, load power, load energy and mechanical-to-load efficiency to be measured directly in the simulation.

## 2.6 CFD and Simulation-Based Performance Evaluation

Computational Fluid Dynamics is widely used to evaluate tidal turbine performance before prototype fabrication because it can estimate flow behavior, torque, loading and power output under different operating conditions. RANS-based CFD and related turbine modelling approaches are commonly applied to tidal stream turbines and turbine arrays to predict thrust, power and wake behavior. For the present project, ANSYS Fluent was used to simulate the turbine under different tidal current velocities and to obtain torque, mass flow rate and mechanical performance data.

The electrical side of the system was then evaluated in MATLAB/Simulink using a simplified PMSM-load model. This combined workflow is suitable for a student-level design study because the hydrodynamic and electrical parts can be connected using operating-point data. The CFD model provides rotor torque and angular speed, while the Simulink model converts these mechanical inputs into electrical output quantities. Standards and guidelines for tidal turbine power performance and tidal turbine design also support the need for systematic performance assessment, although full experimental validation is still required for future work.

## 2.7 Summary of Literature Review and Research Gap

The reviewed literature shows that tidal stream turbines, ducted/open-center turbine arrangements, bidirectional operation, CFD-based hydrodynamic analysis and permanent magnet generator systems are all relevant to the development of small tidal energy systems. Previous studies provide strong support for using ducted or open-center turbine concepts, CFD simulation, and PMSM/PMSG-based electrical conversion. However, many studies focus on either hydrodynamic performance, generator modelling, or large-scale systems separately.

**Table 2.1** Short review of recent literature relevant of the Thesis model.

| Source | Main contribution | Relevance to this thesis |
|---|---|---|
| S. Allsop, C. Peyrard, P. Bousseau, and P. R. Thies, "Adapting Conventional Tools to Analyze Ducted and Open Centre Tidal Stream Turbines," | Studied ducted and open-center tidal turbine behavior using conventional analysis tools. The study identified key issues such as blade loading, stress concentration and performance evaluation. | Supports the choice of an open center ducted turbine concept. It also shows that blade geometry, duct arrangement and structural loading are important in turbine design. |
| M. Maduka and C.W. Li, "Numerical study of ducted turbines in bi-directional tidal flows," Engineering Applications of Computational Fluid Mechanics" | Investigated ducted turbine performance in bi-directional tidal flow using numerical simulation. The study showed that duct geometry affects flow acceleration, suction region, mass flow rate and turbine performance. | Supports the use of a ducted bidirectional turbine for tidal-current energy extraction. It also supports the use of CFD to study flow behavior around the duct and rotor. |
| Yuxiang Zhao, Caixiao Mo, Waniqiang Zhu. "Design and Test for a New Type of Permanent Magnet Synchronous Generator Applied in Tidal Current Energy System" | Designed and tested a direct-drive PMSG for tidal-current energy systems. The work focused on low-speed operation, voltage generation, sealing and generator performance. | Supports the use of a low-speed direct-drive PMSM/PMSG generator in this thesis. It justifies using turbine torque and angular speed as inputs to estimate voltage, current, frequency and load power. |

Table 2.1 shown the research gap addressed in this thesis is the need for a compact and defensible workflow for a Bangladesh coastal application that connects turbine geometry, CFD torque extraction, PMSM electrical simulation and tidal-cycle energy estimation. This project fills that gap by developing a micro open-center bidirectional turbine design, simulating it in ANSYS Fluent over a range of tidal velocities, applying the resulting torque and speed to a PMSM generator model, testing a balanced three-phase resistive load, and estimating daily, monthly and yearly electrical energy output using a velocity-to-power lookup table and tidal-cycle integration. This thesis addresses that gap by developing a simplified but defensible design and simulation workflow for a bidirectional micro tidal turbine system.

# CHAPTER 3
# DESIGN AND MATHEMATICAL MODELING

## 3.1 Design Concept

The proposed system is a bidirectional micro tidal stream turbine. The design features a ducted housing, six curved rotor blades, an open-centered annular region of the rotor and a practical stator-rotor configuration for integration into a future generator. For the SolidWorks assembly in the actual application, the stator is a structure with holes or slots where coils are to be inserted, and the rotor is to be used to embed magnets. This arrangement is a conceptual design for a permanent-magnet generator wrapped around the turbine ring. A turbine was designed to work in low to moderate tidal current velocities. The velocity range used to simulated was between 0.4 m/s and 2.4 m/s. The tip speed ratio (TSR) of turbines was fixed at **3** to relate the speed of the turbines to the speed of water.

## 3.2 Proposed System Concept

The proposed system starts with the tidal current flow, and the 6-blade ducted turbine. Some of the kinetic energy of the water is transformed into mechanical energy in the turbine. Then the torque and angular speed of the mechanical shaft are transferred to the PMSM generator. The PMSM is a motor that converts mechanical energy into three-phase AC electricity. This output is sent directly into a balanced 3-phase, 15Ω, resistive load in the final simplified MATLAB model [Fig. shown as 3.1].

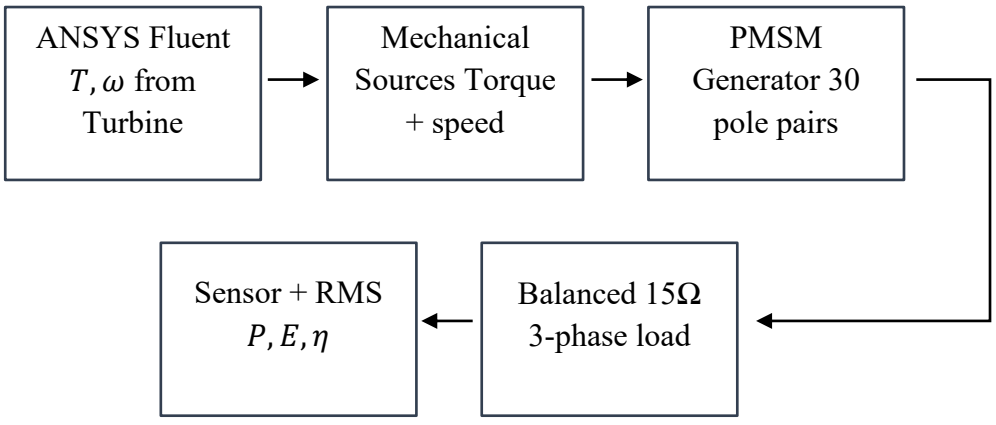



Fig. 3.1. Simplified PMSM-load architecture Simulink Electrical model

## 3.3 Practical Design and Simulation Design

Two design representations were created:

I. **Practical/prototype assembly:** This version has the base structure, support frame, stator housing, coil slot provision, rotor-magnet concept, duct, and blade assembly added in the practical/prototype assembly. It is a depiction of what the turbine might look like if it were actually constructed. [Fig. shown as 3.2].

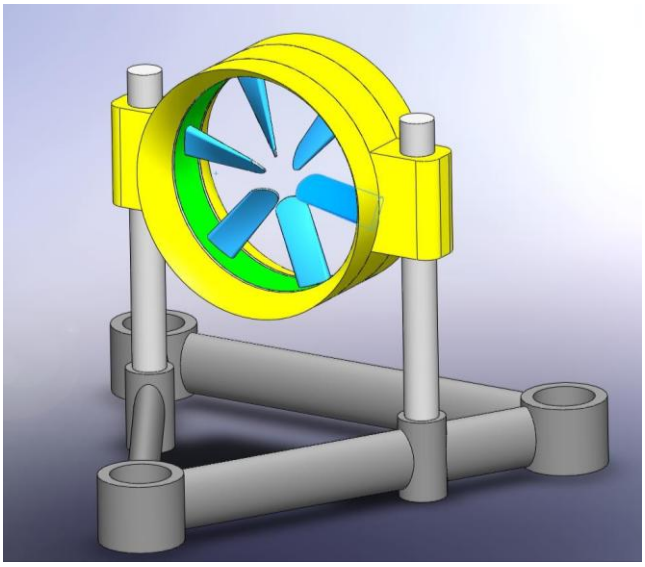


Fig. 3.2. Practical SolidWorks assembly concept with support structure.

II. **Simplified CFD model:** This model without the external base/support structure, with the turbine flow passage and rotor/duct geometry only. The model was imported into ANSYS Fluent and simulated. To reduce computational complexity and focus on hydrodynamic interaction between water flow, duct and rotor blades, the CFD model was simplified [Fig. shown as 3.3].

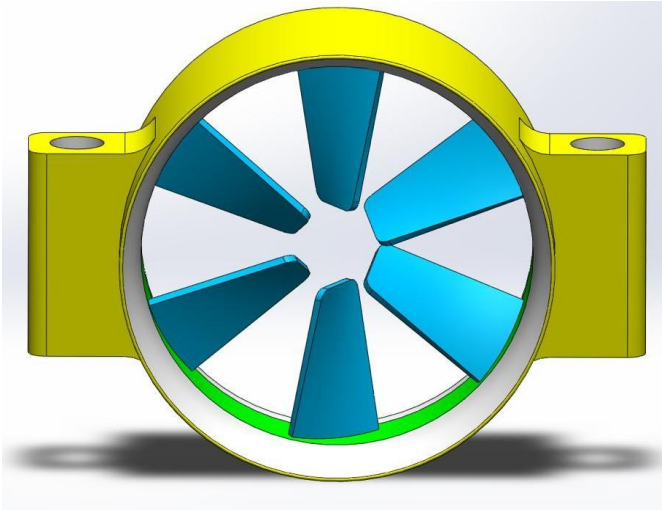


Fig. 3.3. Six-blade CFD without base structure for simulation.

This is significant. The CFD results in this thesis are for geometry with no base. The concept of the practical prototype is explained using the full base design.

### 3.4 Turbine Geometry and Design Parameters

The turbine geometry is a curved duct with six blades on the rotor, an open centered hub region and a viable concept for a stator-rotor assembly. The practical SolidWorks model comprises the base/support structure, the arrangement of coil slots in the stator, and the concept of the rotor magnets. The simplified CFD model eliminates the external base structure to allow the hydrodynamic analysis to be focused on the rotor, duct and fluid region [Fig. shown as 3.4].

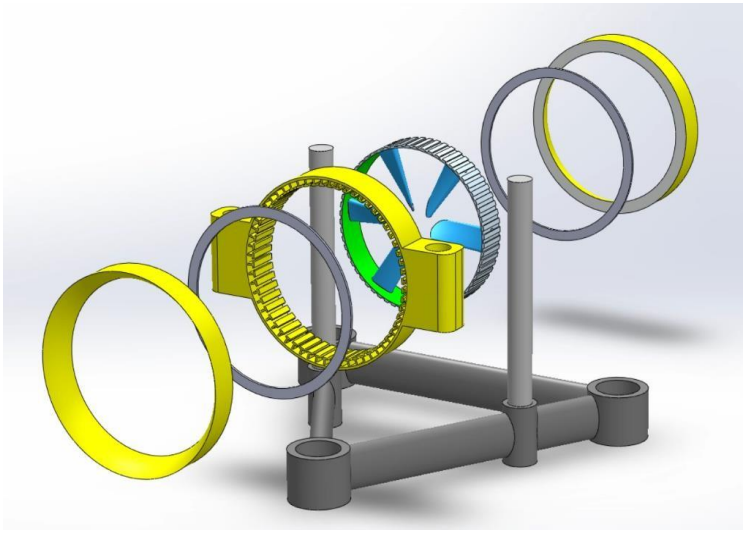


Fig. 3.4. Assembly of Six-blade CFD Turbine Components.

The exploded view shows the practical assembly of the proposed bidirectional micro tidal stream turbine. Main components are the duct, rotor bladders, stator ring, generator housing, alignment rings and support frame. The duct leads the tidal flow to the turbine, and open-center design blades permit the water to pass through the center which enables the turbine to function in both flood and ebb tide directions. The stator portion has a plurality of slots where windings are located, and the rotor may have permanent magnets in it to generate electricity. In general, the design illustrates that the simulated turbine could be scaled down and made into a practical prototype for small-scale tidal energy extraction.

The blue blades are turbine rotor blades that are installed in the duct. The rotor comprises several blades surrounding an open inner area. This configuration has an open center through which water can flow as the blade area around it harvests the energy from the flowing tidal current. The turbine will be designed to work in both directions of tidal flow, with the blade and duct configuration that allows for this.

The yellow ring with internal slots represents the stator section of the generator. The slots are intended for placing copper windings, while the rotor section can carry permanent magnets. As the rotor rotates due to tidal flow, relative motion between the rotor magnets and stator windings can produce electrical power. This makes the design suitable for direct integration with a permanent magnet generator system.

The grey circular rings on both sides are not just decorative but serve as functional and alignment elements as well. These parts are used to maintain proper spacing between the duct, stator and rotor assembly. They also assist in mechanical assembly and maintain the correct positioning of the rotating part. The supporting base frame (the grey part) is used to stabilize the turbine and enable the whole system to be installed in a real tidal flow site

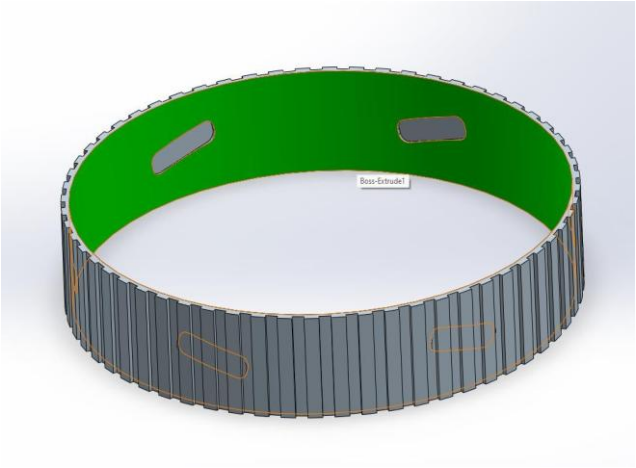



Fig. 3.5. Six-blade rotor and ducted open-centered turbine geometry.

The rotor section comprises six blades that are curved and spaced around the open center turbine passage. This blade configuration is designed to engage with the incoming tidal current and convert the kinetic energy of the moving water to rotational mechanical energy. The open-center design gives water freedom to flow through the center whilst the surrounding blades extract energy from the flow. The geometry of blades can be designed to work in both directions of the tide, making this type of rotor suitable for bidirectional tidal operations [Fig. shown as 3.5].

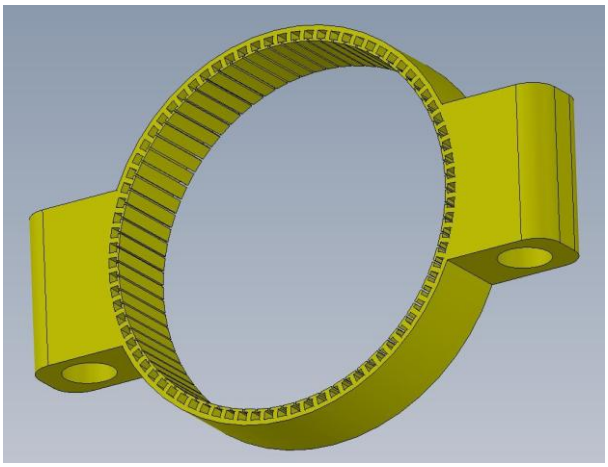


Fig. 3.6. Stator with embeded coils.

This is a view of the stator with coil spaces around the inside of the yellow ring. The practical electric design is such that the rotor with permanent magnets rotates inside the stator. The rotor is rotated by the tidal flow and the varying magnetic field cuts through the stator coils embedded within, inducing a voltage. Hence, this stator configuration constitutes

the primary electrical power generating part of the turbine, which changes the mechanical rotation provided by the flowing water into electrical power [Fig. shown as 3.6].

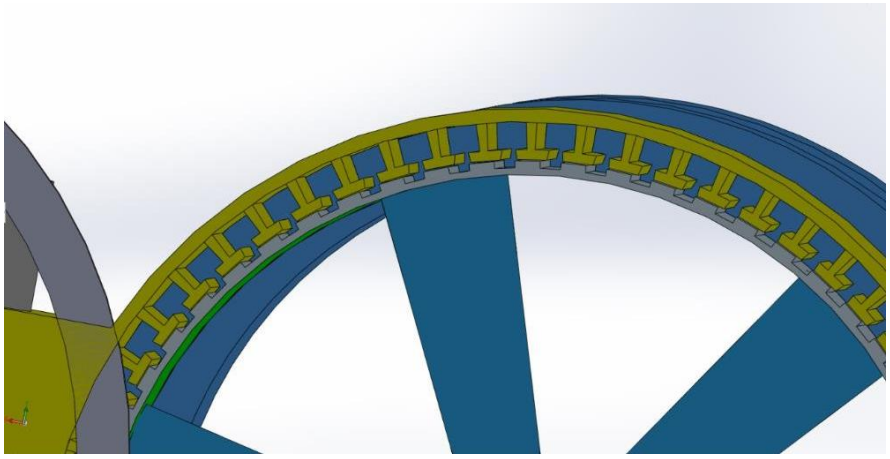


Fig. 3.7. Stator and coil-slot arrangement.

In fig 3.7 shown the outer yellow ring shows the stator structure of the turbine-generator assembly. In the stator, there are a number of evenly spaced slots around the inner circumference of the structure that are added to accommodate the copper windings/coils. These slots are used to help establish a uniform circular array of coils around the rotor to enable electromagnetic induction during movement of permanent magnets on the rotor through these coils. The interaction between the magnetic field in the rotor and the winding in the stator is enhanced because of the close spacing of the slots. Table 3.1 shows calculated parameters for turbine design.

**Table 3.1** The main turbine dimensions used in the project are summarized below.

| Parameter | Value |
|---|---|
| Duct diameter | 120 cm = 1.20 m |
| Duct radius | 60 cm = 0.60 m |
| Rotor diameter | 108 cm = 1.08 m |
| Rotor radius | 54 cm = 0.54 m |
| Hub/open-center diameter | 22 cm = 0.22 m |
| Hub/open-center radius | 11 cm = 0.11 m |
| Number of blades | 6 |
| Blade curve angle | Approximately 15 degrees |
| Blade length from base to tip | Approximately 43 cm |
| Blade base length | Approximately 25.91 cm |
| Rotor width | Approximately 20.19 cm |
| Duct one-side width | Approximately 20.09 cm |
| Total duct width | Approximately 57.37 cm |
| Blade width near tip | Approximately 18.81 cm |
| Blade width near middle | Approximately 20.85 cm |
| Blade base thickness | Approximately 2.92 cm |
| Blade tip thickness | Approximately 2.00 to 2.17 cm |
| Blade-to-blade separation | Approximately 24.45 cm |
| Annular swept area | 0.878 m^2 |

### 3.5 Annular Swept Area Calculation

The effective swept area of the turbine is not the area of a full circle as this is an open-centered turbine. The effective swept area, however, is the area of the annulus between the outer radius of the rotor and the radius of the inner hub/open center. So, the swept area of the ring will be:

$$A = \pi (R_{rotor}^2 - R_{hub}^2) \quad (3.1)$$

Where, $R_{rotor} = 0.54\, m$ and $R_{hub} = 0.11m$

$$\text{Thus, } A = \pi (0.54^2 - 0.11^2)$$

$$A = \pi (0.2916 - 0.0121)$$

$$A = \pi (0.2795)$$

$$A \approx 0.878\, m^2$$

Therefore, the effective annular swept area of the open-centered turbine is approximately:

$$A \approx 0.878\, m^2$$

This swept area was utilized to interpret design of the turbine geometry. The hydraulic power that was measured in Plane 1 was, however, used directly together with the inlet velocity for the corrected power calculation available in hydraulic from ANSYS Fluent. This was done using the kinetic energy rate expression:

$$P_{avail} = \frac{1}{2} \dot{m} V^2 \quad (3.2)$$

where ṁ is the mass flow rate through the reference plane and V is the inlet water velocity.

### 3.6 Tip to speed Ratio, Rotor Speed and Angular Speed

The tip-speed ratio is an important parameter in tidal turbine analysis because it relates the blade tip speed to the incoming water velocity. It is defined as:

$$TSR = \frac{\omega R}{V} \quad (3.3)$$

where TSR is the tip-speed ratio, ω is the mechanical angular speed of the rotor, R is the rotor radius, and V is the incoming tidal water velocity.

In this study, a constant tip-speed ratio of:

$$TSR = 3$$

was used for all operating points. Rearranging the tip-speed ratio equation gives the angular speed of the rotor:

$$\omega = \frac{TSR \times V}{R}$$

Since the rotor radius is R = 0.54 m, the angular speed increases linearly with water velocity. The corresponding rotor speed in revolutions per minute is calculated as:

$$n = \frac{60\omega}{2\pi}$$

For example, at a tidal velocity of $V = 2.1\ m/s$:

$$\omega = \frac{3 \times 2.1}{0.54}$$

$$\omega = 11.67\ rad/s$$

Therefore, for the 2.1 m/s representative operating point, the rotor angular speed is approximately 11.67 $rad/s$ and the corresponding rotational speed is approximately 111.41 rpm. This rotor speed was used in the ANSYS Fluent rotating cell zone and moving wall boundary settings.

### 3.7 Available Hydraulic Power

The available hydraulic power represents the kinetic energy rate of the water flow passing through the turbine reference plane. In this study, the available hydraulic power was calculated using the mass flow rate obtained from ANSYS Fluent at Plane 1 and the corresponding inlet water velocity. The expression used is:

$$P_{avail} = \frac{1}{2}\ \dot{m}V^2 \tag{3.4}$$

Where $P_{avail}$ is the available hydraulic power, $\dot{m}$ is the mass flow rate through Plane 1, and V is the inlet water velocity.

This method is appropriate because the mass flow rate directly represents the amount of water passing through the selected reference plane per unit time. Therefore, using $\dot{m}$ from Plane 1 avoids overestimating the available power from the larger inlet-domain flow.

For example, at a tidal velocity of $V = 2.1\ m/s$ , the mass flow rate obtained from ANSYS Fluent was:

$$\dot{m} = 2742.07\ kg/s$$

Thus, the available hydraulic power is:

$$P_{availe} = \frac{1}{2} \times 2742.07\ \times (2.1)^2$$

$$P_{availe} = 6046.26\ W$$

Therefore, the available hydraulic power at 2.1 m/s is approximately:

$$P_{availe} = 6.046\ kW$$

This value was used in the corrected ANSYS result table and provides a more realistic basis for evaluating turbine performance than using the mass flow rate from the entire inlet domain.

### 3.8 Torque and Mechanical Shaft Power

The turbine torque was obtained from ANSYS CFD-Post about the global Z-axis, since the turbine rotor was defined to rotate about the Z-axis in the simulation. In the corrected dataset, the torque acting on the blade surface was taken as the turbine torque for the simplified CFD interpretation.

The mechanical shaft power was calculated from the turbine torque and angular speed using:

$$P_{mech} = T\omega \tag{3.5}$$

Where $P_{mech}$ is the mechanical shaft power, T is the turbine torque, and ω is the angular speed of the rotor.

For example, at a tidal velocity of $V = 2.1\ m/s$, the turbine torque was:

$$T = 288.16\ N.m$$

and the angular speed was:

$$\omega = 11.67\ rad/s$$

Therefore, the mechanical shaft power is:

$$P_{mech} = 288.16 \times 11.67$$

$$P_{mech} = 3362.83\ W$$

Thus, at the 2.1 m/s operating point, the turbine delivered approximately 3362.83W of mechanical shaft power to the generator.

### 3.9 Hydraulic to Mechanical Turbine Efficiency

The hydraulic-to-mechanical turbine efficiency represents the percentage of available hydraulic power that is converted into useful mechanical shaft power by the turbine. It was calculated using:

$$\eta_t = \frac{P_{mech}}{P_{avail}} \times 100 \quad (3.6)$$

Where $\eta_t$ is the turbine efficiency, $P_{mech}$ is the mechanical shaft power, and $P_{avail}$ is the available hydraulic power.

For the representative operating point at V = 2.1 m/s:

$$P_{mech} = 3362.83\ W$$

$$P_{avail} = 6046.26\ W$$

Therefore,

$$\eta_t = \frac{3362.83}{6046.26} \times 100$$

$$\eta_t = 55.62\%$$

This value indicates that approximately 55.62% of the available hydraulic kinetic power passing through the selected reference plane was converted into mechanical shaft power at this operating point.

### 3.10 PMSM Generator and Electrical Frequency

The permanent magnet synchronous machine (PMSM) converts the mechanical shaft rotation of the turbine into three-phase electrical output. In a PMSM, the electrical angular speed is related to the mechanical angular speed by:

$$\omega_e = p\omega_m \tag{3.7}$$

where $\omega_e$ is the electrical angular speed, $\omega_m$ is the mechanical angular speed, and $p$ is the number of pole pairs.

The corresponding electrical frequency is calculated as:

$$f_e = \frac{\omega_e}{2\pi} \tag{3.8}$$

Substituting $\omega_e = p\omega_{\dot{m}}$

$$f_e = \frac{p\omega_{\dot{m}}}{2\pi} \tag{3.9}$$

In this study, the selected PMSM model uses 30 pole pairs, equivalent to 60 magnetic poles. A high pole-pair number is suitable for low-speed direct-drive tidal turbine applications because it allows a useful electrical frequency to be generated at relatively low mechanical rotational speeds, without requiring a gearbox.

For example, at V = 1.9 m/s, the mechanical angular speed was:

$$\omega_m = 10.56\, rad/s$$

Using $p = 30$

$$f_e = \frac{30 \times 15.6}{2\pi}$$

$$f_e = 50.42\, Hz$$

The corresponding rotor speed is,

$$N = \frac{60\omega_m}{2\pi}$$

$$N = \frac{60 \times 10.56}{2\pi}$$

$$N \approx 100.8\, rpm$$

Therefore, at the 1.9 m/s operating point, the generator produces an electrical frequency close to 50 Hz while the turbine rotor speed remains only about 100.8 rpm. This demonstrates the suitability of a high-pole-count PMSM for low-speed tidal energy conversion.

### 3.11 Permanent Magnet Flux Linkage Calculation for 0.218Wb

The permanent magnet flux linkage used in the PMSM block was selected as:

$$\lambda_m = 0.218\, Wb$$

This value was justified by using the generator back-EMF relationship. For a sinusoidal PMSM, the approximate no-load phase RMS back-EMF can be expressed as:

$$E_{ph,rms} = \frac{\omega_e \lambda_m}{\sqrt{2}} \tag{3.10}$$

where $E_{ph,rms}$ is the phase RMS back-EMF, $\omega_e$ is the electrical angular speed, and $\lambda_m$ is the permanent magnet flux linkage.

Rearranging the equation gives:

$$\lambda_m = \frac{\sqrt{2}\, E_{ph,rms}}{\omega_e} \tag{3.11}$$

The design target was to obtain useful low-voltage three-phase generator output in the strong-flow operating region. In the earlier DC-bus concept, a nominal DC bus voltage of 120 V was considered. For a three-phase diode bridge rectifier, the average DC output voltage can be approximated as:

$$V_{dc} \approx 1.35 V_{LL,rms}$$

Ignoring small diode and loading effects, a 120 V DC bus corresponds to a line-to-line RMS voltage of approximately:

$$V_{LL,rms} = \frac{120}{1.35}$$

$$V_{LL,rms} \approx 89\,V$$

Therefore, a target line-to-line RMS voltage in the range of approximately 89 V to 94 V was considered reasonable.

At the representative high-flow operating point of V = 2.1 m/s:

$$\omega_m = 11.67\,rad/s$$

and $p = 10$

Therefore, the electrical angular speed is:

$$\omega_e = p\omega_m$$

$$\omega_e = 30 \times 11.67$$

$$\omega_e = 350.1\,rad/s$$

If the target line-to-line RMS voltage is selected as approximately:

$$V_{LL,rms} = 93.4\,V$$

Then the corresponding phase RMS voltage is:

$$V_{ph,rms} = \frac{V_{LL,Rms}}{\sqrt{3}} \tag{3.12}$$

$$V_{ph,rms} = \frac{93.4}{\sqrt{3}}$$

$$V_{ph,rms} \approx 53.9\,V$$

Using the flux linkage equation:

$$\lambda_m = \frac{\sqrt{2} \times 53.9}{350.1}$$

$$\lambda_m \approx 0.218\, Wb$$

Therefore, a flux linkage of 0.218 Wb was chosen as a reasonable value to develop the desired generator voltage level at the high flow operating point. Simplified loading model (model #2): Same flux linkage is used as it gives the same phase RMS voltage values as simulation results.

### 3.12 Three-Phase Resistive Load Power Calculation

The final MATLAB/Simulink model uses a balanced three-phase resistive load of 15 Ω per phase. Since the load is balanced and purely resistive, the power factor is assumed to be approximately unity:

$$cos\emptyset \approx 1$$

The phase RMS voltage and phase RMS current were measured using voltage and current sensors followed by RMS blocks. The per-phase load power was calculated as:

$$P_{ph} = V_{ph,rms}\, I_{ph,rms} \tag{3.13}$$

where $P_{ph}$ is the per-phase load power, $V_{ph,rms}$ is the phase RMS voltage, and $I_{ph,rms}$ is the phase RMS current.

Since the system is a balanced three-phase load, the total three-phase load power was calculated as:

$$P_{load} = 3P_{ph} \tag{3.14}$$

Therefore:

$$P_{load} = 3V_{ph,rms}\, I_{ph,rms} \tag{3.15}$$

This is why the Simulink model first multiplies the measured phase RMS voltage and phase RMS current to obtain the per-phase power and then multiplies the result by 3 to obtain the total three-phase load power.

The line-to-line RMS voltage was calculated separately using:

$$V_{LL,rms} = \sqrt{3} V_{ph,rms} \tag{3.16}$$

This conversion was used only to report the line-to-line voltage of the generator output. It was not used directly in the total three-phase load power calculation, since the load power was calculated using the phase RMS voltage and phase RMS current.

For example, at a tidal velocity of V = 1.4 m/s:

$$V_{ph,rms} = 34.34\ V$$

$$I_{ph,rms} = 2.289\ A$$

Therefore:

$$P_{load} = 3\ \times 34.34\ \times 2.289$$

$$P_{load} = 235.8\ W$$

This value is the total three-phase electrical power delivered to the balanced resistive load and is the value reported in the electrical output table.

### 3.13 Mechanical to load Efficiency

Mechanical-to-load efficiency represents the percentage of mechanical shaft power that is converted into useful electrical power delivered to the load. It was calculated as:

$$\eta_{load} = \frac{P_{load}}{P_{mech}} \times 100$$

where $\eta_{load}$ is the mechanical-to-load efficiency, $P_{load}$ is the total three-phase load power, and $P_{load}$ is the mechanical shaft power supplied to the PMSM generator.

This efficiency is different from the hydraulic-to-mechanical turbine efficiency. The hydraulic-to-mechanical efficiency describes how much available hydraulic power is converted into turbine shaft power, whereas the mechanical-to-load efficiency describes how much of the shaft power finally appears as electrical power in the load. Therefore, the mechanical-to-load efficiency includes the effects of generator performance, electrical loading, and load-matching behavior.

For example, at a tidal velocity of V = 1.4 m/s:

$$P_{mech} = 918.76\,W$$

$$P_{load} = 235.8\,W$$

Therefore:

$$\eta_{load} = \frac{235.8}{918.76} \times 100$$

$$\eta_{load} = 25.67\%$$

This means that at the 1.4 m/s operating point, approximately 25.67% of the mechanical shaft power was delivered as electrical power to the three-phase resistive load. The remaining difference represents generator losses, electrical loading effects, and load-matching limitations in the simplified model.

### 3.14 Load Energy and Long-Term Energy Estimation

For each Simulink operating point, the load energy was calculated by integrating the three-phase load power over the simulation time. The simulation time for each operating point was 20 seconds. Therefore, the load energy in joules was calculated as:

$$E_{load} = \int P_{load}\,(t)dt \tag{3.17}$$

where $E_{load}$ is the load energy and $P_{load}$ is the instantaneous or measured load power as a function of time.

Since the simulation time was only 20 seconds, the generated energy for a single simulation run is small. Therefore, this value should not be confused with daily energy production. The

20-second simulations were used to obtain steady operating-point electrical output values at different tidal velocities.

To estimate long-term energy production, the 21 simulated operating points were used as a velocity-to-power lookup table. In this method, the tidal velocity is treated as the input and the corresponding three-phase load power is treated as the output:

$$v \rightarrow P_{load}$$

A smooth tidal velocity profile was then generated over one lunar tidal day of approximately 24.84 hours. Since the turbine is considered bidirectional, the tidal current velocity magnitude was used. At each step in the tidal cycle, the corresponding load power was estimated by interpolation using the 21 simulated operating points. The total energy over one lunar tidal day was then calculated by integrating the interpolated load-power curve over time:

$$E_{day} = \int_{0}^{24.84h} P_{load}\,(t)dt$$

This method gives a time-based energy estimate rather than a simple average of the 21 operating-point powers. The final estimated energy values obtained from this method were:

$$\mathrm{E_{day}} = 6.675 \text{ kWh per lunar tidal day}$$

$$E_{month} = 193.48\ kWh\ per\ 30\ days$$

$$E_{year} = 2353.99\ kWh/yaer$$

These results represent the estimated electrical energy delivered to the three-phase resistive load using the simulated PMSM generator output and the assumed tidal velocity variation over a full lunar tidal day. This approach is more realistic than using a single constant velocity because the tidal current velocity changes continuously throughout the tidal cycle.

# CHAPTER 4
# PROJECT IMPLEMETATION

## 4.1 Overall Methodology

The project workflow consists of four connected stages:

- SolidWorks modelling: Development of turbine geometry and practical assembly.
- ANSYS Fluent CFD simulation: Hydrodynamic analysis for different water velocities.
- Data processing: Calculation of torque, mechanical shaft power, available hydraulic power, and efficiency.
- MATLAB/Simulink electrical modelling: Conversion of mechanical input into generator-side DC output and load-side AC output.

The simulation methodology is as follows: First, SolidWorks was used to prepare the geometry, then ANSYS Fluent was applied to simulate the hydrodynamic performance of the simulated pumps, the data was extracted from ANSYS Fluent using CFD-Post function calculator and it was used to simulate PMSM generator in MATLAB/Simulink; after that the table was prepared, plotted and the energy yield was estimated. This chapter explains the implementation of each stage and how the simplified PMSM-load system was chosen for the thesis.

The values for torque and angular speed for each water velocity are the principal values of interest that connect ANSYS with MATLAB. The above values were set for the PMSM shaft in Simulink.

## 4.2 SolidWorks Modelling

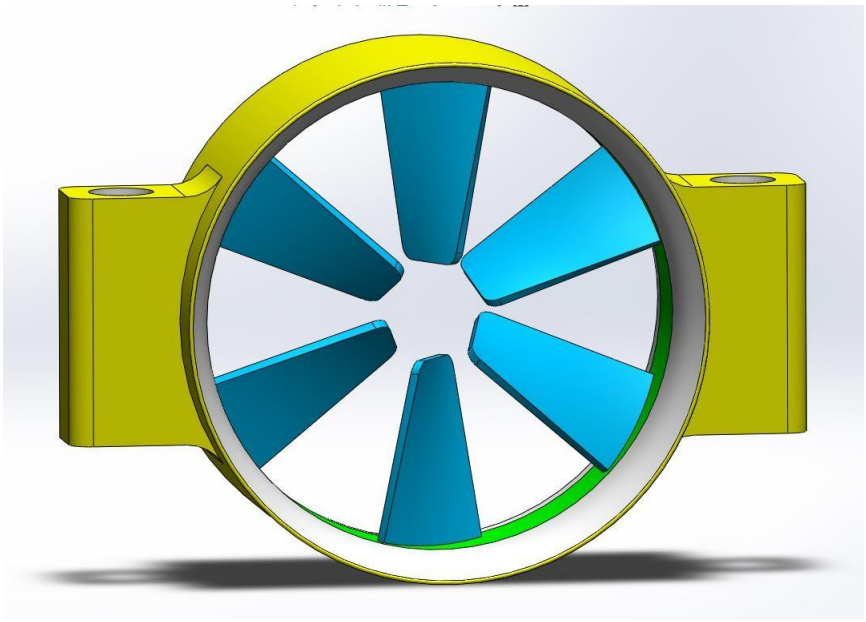


Fig. 4.1. Six-bladed design with Rotor angle 13 degree.

The geometry of the simplified no-base turbine was generated in the SolidWorks stage, and the practical turbine assembly was also produced. The practical assembly consists of a supporting base, duct, stator, coil-slot concept, rotor and six curved blades. Simplified geometry eliminates the need for an external support base for CFD analysis. This is acceptable since the objective of the CFD is to evaluate the hydrodynamic torque, and mass-flow behavior of the turbine rotor/duct region.

The rotor has 6 blades and has around 13 degrees of rotor blade curvature. Blades are broader at the base and taper towards the tip. The stator ring has holes where the coils are to be installed, and the rotor will have embedded magnets. This helps to develop a future practical PMSM/PMSG type generator concept.

## 4.3 ANSYS Fluent Geometry and Mesh

The turbine geometry wash simplified and imported to list ANSYS Design Modeler And meshed for fluent. The model included a rotor and stator/fluid domains. The rotor zone was given a rotational movement, and the stator zone was given a stationary movement. Mesh interfaces between the rotating and stationary regions were employed. The imported

geometry was prepared with enclosures and Boolean operations to provide the fluid domain to be solved around the turbine.

In geometry preparation, two enclosure regions were used. Boolean operations were used to isolate the fluid domains and create the computational domain. Two large cell areas were incorporated in the final model:

- **Rotor zone:** Rotating fluid region around the rotor blades.
- **Stator zone:** Stationary surrounding fluid region.

The rotor region is where the kinetic energy of the water is absorbed, and energy is extracted here at this region specifically. This region is very crucial as the turbine extracts most of its power from this central region of the turbine. The water gets accelerated due to the curvature of the duct inside the inner region. The blades of the rotors must be built with sturdy and flexible material so it can bend and withstand the strong jet stream from the inlet. There is also a hollow circle at the center called the hub. This region is hollow so that small fishes can actually sweep past uninterrupted through the turbine. Therefore, less damage is impacted by the fishes. We had to assign a speed of 2.4m/s or any water velocity speed.

The stator region is the stationary part of the turbine. It does not move while the rotor zone only moves. In ANSYS simulation, we do not need to assign any values to the stator region. The values are not important here at this point. Since this region is where the water us flowing through the inlet of the turbine. The turbine has a few stator regions where the base of it is strictly attached to it for stability purposes as well as for the underwater turbine structure itself. Fluid is supposed to flow from this region. As the water flows from the inlet to the stator region, the walls of the stator zone are there to absorb the kinetic energy produced by the water by the turbine blades. So, the rotor and the stator region both work together here. One is moving while the other is stationary. By using this method, we have modelled the turbine in SolidWorks and used that same model to simulate in a domain where the turbine has inlet flow of water and an outlet flow of water.

## 4.4 Mesh Generation and Mesh Settings

Figure 4.2 shows the mesh generated for the cylindrical computational fluid domain used in the ANSYS Fluent simulation. The turbine model was placed inside this fluid domain so that the tidal flow around the rotor and duct could be analyzed numerically. An unstructured mesh was used because it can represent the cylindrical domain and turbine geometry more easily than a simple structured mesh. The mesh divides the fluid region into many small elements, allowing ANSYS Fluent to solve the governing flow equations at different locations in the domain. A suitable mesh is important because the accuracy of the CFD results, such as velocity distribution, torque, mass flow rate and pressure variation, depends strongly on the quality of the mesh. The generated mesh was therefore used as the computational basis for the tidal turbine flow simulation.

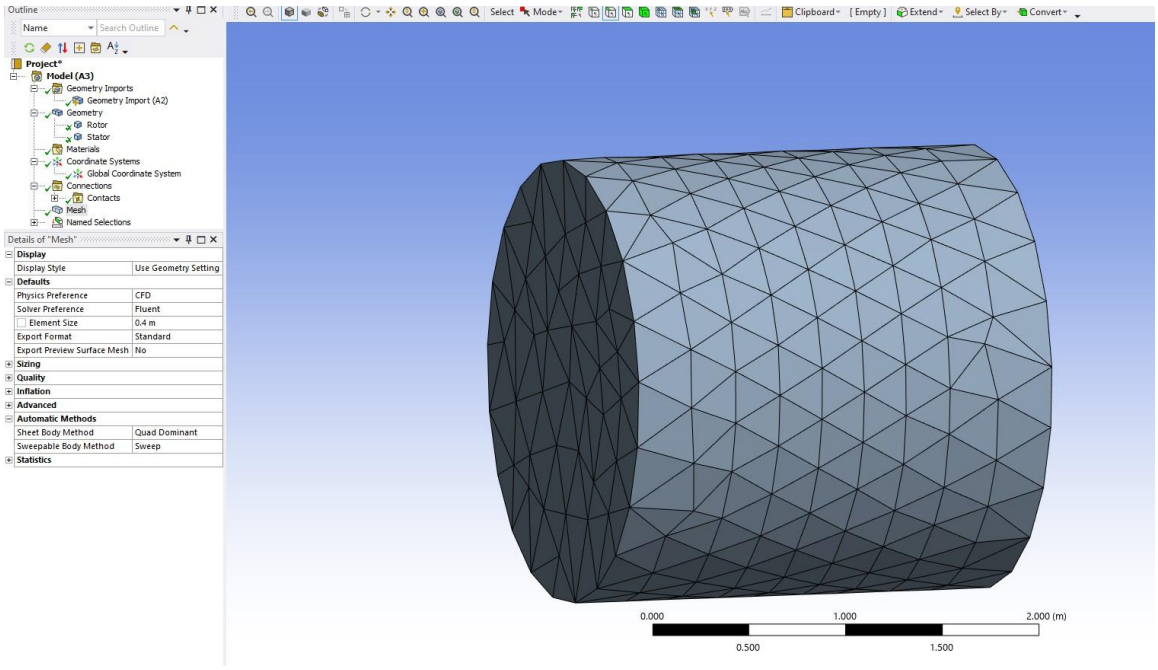
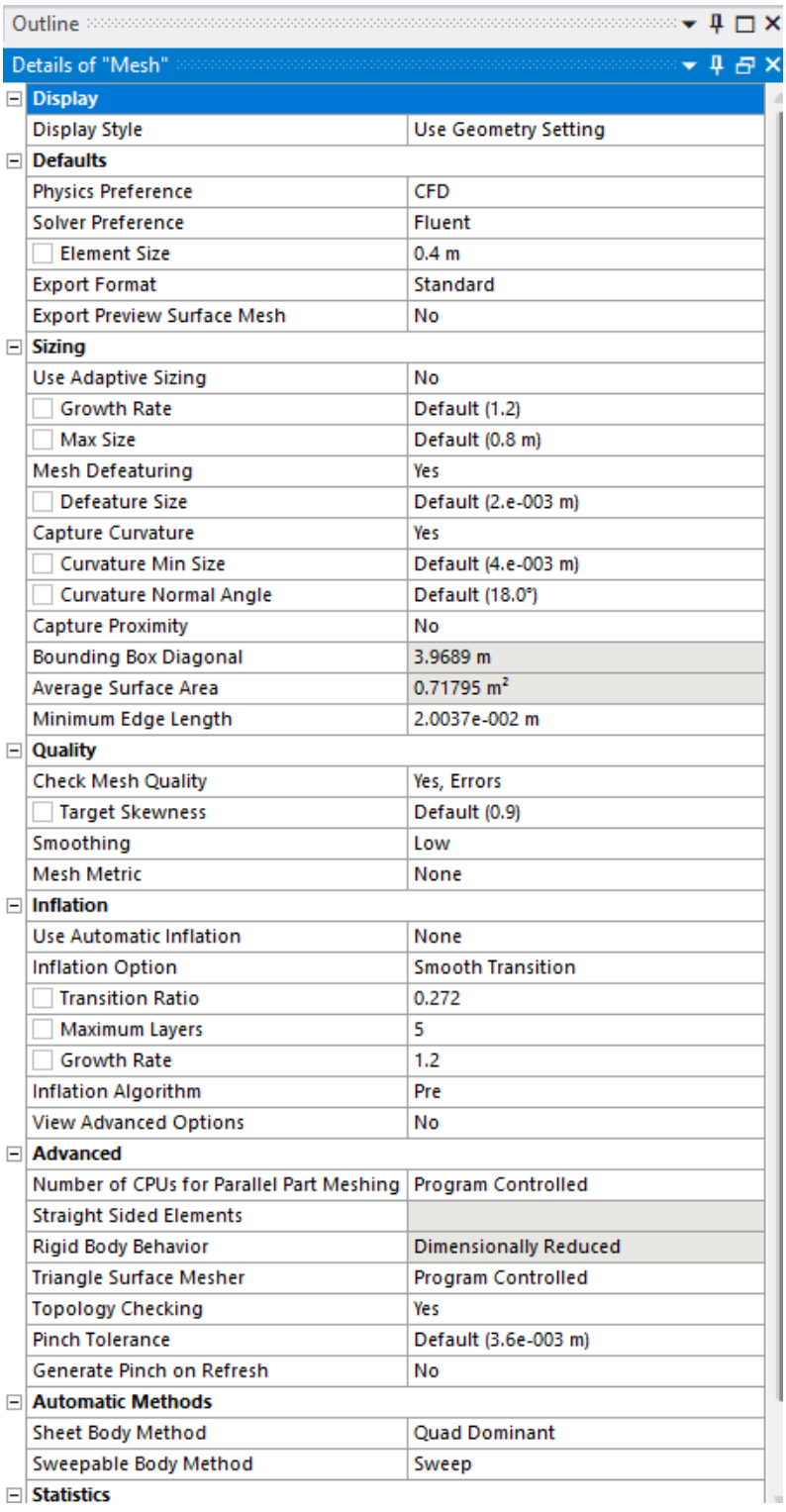



Fig. 4.2. ANSYS mesh of the Cylindrical Computational fluid domain used for CFD simulation



Outline

Details of "Mesh"

| | |
|---|---|
| **Display** | |
| Display Style | Use Geometry Setting |
| **Defaults** | |
| Physics Preference | CFD |
| Solver Preference | Fluent |
| Element Size | 0.4 m |
| Export Format | Standard |
| Export Preview Surface Mesh | No |
| **Sizing** | |
| Use Adaptive Sizing | No |
| Growth Rate | Default (1.2) |
| Max Size | Default (0.8 m) |
| Mesh Defeaturing | Yes |
| Defeature Size | Default (2.e-003 m) |
| Capture Curvature | Yes |
| Curvature Min Size | Default (4.e-003 m) |
| Curvature Normal Angle | Default (18.0°) |
| Capture Proximity | No |
| Bounding Box Diagonal | 3.9689 m |
| Average Surface Area | 0.71795 m² |
| Minimum Edge Length | 2.0037e-002 m |
| **Quality** | |
| Check Mesh Quality | Yes, Errors |
| Target Skewness | Default (0.9) |
| Smoothing | Low |
| Mesh Metric | None |
| **Inflation** | |
| Use Automatic Inflation | None |
| Inflation Option | Smooth Transition |
| Transition Ratio | 0.272 |
| Maximum Layers | 5 |
| Growth Rate | 1.2 |
| Inflation Algorithm | Pre |
| View Advanced Options | No |
| **Advanced** | |
| Number of CPUs for Parallel Part Meshing | Program Controlled |
| Straight Sided Elements | |
| Rigid Body Behavior | Dimensionally Reduced |
| Triangle Surface Mesher | Program Controlled |
| Topology Checking | Yes |
| Pinch Tolerance | Default (3.6e-003 m) |
| Generate Pinch on Refresh | No |
| **Automatic Methods** | |
| Sheet Body Method | Quad Dominant |
| Sweepable Body Method | Sweep |
| **Statistics** | |

Fig. 4.3. Mesh details for Six-bladed design with Rotor angle 13 degree

The mesh was generated using ANSYS Meshing. The mesh settings included:

- **Physics Preference:** CFD.
- **Solver Preference:** Fluent.
- **Element size:** approximately 0.4 m in the global setting.
- Curvature Capture Enabled.
- Mesh quality check enabled.
- Inflation option using smooth transition.
- Automatic methods including sweep/quad-dominant settings where applicable.

The rotor and stator areas were meshed as separate areas. The number of nodes and elements for the rotor region in the available screenshots are high, suggesting the computational meshes were able to capture the blade/rotor geometry. A mesh independence study should be performed for future refinement to ensure that torque does not vary significantly with further mesh refinement [Fig. shown as 4.3].

## 4.5 Fluid Properties and Material Selection

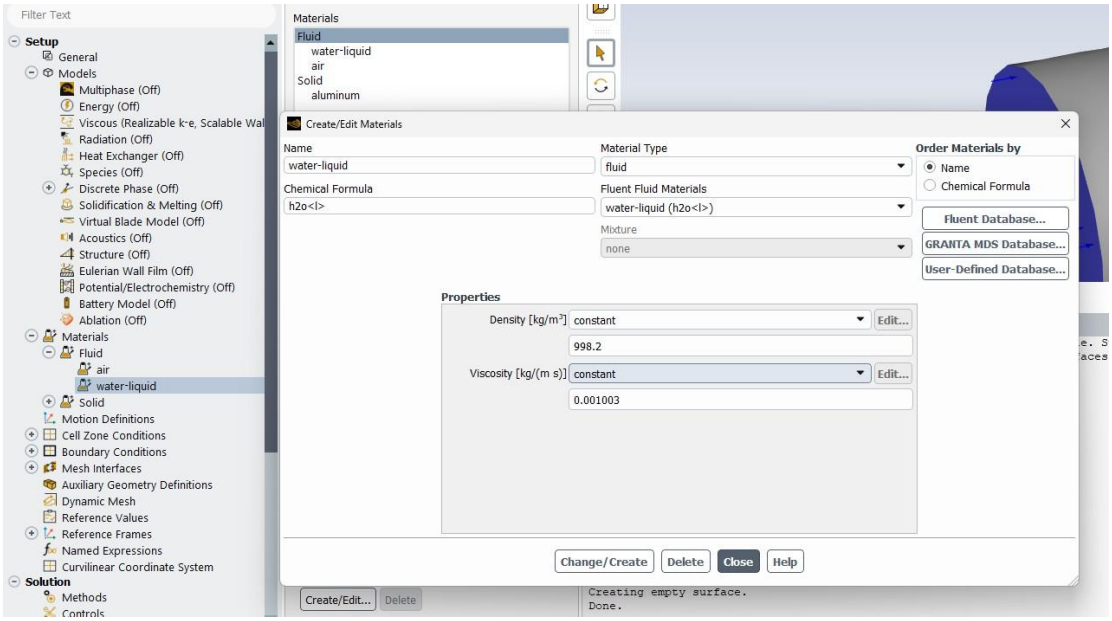



Fig. 4.4. Fluid Properties.

Figure 4.4 show simulations used water-liquid as the main fluid material. From the ANSYS material setup, Table 4.1 shown the water-liquid properties were:

**Table 4.1** The water-liquid Properties

| Property | Value |
|---|---|
| Density | 998.2 kg/m^3 |
| Dynamic viscosity | 0.001003 kg/(m.s) |

Air and aluminum were also available in the material list, but the hydrodynamic simulation used water-liquid for the fluid zones. Table 4.2 shown as ANSYS setup and data extraction method.

**Table 4.2** Summary of ANSYS Fluent setup and data extraction method

| Item | Setting |
|---|---|
| Software | ANSYS Fluent / CFD-Post |
| Model type | Transient pressure-based CFD |
| Fluid material | Water-liquid |
| Water density | 998.2 kg/m^3 |
| Water viscosity | 0.001003 kg/(m.s) |
| Turbulence model | Realizable k-epsilon with scalable wall functions |
| Velocity range | 0.4 m/s to 2.4 m/s |
| Tip-speed ratio | TSR = 3 |
| Inlet condition | Velocity inlet |
| Outlet condition | Pressure outlet, 0 Pa gauge |
| Rotor motion | Rotating frame / moving wall about global Z-axis |
| Torque extraction | Function Calculator, torque about global Z-axis |
| Mass flow extraction | Function Calculator, mass flow through Plane 1 |

## 4.6 Boundary Conditions

The Boundary conditions were defined in ANSYS Fluent to represent the tidal water flow through the computational domain. The upstream face of the cylindrical domain was assigned as the velocity inlet, where the tidal current velocity was specified for each operating case. The downstream face was defined as the pressure outlet so that water could leave the domain naturally after passing through the turbine. The outer cylindrical wall was treated as a wall boundary to enclose the flow region, while the rotor blade and hub surfaces were assigned as moving wall surfaces to represent turbine rotation. The rotor and stator regions were also defined separately so that the rotating part of the turbine could be simulated relative to the stationary fluid domain. These boundary conditions allowed the CFD model to calculate the flow field, pressure variation, mass flow rate and torque generated by the turbine.

### 4.6.1 Velocity Inlet

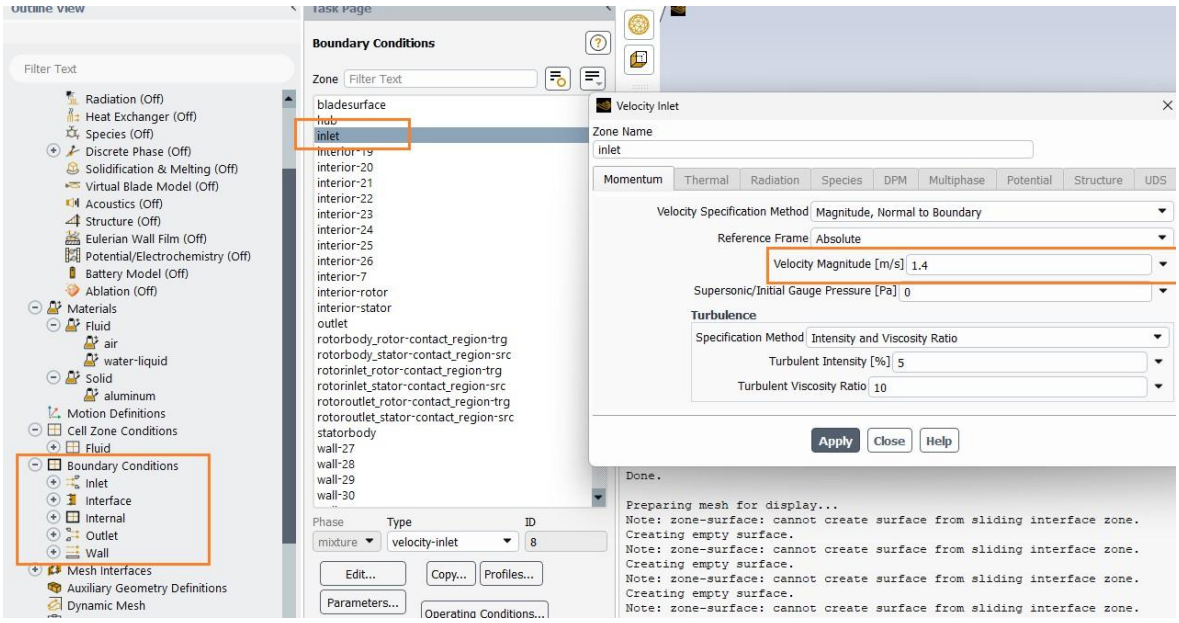



Fig. 4.5. Velocity Inlet boundary condition applied at the upstream boundary of the computational domain.

The velocity inlet boundary condition was used at the inlet of the computational domain as depicted in figure 4.5. The tidal current velocity used for each operating case was

varied to change the inlet velocity magnitude from 0.4 m/s to 2.4 m/s. The velocity direction was set to be perpendicular to the inlet boundary such that the flow of water was along the turbine axis into the domain. The turbulence intensity and the turbulent viscosity ratio were used to define the inlet turbulence condition. So, we fixed a turbulence intensity of 5% and the turbulent viscosity ratio to be of 10. With this configuration, each CFD case was able to simulate a different speed of the tidal flow without changing the geometry of the turbine or the domain configuration. This is very useful as we have seen after running the simulation.

### 4.6.2 Pressure Outlet

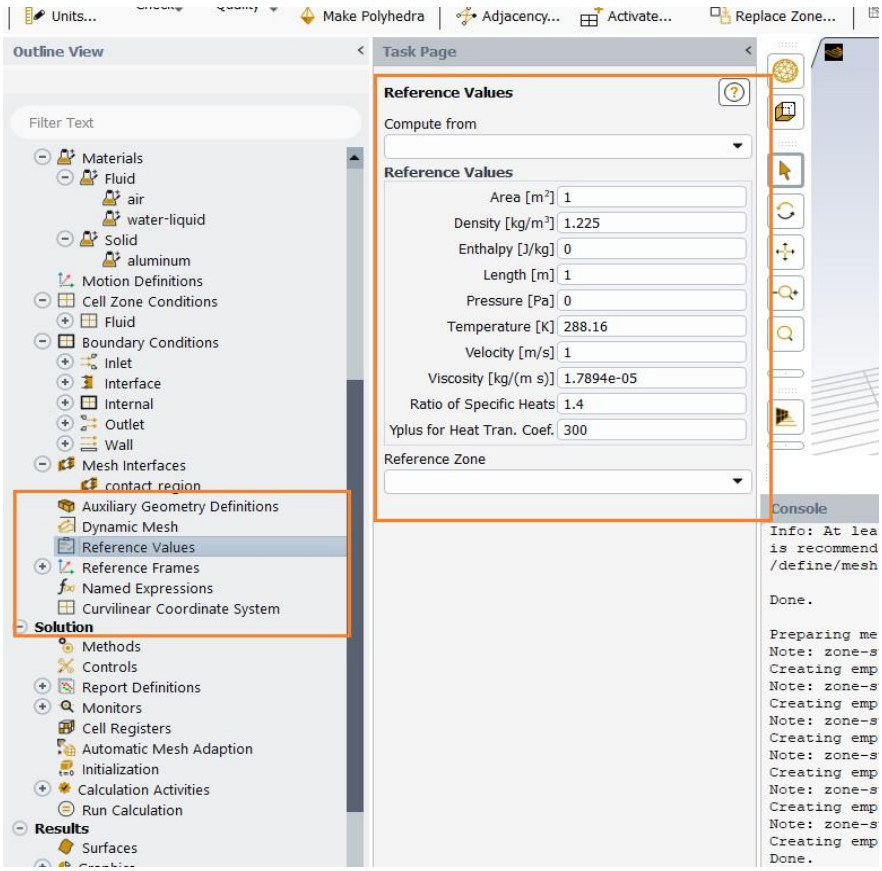



Fig. 4.6. Pressure Outlet boundary condition steup in ANSYS Fluent.

The downstream edge was assumed to be a pressure outlet. This outlet gauge pressure was set to 0 Pa, which acts as a reference pressure and the flow naturally exits the computational domain at this location. The other specifications for the backflow turbulence were the intensity and the viscosity ratio: backflow turbulent intensity is 0.05 and the viscosity ratio is 0.1 [Fig. shown as 4.6].

### 4.6.3 Rotor and Stator Cell Zones

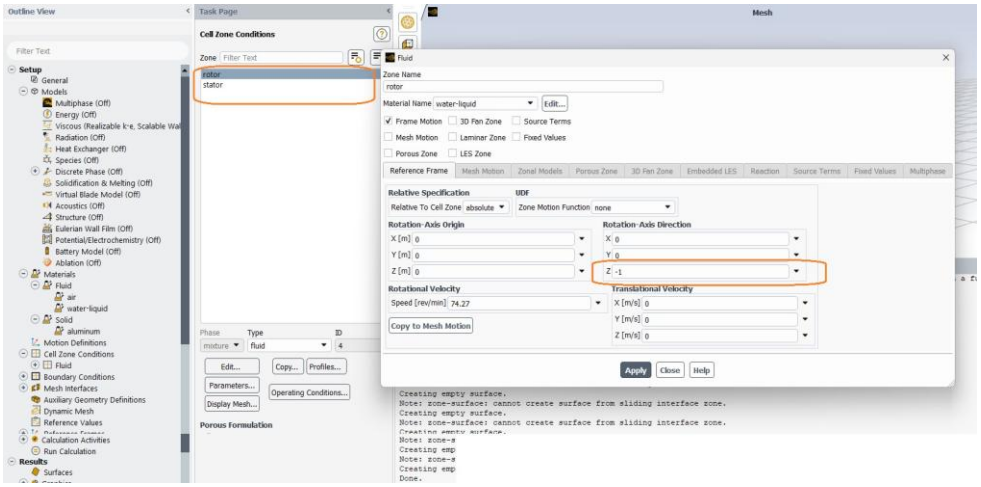



Fig. 4.7. Rotor and Stator Cell Zones seetings in ANSYS Fluent.

A frame motion around the global Z-axis and water were assigned to the rotor cell zone. The calculated rpm for that velocity was chosen to be the rotational velocity in rev/min. The surface of the blade and the hub were considered as moving walls for the adjacent rotor zone. The Z-axis torque was used for turbine torque extraction due to the rotation of the rotor around the Z-axis. The region of the stator remained stationary. Mesh interfaces were used to connect the rotor and stator regions [Fig. shown as 4.7].

### 4.6.4 Moving Wall Surface

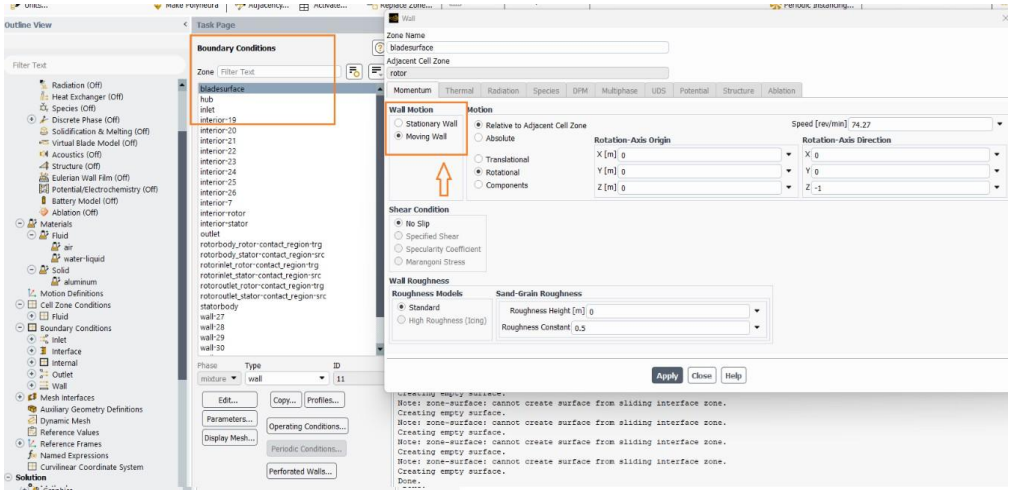



Fig. 4.8. Moving wall boundary condition applied to rotor blade and hub surface.

The blade surface and the hub were modeled as moving wall surfaces of the rotor region. They were given a rotational movement with respect to the global Z-axis. Later these surfaces were used for torque extraction [Fig. shown as 4.8].

## 4.7 Solution Methods and Transient Simulation Settings

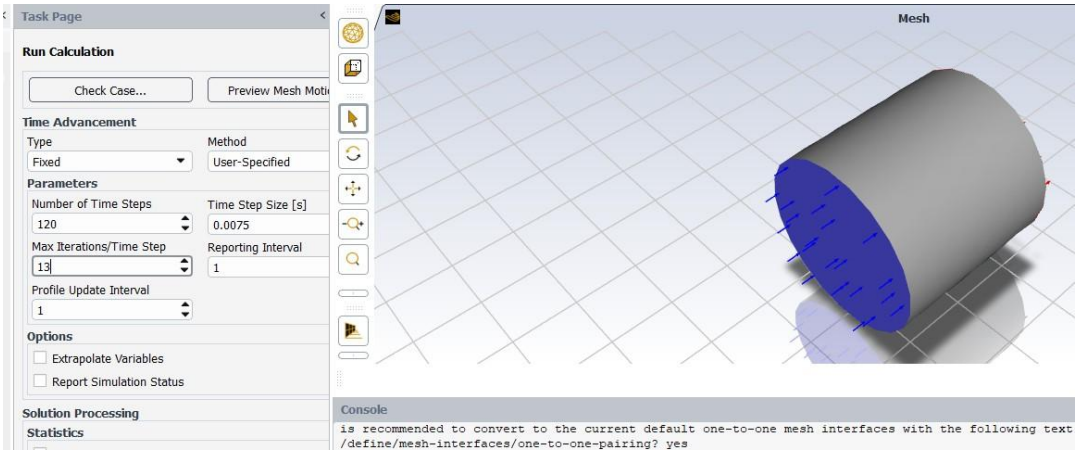



Fig. 4.9. Transient simulation settings for one rotor revolution ANSYS Fluent.

The simulation with the CFD was carried out as a transient operating point simulation. The solver was chosen as the pressure-based solver. The SIMPLE pressure-velocity coupling scheme was used. Least-squares cell-based gradint, second-order pressure, second-order upwind momentum and first-order upwind turbulence quantities were included in the spatial discretization [Fig. shown as 4.9].

The table 4.3 shown as simulations were initially carried out using:

**Table 4.3** Simulations time step size, Number of time steps and Maximum iterations per time step

| Parameter | Value |
|---|---|
| Time step size | 0.0075 s |
| Number of time steps | 120 |
| Maximum iterations per time step | 13 |

Subsequent tests revealed that varying the number of steps in time will affect the torque value, particularly at lower rpm, where one full revolution will take longer physical simulation time. Thus, one constraint of the data set of the present CFD is that periodic torque convergence may not be achieved for some operating points. Better future method would be at least one revolution of a rotor for each case, and torque would be taken from the end of each simulation to get the average torque.

## 4.8 Representative ANSYS Case at 2.1 m/s

**Table 4.4** Representative ANSYS Case documentation for V = 2.1 m/s

| Parameter | Value |
|---|---|
| Water velocity | 2.1 m/s |
| Rotor speed | 111.41 rpm |
| Angular speed | 11.67 rad/s |
| Time steps | 120 |
| Time step size | 0.0053 s (documented setting) |
| Maximum iterations per time step | 13 |
| Mass flow rate at Plane 1 | 2742.07 kg/s |
| Blade-surface torque about Z-axis | 288.16 N.m |
| Force on blade surface about Z-direction | approximately -489.24 N |
| Average velocity on blade surface | 2.9282 m/s |
| Average outlet velocity | 2.11806 m/s |
| Available hydraulic power | 6046.264 W |
| Mechanical shaft power | 3362.83 W |
| Hydraulic-to-mechanical efficiency | 55.62% |

A representative high-flow case was observed at the water velocity of V = 2.1 m/s. The calculated rotor speed for this case was 111.41 rpm, and the angular speed was 11.67 rad/s. For the transient run, 120-time steps were used, with a time step that was captured at about 0.0075 s and a maximum of 13 iterations per time step. This is a representative case to illustrate the precise procedure followed in creating the other velocity cases. Also, to ensure that the turbine completes one full revolution to verify that the values of the performance characteristics are correct [Table shown as 4.4]

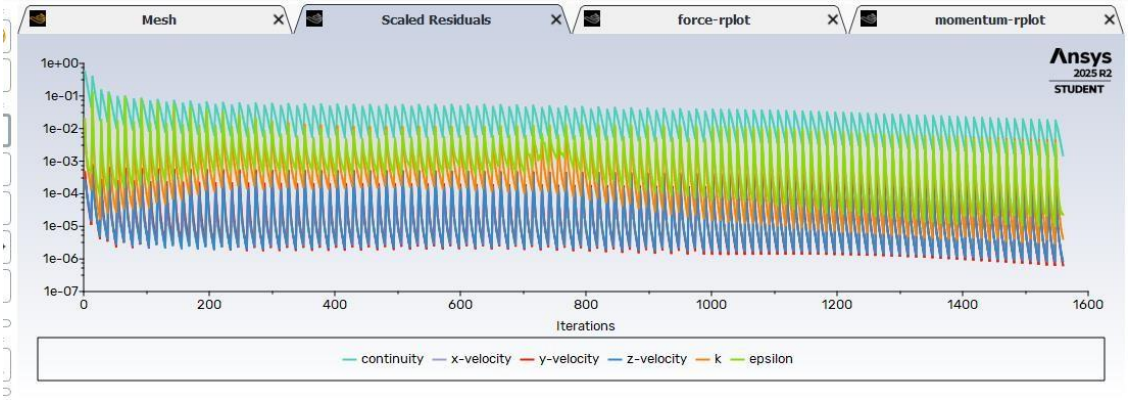



Fig. 4.10. Example residual covergence plot from ANSYS Fluent.

The behavior of the iterative solution is displayed in the residual plot. Transient sliding or rotating simulations may have some oscillations in the residuals because the rotor position and flow field are constantly changing. The key sign is that no matter how many terms you calculate, the residuals should eventually get to a stable repeating band and not diverge [Fig. shown as 4.10].

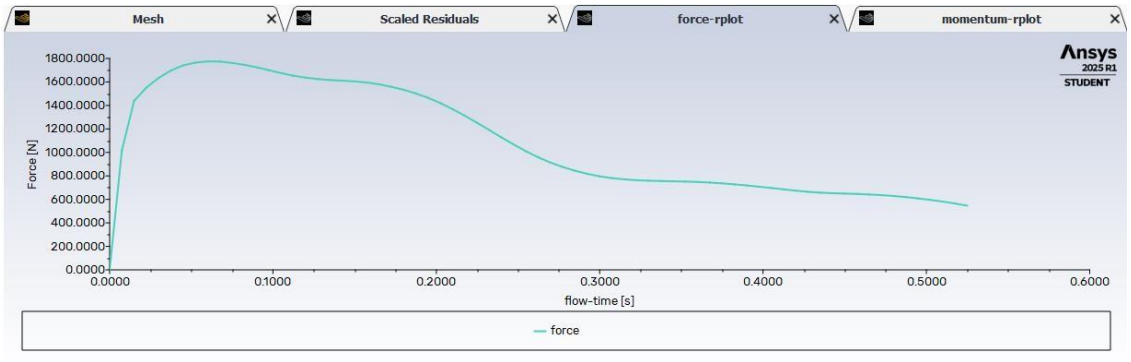



Fig. 4.11. Example force monitor plot from ANSYS Fluent.

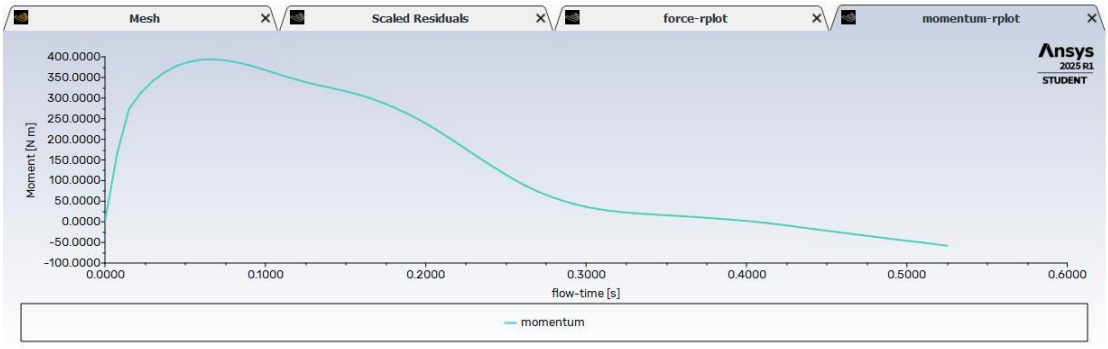



Fig. 4.12. Example moment/torque monitor plot from ANSYS Fluent.

The reason for the rise in the force and moment monitor plots at first is that the flow field is developing around the rotor. The force and moment approach to the transient start-up enters into a gentler region. Then, the final/torsion-stable torque is applied for the performance table [Fig. shown as 4.11 & 4.12].

## 4.9 Torque Extraction Method

CFD-Post was used to extract torque using the Function Calculator. The rotor was specified to be rotating about the global Z-axis, so torque was calculated about the global Z-axis.

The total turbine torque was calculated as:

$$T_{total} = T_{blade\ surface} \tag{4.1}$$

The torques on the surfaces of the stator, duct, inlet, outlet and contact-region were not considered since they are not the torque producing rotating surfaces.

## 4.10 Hydraulic performance Calculation Method

The turbine is run inside the simulation domain in ANSYS software where we are able to obtain the Torque, the Force on the propeller, the mass flow rate. With these values from the function calculator, we can use the conventional formulas to calculate the Mechanical Power the turbine produces after each complete rotation of the blades, as well as the Available Hydraulic Power in free flow water in the region of Plane.

### 4.10.1 Mechanical Shaft Power Calculation

Mechanical shaft power was calculated from:

$$P_{mech} = T\omega \tag{4.2}$$

where T is total turbine torque and omega is angular speed in rad/s.

For example, at V = 2.1 m/s:

$$T = 288.16\ N.m$$

$$\Omega = 11.67\ rad/s$$

$$P_{mech} = 288.16 \times 11.67 = 3362.83W$$

This matches the value used in the turbine operating table.

### 4.10.2 Available Hydraulic Power Calculation

The actual mass flow rate for the ANSYS table is the mass flow out of Plane 1 and not the mass flow of the big inlet-domain. This is crucial since the available power should model the flow of energy through the appropriate turbine/reference region. A different larger mass flow rate at an improper boundary can make the calculated turbine efficiency lower, and the available power higher. The table shows efficiencies of about 50-56% which are more uniform.

The formula used is: $P_{avail} = \frac{1}{2}\dot{m}V^2$ (4.3)

### 4.10.3 Turbine Efficiency Calculation

The hydraulic-to-mechanical turbine efficiency was calculated as:

$$\text{Efficiency} = \frac{Mechanical\ Powe}{Available\ Power\ in\ Plane\ 1} \times 100\% \tag{4.4}$$

This efficiency represents the fraction of available hydraulic power converted into mechanical shaft power in the CFD operating-point analysis.

## 4.11 Torque Extraction Method

The actual mass flow rate for the ANSYS table is the mass flow out of Plane 1 and NOT the mass flow of the big inlet-domain. The value has been taken from the Function

Calculator from POST-ANSYS window after running and completing the simulation of the turbine in ANSYS Fluent. The torque was taken from the region of the blade surface of the turbine only. After acquiring the Torque, the formula is applied to find the Mechanical Power produced by the turbine after completing the simulation. Torque is one of the most critical values needed to find the mechanical shaft power, the available hydraulic power and the efficiency of the turbine.

This method is the only method to fin out the total torque generated by the turbine blades. Noting that there are six blades all together, so all 6 blades contribute to the force exerted by the turbine.

## 4.12 MATLAB/SIMULINK Electrical Model

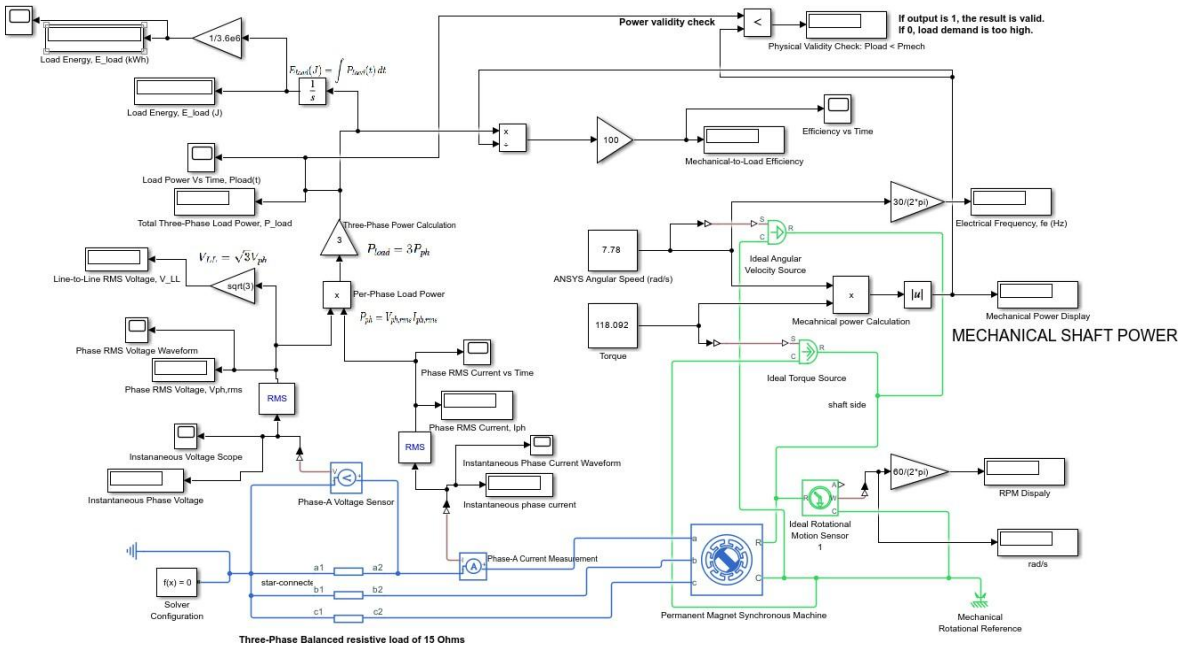



Fig. 4.13. MATLAB/Simulink model for the electrical power generation.

In figure 4.13 shows the simplified PMSM-load configuration has been used in the final MATLAB/Simulink model. The mechanical side consists of the ideal angular velocity source, ideal torque source, ideal rotational motion sensor, mechanical rotational reference and PMSM mechanical port. Mechanical inputs are the ANSYS torque and angular speed. For the electrical side, it has a PMSM three-phase terminals directly connected with a balanced 15 ohm three-phase resistive load in a star configuration.

The voltage and current in phase-A is measured by voltage and current sensors. RMS blocks calculate the RMS value for instantaneous AC waveforms. The total load power is $P_{load} = 3V_{ph,rms}\, I_{ph,rms}$ In calculating load energy, an integrator is used. Mechanical-to-load efficiency = (load power / mechanical shaft power) x 100. A physical validity check is done between load power and mechanical power, which showed impossible load possibilities.

The figure 4.14 shows how MATLAB/Simulink model was developed in MATLAB Simscape Electrical. The main components were:

- Ideal Angular Velocity Source
- Ideal Torque Source
- Ideal Rotational Motion Sensor
- Permanent Magnet Synchronous Machine (PMSM)
- DC Voltage and Current Sensors
- Voltage sensor
- Current sensor
- Gain block for Line-to-Line calculation
- Balanced three-phase resistive load of 15 Ohms
- PS-Simulink Converters
- RMS Voltage and Current Measurement Blocks
- Product Blocks for Power Calculation
- Integrator Blocks for Energy Calculation
- Display and Scope Blocks
- Electrical Reference and Mechanical Rotational Reference
- Solver Configuration Block

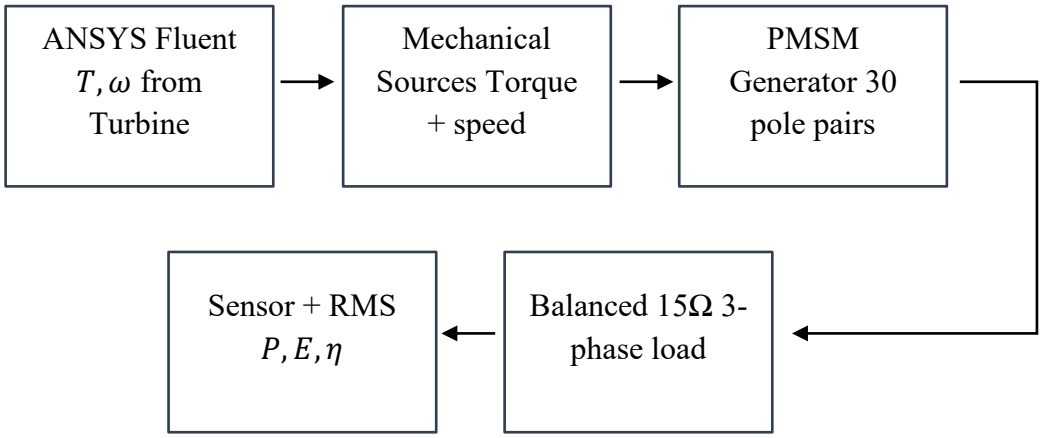



Fig. 4.14. MATLAB/Simulink electrical architecture for the PMSM turbine generator system

**Table 4.5** MATLAB/Simulink PMSM-load model parameter summary

| **Parameter** | **Value** |
|---|---|
| Electrical connection | Expanded three-phase ports |
| Winding type | Wye-wound |
| Number of pole pairs | 30 |
| Permanent magnet flux linkage | 0.218 Wb |
| Stator d-axis inductance, Ld | 0.00019 H |
| Stator q-axis inductance, Lq | 0.00025 H |
| Stator resistance per phase, Rs | 0.3 ohm |
| Rotor inertia | 0 or 0.01 kg.$m^2$ depending on tested model.<br>Finally, simplified source-driven model uses ideal imposed speed |
| Load resistance | 15 ohm per phase, star-connected |
| Simulation stop time | 20 s |
| Solver | Variable-step ode23t, maximum step size $1e^{-4}$ s |
| Simscape local solver | Trapezoidal rule, sample time $1e^{-4}$ s |

The Simulink model was created with a stop time of 0.2 s. The ode solver ode23t was used with maximum step size of 1e-4 which is relative to the tolerance of 0.0001. The time-based equation formulation block in the Simscape Solver Configuration block was used, also the fixed-cost runtime consistency iterations were used [Table shown as 4.5]

## 4.13 Data Processing Workflow

- From TSR = 3, calculate angular speed and rpm for each of the tidal velocities.
- Start ANSYS Fluent and use the same inlet velocity and rotor rpm.
- Extract mass flow rate at Plane 1 and z-axis torque on the blade surface.
- Compute the available hydraulic power as $P_{avail} = \frac{1}{2} \dot{m} V^2$.
- Use $P_{mech} = T\omega$ to determine mechanical shaft power.
- Apply torque and angular speed to the model of PMSM generator in MATLAB/Simulink

# CHAPTER 5
# INVESTIGATIONS, RESULTS AND DISCUSSION

## 5.1 Overview of Result Structure

The results are presented in the following sections: hydraulic-mechanical turbine performance, simplified PMSM electrical output, selected operating point comparison, load-resistance investigation, waveform interpretation and long-term energy estimation. The final dataset contains 21 velocity cases ranging from 0.4 m/s to 2.4 m/s. The three points identified with markers are low flow of 0.7 m/s, medium flow of 1.4 m/s and high flow of 2.1 m/s.

## 5.2 Turbine Operating Conditions and Hydraulic-Mechanical Performance

We fixed a TSR value of 3 for all the observations from the table below. TSR 3 is ideal for our low-speed direct drive turbines in shallow waters. We set different water velocities ranging from 0.4m/s to 2.4m/s. We calculated the angular Rotor speed using the formulas and selected each speed for the corresponding water velocities. We were able to find the values for the Torque and the Mass flow rate for each individual observation. We then calculated the Mechanical shaft power produced by the turbine under water, also calculated the Available Hydraulic power in Plane of the turbine and lastly calculated the Turbine Efficiency. As can be seen from the table, as the water current increases, the Rotor speed of the turbine increases the Torque produced by the turbine blade increase, the Mass flow rate increases, the Mechanical Shaft Power Increases and the Available hydraulic power increases as well.

**Table 5.1** Turbine operating conditions and hydraulic-mechanical performance.

| Experiment No. | TSR | Tidal Velocity (m/s) | Rotor Speed (RPM) | Angular speed (rad/s) | Torque (N.m) | Mass Flow Rate, (kg/s) | Mechanical Shaft Power, Pmech (W) | Available Hydraulic Power, Pavail | Turbine Efficiency (%) |
|---|---|---|---|---|---|---|---|---|---|
| 1 | 3 | 0.4 | 21.22 | 2.22 | 9.9681 | 528.309 | 22.13 | 42.264 | 52.35 |
| 2 | 3 | 0.5 | 26.53 | 2.78 | 15.872 | 658.432 | 44.13 | 82.304 | 53.61 |
| 3 | 3 | 0.6 | 31.83 | 3.33 | 22.197 | 791.972 | 73.92 | 142.554 | 43.28 |
| 4 | 3 | 0.7 | 37.14 | 3.89 | 31.1886 | 920.37 | 121.32 | 226.49 | 53.80 |
| 5 | 3 | 0.8 | 42.44 | 4.44 | 40.065 | 1053.08 | 177.89 | 336.985 | 52.79 |
| 6 | 3 | 0.9 | 47.75 | 5.00 | 50.822 | 1184.01 | 254.11 | 479.524 | 52.99 |
| 7 | 3 | 1.0 | 53.05 | 5.56 | 65.010 | 1309.67 | 361.46 | 654.835 | 55.20 |
| 8 | 3 | 1.1 | 58.36 | 6.11 | 80.1761 | 1437.05 | 489.875 | 869.415 | 56.35 |
| 9 | 3 | 1.2 | 63.66 | 6.67 | 93.223 | 1571.03 | 621.80 | 1131.141 | 54.97 |
| 10 | 3 | 1.3 | 68.97 | 7.22 | 102.687 | 1714.06 | 741.400 | 1448.381 | 51.19 |
| 11 | 3 | 1.4 | 74.27 | 7.78 | 118.092 | 1846.7 | 918.76 | 1809.766 | 50.76 |
| 12 | 3 | 1.5 | 79.60 | 8.33 | 137.803 | 1975.43 | 1147.90 | 2222.358 | 51.65 |
| 13 | 3 | 1.6 | 84.88 | 8.89 | 158.625 | 2103.40 | 1410.18 | 2692.352 | 52.37 |
| 14 | 3 | 1.7 | 90.19 | 9.44 | 176.826 | 2237.43 | 1669.24 | 3233.086 | 51.63 |
| 15 | 3 | 1.8 | 95.49 | 10.00 | 198.966 | 2367.58 | 1989.66 | 3835.479 | 51.88 |
| 16 | 3 | 1.9 | 100.80 | 10.56 | 226.123 | 2493.79 | 2387.86 | 4501.291 | 53.05 |
| 17 | 3 | 2.0 | 106.10 | 11.11 | 263.018 | 2612.07 | 2922.13 | 5224.140 | 55.94 |
| 18 | 3 | 2.1 | 111.41 | 11.67 | 288.16 | 2742.07 | 3362.83 | 6046.264 | 55.62 |
| 19 | 3 | 2.2 | 116.71 | 12.22 | 314.5 | 2874.16 | 3843.19 | 6955.467 | 55.25 |
| 20 | 3 | 2.3 | 122.02 | 12.78 | 345.93 | 3001.78 | 4420.99 | 7939.708 | 55.68 |
| 21 | 3 | 2.4 | 127.32 | 13.33 | 372.133 | 3136.65 | 4960.53 | 9033.520 | 54.91 |

Table 5.1 shows the hydraulic-mechanical performance of proposed open center tidal turbine for different tidal current velocities between 0.4 m/s to 2.4 m/s. The tip-speed ratio always remained the same and the rotor speed and the angular speed for each velocity were calculated. The ANSYS Fluent simulation result provided the torque and mass flow rate, which were then used to calculate mechanical shaft power, available hydraulic power and turbine efficiency. It can be seen from the table that as the tidal velocity increases, there is a noticeable increase in rotor speed, torque, mass flow rate and shaft power. The mechanical shaft power was raised from 22.13W at 0.4 m/s to 4960.53W at 2.4 m/s. To this end we identified three representative operating points: at 0.7 m/s, 1.4 m/s and 2.1 m/s water velocity. The turbine generated 121.32W at 0.7 m/s, 918.76W.

At 1.4 m/s and 3362.83W at 2.1 m/s. The calculated turbine efficiency was also found to be mainly between 50 to 56 percent, which indicated that the turbines had a consisted hydraulic performance within the operating range. So, the table lists the key hydraulic data inputs needed for the subsequent PMSM generator and electrical load analysis.

### 5.2.1 Mechanical Shaft Power vs Tidal Velocity

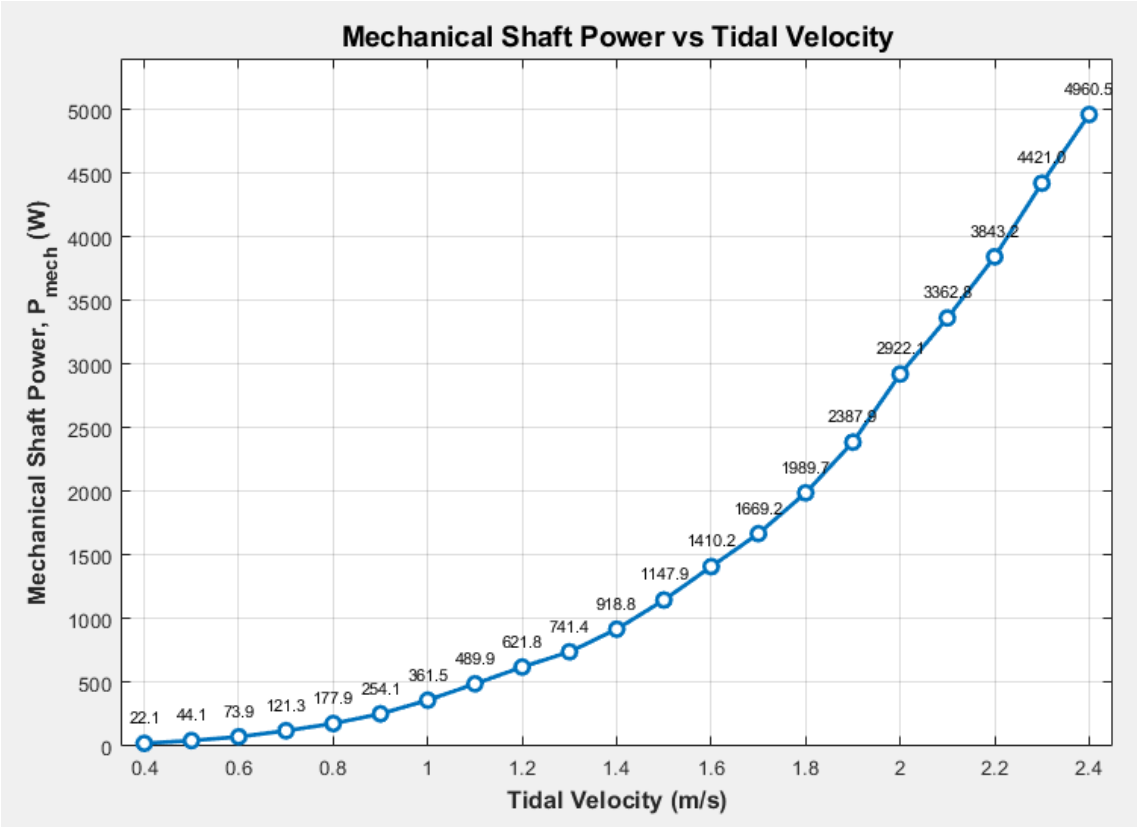



Fig. 5.1. Mechanical shaft power output of the turbine at different tidal current velocities.

Figure 5.1 shows the variation of mechanical shaft power with tidal current velocity. The mechanical shaft power was calculated from the ANSYS Fluent torque result and the corresponding rotor angular speed using Mechanical Shaft Power = $T \times \omega$. The graph shows an increasing trend as we can see, where the shaft power rises from about 22.1W at 0.4 m/s to 4960.5W at 2.4 m/s. This increase is not linear, because the available kinetic energy in flowing water increases strongly with velocity. As the tidal velocity increases, both the torque produced on the turbine rotor and the angular speed increase, resulting in a rapid rise in mechanical shaft power. The result confirms that higher tidal current velocities provide significantly greater mechanical energy to the turbine shaft, which can then be supplied to the PMSM generator for electrical power conversion.

### 5.2.2 Mechanical Shaft Power and Available Hydraulic Power vs Tidal Velocity

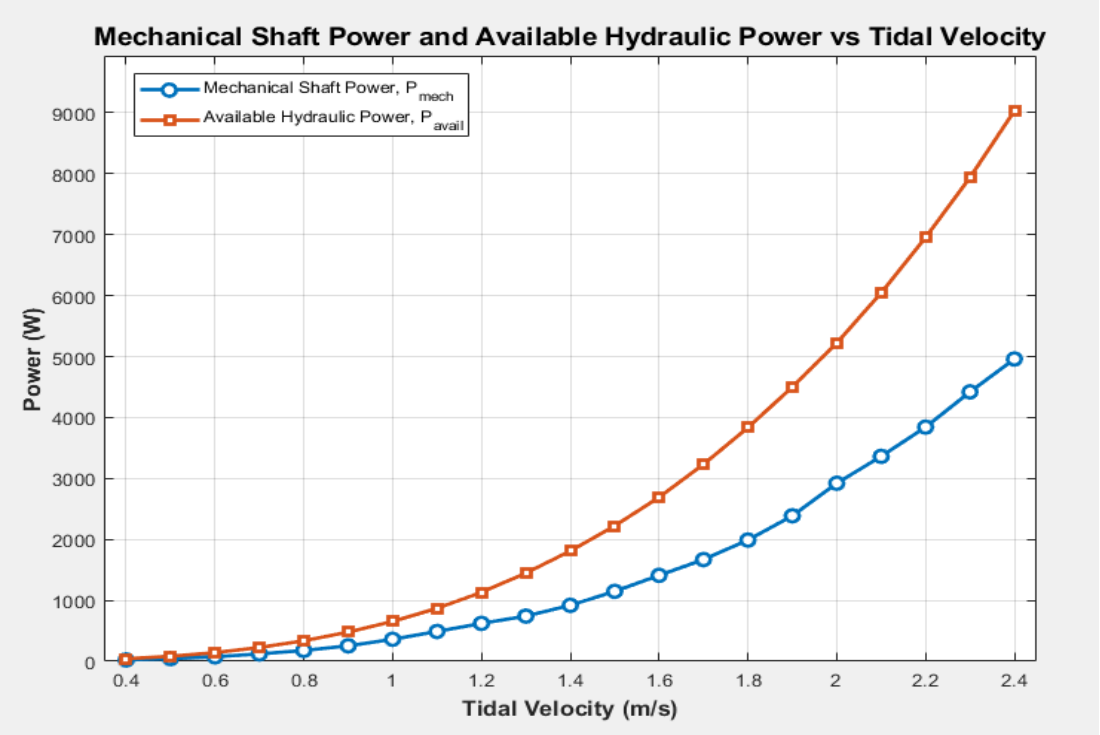



Fig. 5.2. Comparison between available hydraulic power and extracted mechanical shaft power at different tidal velocity.

The comparative available hydraulic power of the tidal flow and the mechanical shaft power output of the turbine is shown in figure 5.2 Both quantities increase as the velocity of the tide increases, but the hydraulic power available is greater than the mechanical shaft power at all operating points. This is normal since it is impossible to obtain all the K.E. of the flowing water in useful shaft power from the turbine. Flow separation, wake formation, turbulence, blade drag, and other hydrodynamic losses cause a loss of part of the available energy. Available hydraulic power at 2.4 m/s is around 9033.52W and the extracted mechanical shaft power is around 4960.53W. The difference between the two curves thus indicates the hydraulic energy lost in the conversion. This comparison can be used to verify that the turbine output is physically sound as the shaft power extracted is less than the hydraulic power available over the velocity range tested.

### 5.2.3 Turbine Efficiency vs Tidal Velocity

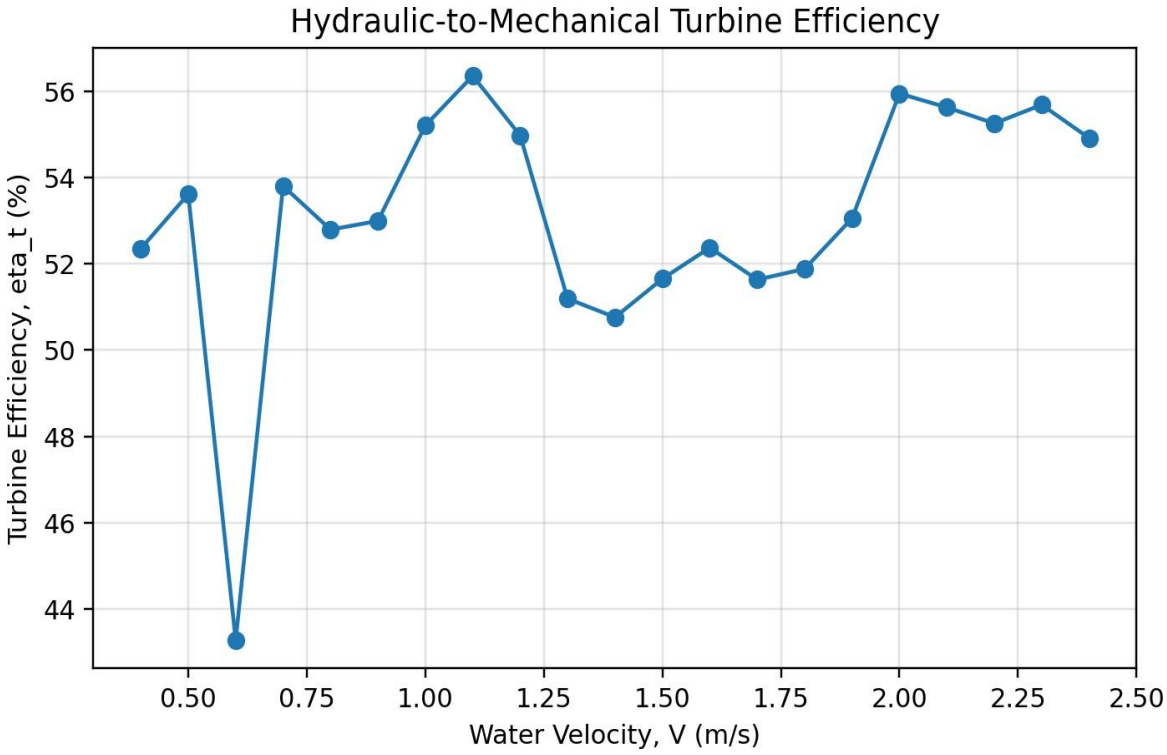



Fig. 5.3. Variation of hydraulic-to-mechanical turbine efficiency with tidal current velocity for the proposed open-center tidal turbine.

The hydraulic-to-mechanical efficiency of a turbine at various tidal current velocities is shown in figure 5.3. The efficiency was determined by dividing the mechanical shaft power extracted by the rotor by the hydraulic power available in the flow. The overall performance is relatively consistent within the tested velocity range, as indicated by the result which is mostly within the stable range of around 50–56%. A lower efficiency value exists around 0.6 m/s which may result from lower torque generation, lower flow stability or lower numerical sensitivity at lower speed operation. From this point onward efficiency is more stable with higher efficiencies at multiple operating points, particularly at 1.1 m/s and greater than 2.0 m/s. To conclude, the graph shows that the proposed open-center tidal turbine is able to convert a steady fraction of the available tidal hydraulic power into useful mechanical shaft power throughout the tidal velocity range in this study.

## 5.3 Tidal Cycle Representation and Turbine Operating Variation

This section is used to denote the tidal cycle, and the impact of it on the turbine operation. Only a single lunar tidal day, a rise and fall of water level, creates two high and two low tides. But the turbine output is primarily dependent on the tidal current velocity and not just tide's height. The current velocity is slow during slack-water periods between high and low tide, and the turbine output is low. This is because the tidal velocity is highest from high tide to low tide and the maximum output of the turbine is available at this period. The turbine is bidirectional, and both the ebb and flood tide currents are deemed to be useful for generating power.

### 5.3.1 Tide Height Variation Over One Lunar Tidal Day

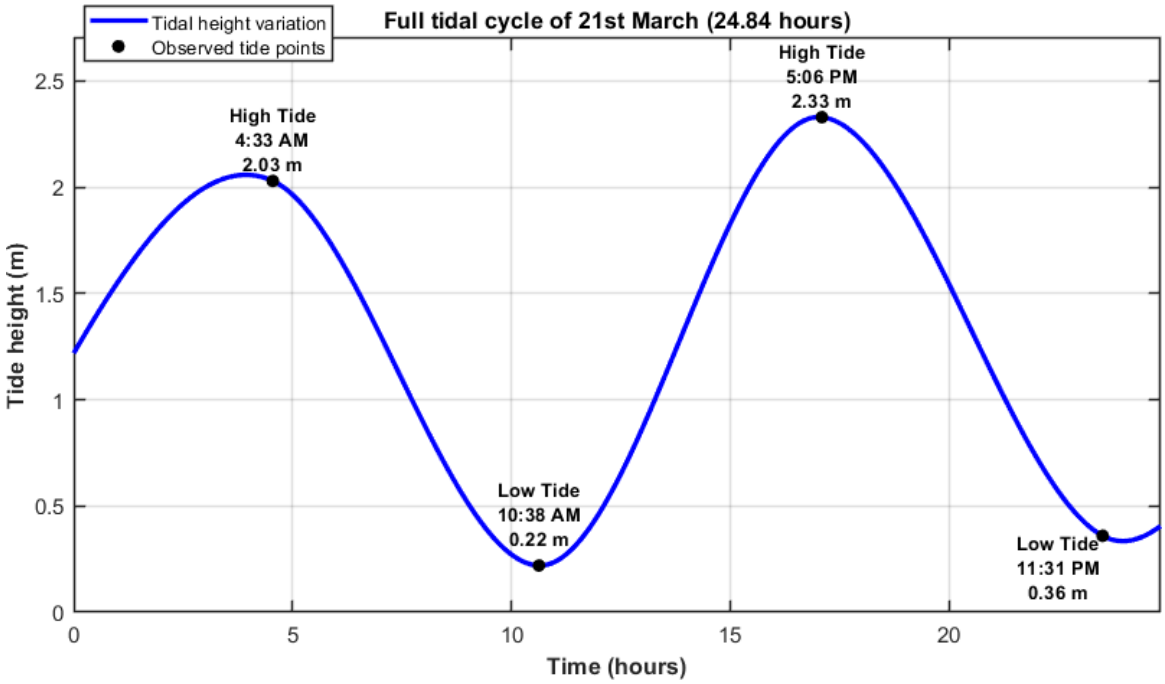



Fig. 5.4. Tidal height variation over one lunar tidal day showing two high tide and two low tide.

The X axis in figure 5.4 is the change in tidal height throughout a full lunar tidal day (24.84 hours). The level of the tide is periodic as we can see. Therefore, this actually shows that there will be two high and two low tides during a complete tidal period for full lunar tidal day. The first high tide occurs at about 4.33 am at a height of 2.03 m and the second high tide is at a height of 2.33 m at 5.06 pm shown in the graph. Additionally, the data for

the two low tide observations are at 10:38 am and 11:31 pm and the corresponding low tide heights are 0.22 m and 0.36 m, respectively. The graph shows the characteristics of semi diurnal tides, two high and low tides in the course of a lunar tide day. Note that maximum power of the turbine doesn't occur at low or high tide. Extremes of water-levels are a coincidence of high and low tides with the change of the direction of water. The strength of the Tidal Current is low – near imperceptible at this time. The points are when slack tide occurring. However, the tide height graph can be used as a guide to the tide cycle and the amount of power available to the tide for generation by these turbines is largely dependent on the velocity of the tide rather than the tide height.

The result is important it shows the turbine should be considered to operate in both rising and falling tide. Water level is periodically varying and so is the flow as well during the cycle. A bidirectional turbine is therefore suitable, which can generate energy even during flood and ebb tide without the need to switch the direction of the turbine.

### 5.3.2 Tidal Current Velocity Variation Over One Lunar Tidal Day

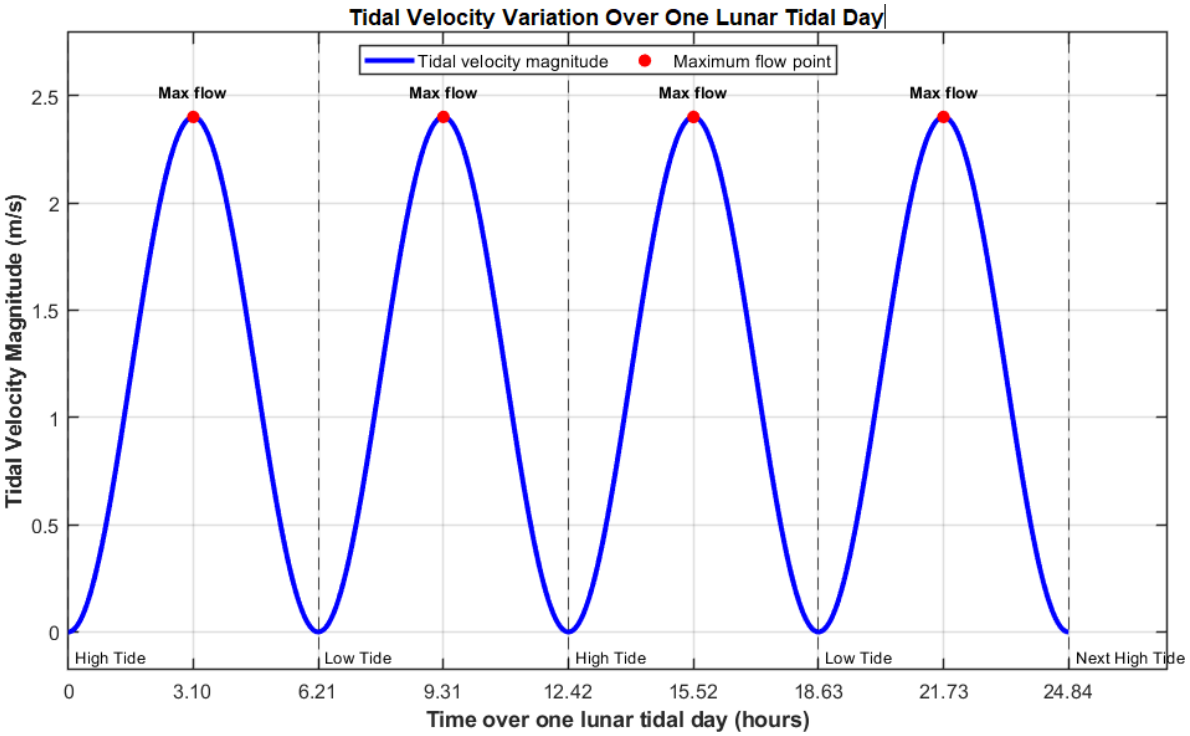



Fig. 5.5. Tidal current velocity meginude over one lunar tidal day showing maximum flow and slack tide points.

In Figure 5.5, the velocity of the above-mentioned tides is shown as a tidal current magnitude in figure above (over 1 lunar tidal day). There are four different maximum velocities, about 2.4 m/s. At times of maximal flow (between high and low tide) these high velocities occur. The velocity reaches a minimum at slack tide points, around 0 h, 6.21 h, 12.42 h, 18.63 h and 24.84 h. The graph shows the magnitude of the velocity and flood and ebb are both positive. This is appropriate for the proposed turbine as the turbine is considered to be bidirectional. These max flow values are at approximately 3.10h, 9.31h, 15.52h and 21.73h, which is where the turbine is expected to produce the greatest amount of power. The same velocity profile was also used for the calculation of daily energy production. Twenty-one velocities to power simulated results were used and power was interpolated for the entire tide day. Next, the energy output was determined by integration of the power over time.

### 5.3.3 Relationship between Tide Height and Water Current Velocity

In The tide height and current velocity graphs will coincide, though not necessarily at the same point in the graph. The vertical distance from the crest to the trough of the tide wave is the vertical period of the rise and fall of the water, and the horizontal distance it moves to turn the turbine is the velocity of the current.

The water level is at its maximum or minimum at high and low tide, but the flow momentarily stops and then reverses direction. So the current at these points tends to be small. The greatest current occurs between high and low tide when the current is greatest. This is because the maximum flow will produce the maximum power generation from turbines, and slack tide will produce minimal power generation.

This is beneficial for the use of a bidirectional tidal turbine as the turbine can provide power for both flood and ebb tides.

### 5.3.4 Turbine RPM Variation Over One Lunar Tidal Day

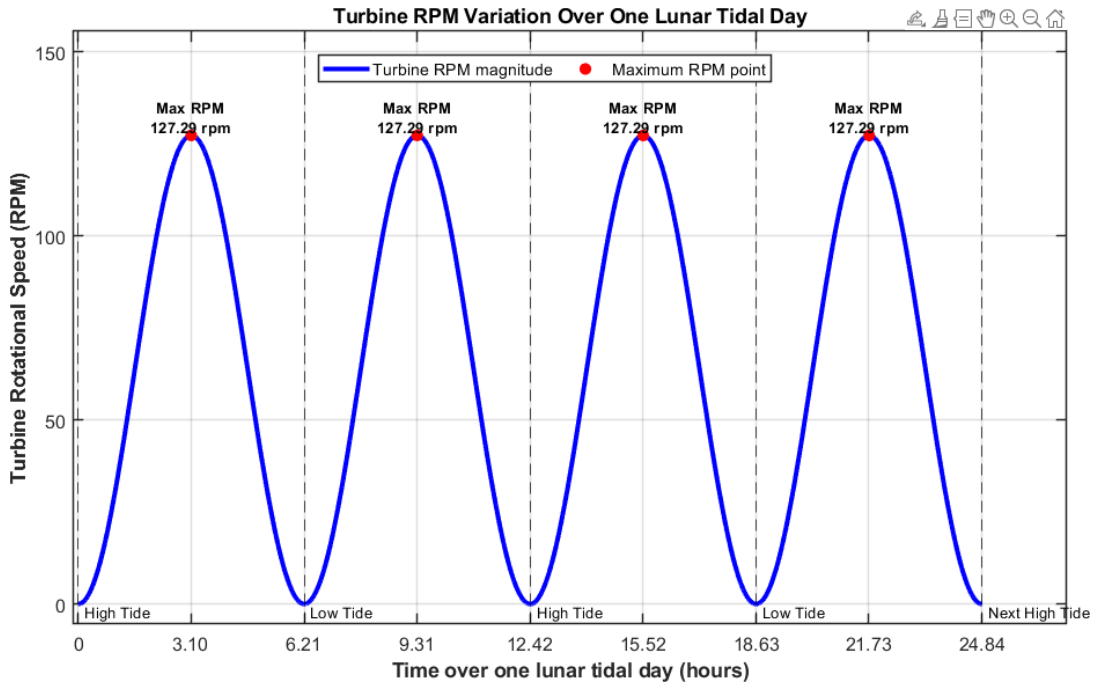



Fig. 5.6. Turbine rotational speed variation over one lunar tidal day based on tidal current velocity profile.

Figure 5.6 is the change in turbine RPM for a lunar tidal day (LTD). The RPM curve is the same as the tidal current velocity graph as the turbine speed was determined with a constant tip speed ratio, TSR = 3. The faster the tidal velocity, the more RPM's the turbine. At slack tide, velocity is also zero and the RPM of the turbine will be very near to zero.

The tidal velocity has its maximum value of 2.4 m/s the maximum speed of the turbine is around 127.29 rpm. This maximum RPM occurs at approximately 3.10 h, 9.31 h, 15.52 h, and 21.73 h.

The turbine speed was calculated using:

$$TSR = \frac{\omega R}{V}$$

Therefore,

$$\omega = \frac{TSR \times V}{R}$$

And

$$N = \frac{60\ \omega}{2\ \pi}$$

For Maximum velocity conditions: V = 2.4 m/s, TSR = 3 and R = 0.54 m

$$\omega = \frac{3\ \times 2.4}{0.54}\ = 13.33\ rad/s$$

$$N = \frac{13.33\ \times 60}{2\ \pi}\ = 127.3\ rpm$$

This matched the maximum RPM show in the graph.

## 5.4 Electrical Output Characteristics of the PMSM Generator

The final electrical output results obtained from MATLAB/Simulink are given in Table 5.4. In this model, the PMSM generator is directly coupled to a resistive three-phase load with total resistance of 15Ω per phase and balanced. From the turbines ANSYS Fluent simulation, the torque and angular velocity were taken as mechanical inputs to the PMSM generator. The results indicate that as the velocity of the tidal current increases, the phase RMS voltage, phase RMS current, three-phase load power and load energy also increase, and the electrical frequency also increases in general. The load of power increases from 6.451W at 0.4 meters per second to 743.1W at 2.4 m/s. The electrical frequency was calculated using the formula

$$f_e = \frac{p\omega_m}{2\pi}$$

where $p$ =30 pole pairs. The electrical frequency at the representative operating point of 1.9 m/s is ~ 50.42 Hz. This indicates that the high pole PMSM is useful to generate useful electrical frequency under low turbine rotational speed. But the output wouldn't be grid ready because voltage regulation, rectifier and inverter control and protection circuits are still necessary, for actual use in the home or connected to the grid.

**Table 5.2** Simulated Electrical Output Characteristics of the PMSM Generator Connected to a Balanced 15Ω Three-Phase Resistive Load.

| Tidal Current Velocity (m/s) | Angular speed, ω (rad/s) | Torque, T (N·m) | Mechanical Shaft Power (W) | Phase RMS Voltage (V) | Phase RMS Current (A) | Three-Phase Load Power (W) | Mechanical-to-load Efficiency (%) | Three-Phase Load Energy (J) | Three-Phase Load Energy (kWh) | Electrical Frequency, fe (Hz) |
|---|---|---|---|---|---|---|---|---|---|---|
| 0.4 | 2.22 | 9.9681 | 22.13 | 5.679 | 0.3786 | 6.451 | 29.15 | 1268 | 3.5230e-4 | 10.6 |
| 0.5 | 2.78 | 15.872 | 44.13 | 10.39 | 0.6925 | 21.58 | 48.91 | 1498 | 4.1619e-4 | 13.27 |
| 0.6 | 3.33 | 22.197 | 73.92 | 13.34 | 0.8896 | 35.62 | 48.18 | 1774 | 4.9286e-4 | 15.9 |
| 0.7 | 3.89 | 31.1886 | 121.32 | 18.01 | 1.201 | 64.86 | 53.46 | 2106 | 5.8510e-4 | 18.57 |
| 0.8 | 4.44 | 40.065 | 177.89 | 20.48 | 1.365 | 83.89 | 47.16 | 2483.2 | 6.8962e-4 | 21.2 |
| 0.9 | 5.00 | 50.822 | 254.11 | 23.06 | 1.538 | 106.4 | 41.87 | 2916.83 | 8.1023e-4 | 23.87 |
| 1.0 | 5.56 | 65.010 | 361.46 | 24.47 | 1.631 | 119.8 | 33.13 | 3402.58 | 9.4026-4 | 26.55 |
| 1.1 | 6.11 | 80.1761 | 489.875 | 25.74 | 1.716 | 132.5 | 27.41 | 3929.82 | 1.0916e-3 | 29.17 |
| 1.2 | 6.67 | 93.223 | 621.80 | 27.81 | 1.854 | 154.7 | 24.87 | 4517.75 | 1.2549e-3 | 31.85 |
| 1.3 | 7.22 | 102.687 | 741.400 | 29.89 | 1.993 | 178.7 | 24.1 | 5145.3 | 1.4292e-3 | 34.47 |
| 1.4 | 7.78 | 118.092 | 918.76 | 34.34 | 2.289 | 235.8 | 25.67 | 5835.2 | 1.6209e-3 | 37.15 |
| 1.5 | 8.33 | 137.803 | 1147.90 | 37.11 | 2.474 | 275.4 | 23.99 | 6562.99 | 1.8231e-3 | 37.15 |
| 1.6 | 8.89 | 158.625 | 1410.18 | 41.64 | 2.776 | 346.8 | 24.59 | 7355 | 2.0431e-3 | 42.45 |
| 1.7 | 9.44 | 176.826 | 1669.24 | 43.88 | 2.926 | 385.2 | 23.07 | 8183.03 | 2.2731e-3 | 45.07 |
| 1.8 | 10.00 | 198.966 | 1989.66 | 46.3 | 3.086 | 428.7 | 21.55 | 9077 | 2.5214e-3 | 47.75 |
| 1.9 | 10.56 | 226.123 | 2387.86 | 47.68 | 3.179 | 454.7 | 19.04 | 10022.88 | 2.7841e-3 | 50.42 |
| 2.0 | 11.11 | 263.018 | 2922.13 | 49 | 3.267 | 480.3 | 16.44 | 11001.87 | 3.0561e-3 | 53.05 |
| 2.1 | 11.67 | 288.16 | 3362.83 | 51.42 | 3.428 | 528.7 | 15.72 | 12049.76 | 3.3472e-3 | 55.72 |
| 2.2 | 12.22 | 314.5 | 3843.19 | 53.62 | 3.574 | 575 | 14.96 | 13129.02 | 3.647e-3 | 58.36 |
| 2.3 | 12.78 | 345.93 | 4420.99 | 58.21 | 3.881 | 677.7 | 15.33 | 14278.95 | 3.9663-3 | 61.02 |
| 2.4 | 13.33 | 372.133 | 4960.53 | 60.95 | 4.064 | 743.1 | 14.98 | 15458.2 | 4.2940e-3 | 63.65 |

Table 5.2 summarizes the simulated electrical output characteristics of the PMSM generator connected to the balanced 15 Ω three-phase resistive load. As the tidal current velocity increases from 0.4 m/s to 2.4 m/s, the generator receives higher mechanical shaft power from the turbine, resulting in higher electrical output. The phase RMS voltage increases from 5.679 V to 60.95 V, while the phase RMS current increases from 0.3786 A to 4.064 A. Over the same velocity range, the three-phase load power increases from 6.451 W to 743.1 W. The electrical frequency also rises from 10.6 Hz to 63.65 Hz because it is directly related to the mechanical speed of the generator. The highlighted operating points at 0.7 m/s, 1.4 m/s and 2.1 m/s represent low, medium and high flow conditions selected for further comparison. Overall, the table confirms that the PMSM generator output follows the turbine operating condition and increases as the tidal current velocity becomes higher.

### 5.4.1 Three-Phase Load Power vs Water Velocity

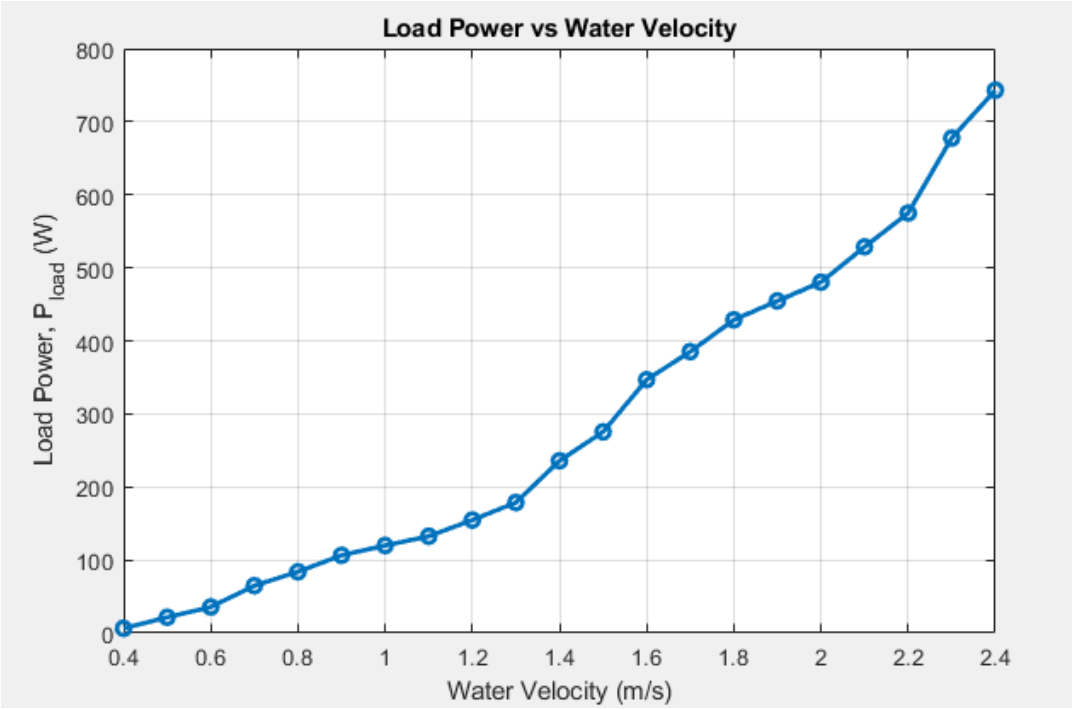



Fig. 5.7. Three-phase load power vs water velocity for the PMSM Generator system.

Figure 5.7 shows the variation in three-phase load power with the tidal water velocity for PMSM generator having a balanced three-phase resistive load. The speed of the water is gradually raised from 0.4 to 2.4 m/s while load power is continuously raised. This trend is because the mechanical shaft power to PMSM generator is higher for higher tidal velocity which leads to higher torque and angular velocity of the turbine. Thus, the voltage and current of the phase created are also increased, and the power of the three-phase load delivered is also increased. The rise is not linear, which indicates that there is a dependence on both turbine speed and generator characteristics and the match between the two.

### 5.4.2 Load Energy (J) vs Water Velocity

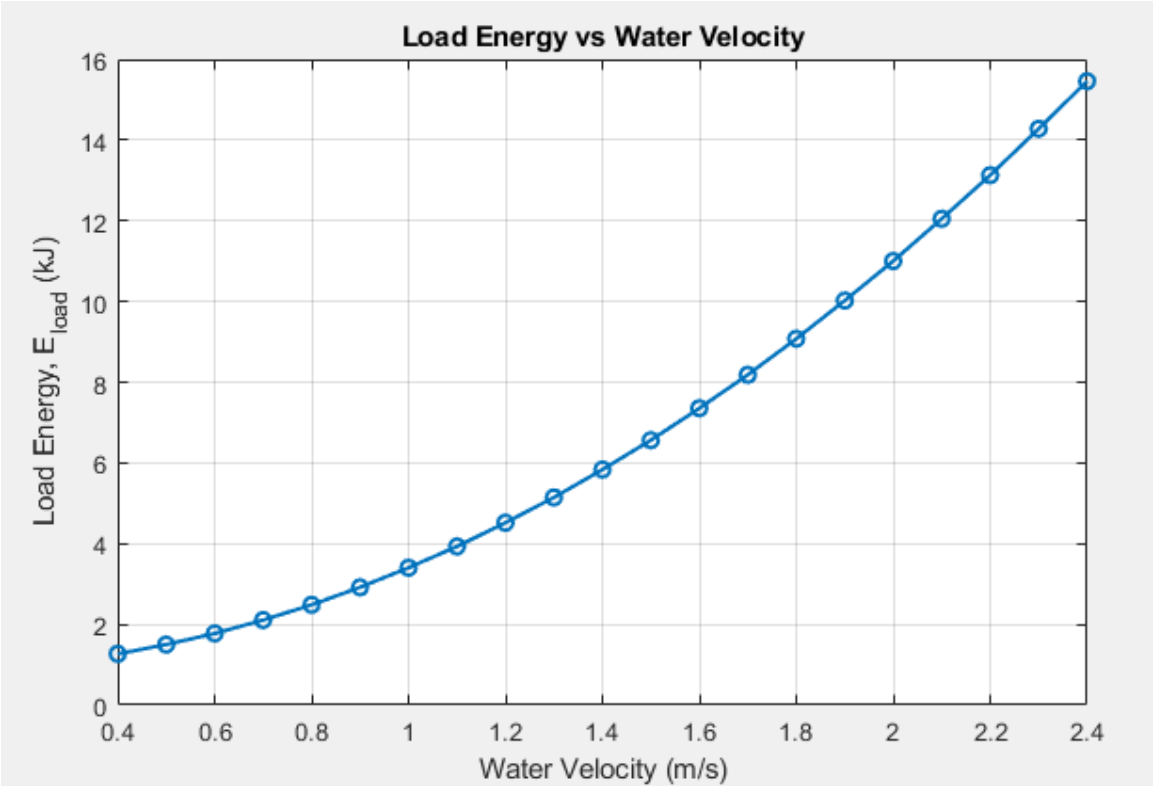



Fig. 5.8. Three-phase load energy in kilojoules vs water velocity for the PMSM generator system.

The load energy output (kJ) is shown as a function of water velocity (m/s) in in figure 5.8. The load of energy will increase as the tidal current speed increases. The increase in tidal current speed will cause the torque of the turbine to increase, the generator speed, and the electrical power generated by the generator will also increase. The more rapid the velocity of water the more electrical energy is produced and sent to the load, and the more load energy that is being accumulated. As the energy is derived by integrating the load power, it has a similar behavior as the load power curve, increasing as the load power curve increases. The energy goes up from about 1.27kJ/0.4m/s to about 15.46kJ/2.4m/s. This result indicates that the greater the turbulent tides the greater the useful energy that can be transferred to the electrical load connected to the system.

### 5.4.3 Load Energy (kWh) vs Water Velocity

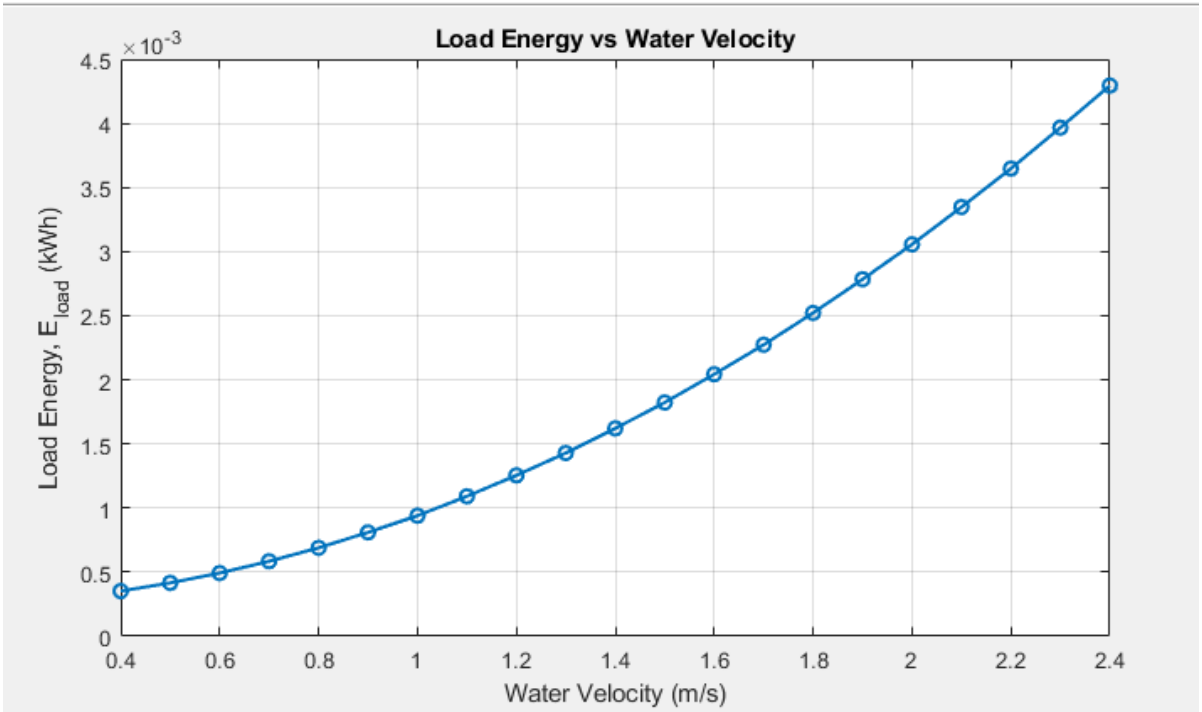



Fig. 5.9. Three-phase load energy in kilowatt-hours vs water velocity for the PMSM generator system.

The load energy (kWh) change with water velocity is shown in Figure 5.9. As with the kilojoule graph, it shows the same energy trend but is expressed in kWh to facilitate the interpretation of the energy in a practical context. The load of energy generated is from $3.523 \times 10^{-4}$ kWh at 0.4 m/s to $4.294 \times 10^{-3}$ kWh at 2.4 m/s for the simulation interval respectively. They appear to be low for this one simulation time period but may be quite large if repeated over the tides or for arrays of turbines. The higher the velocity, the more power a water will generate, which will in turn result in an increase in load energy accumulation. The speed of the water is greatest, and the electric power generated by the turbine-generator system is greatest at the highest speed of the water. Therefore, this graph can be useful to estimate the power output on daily, monthly and yearly basis from the simulated ones.

### 5.4.4 Phase RMS Voltage vs Water Velocity

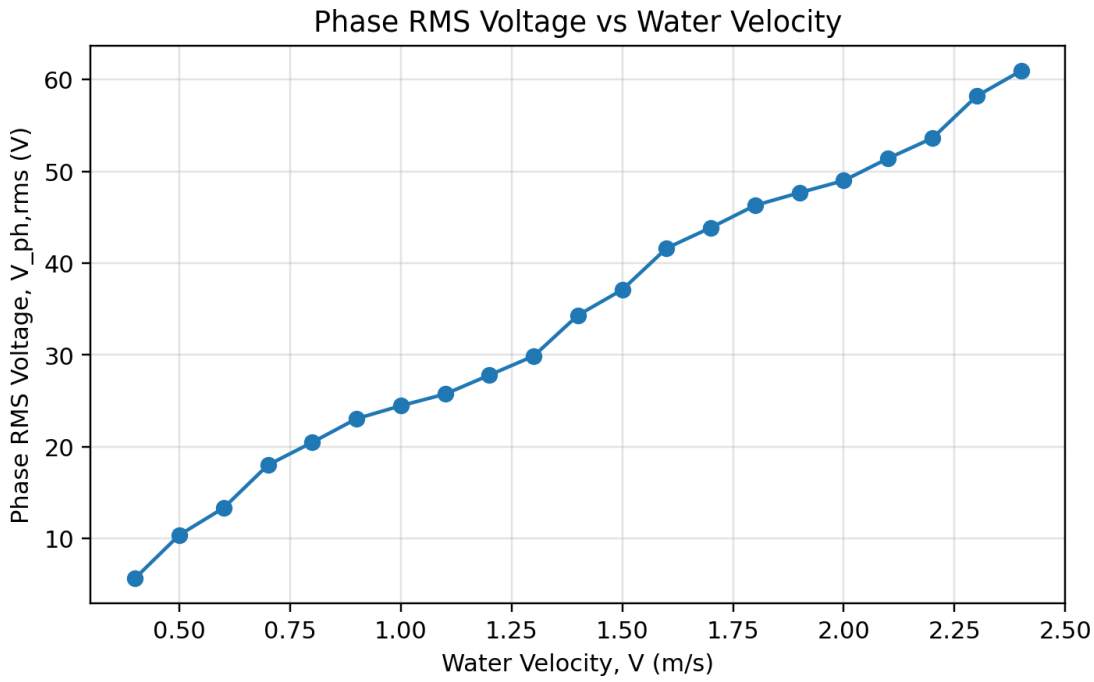



Fig. 5.10. Phase RMS voltage vs water velocity for the PMSM generator connected to a balanced 15Ω load.

The phase RMS voltage is shown as a function of water velocity in figure 5.10. The phase voltage increases almost continuously as the tidal velocity increases. This is because the PMSM generator's output voltage is directly proportional to the speed of the rotor. The higher the velocity of water, the faster the turbine will spin, and the resulting generator electrical frequency and voltage induced will increase. The RMS voltage grows from approximately 5.68V during the speed of m/s up to 60.95V at the speed of 2.4 m/s. This can be used as an indicator of the generator producing more AC voltage if the tidal flow is under a greater force. The higher the generator speed is, the higher the back EMF is generated and the higher the phase voltage at the load terminals. Hence, it can be seen from the trend of the PMSM output voltage with respect to the applied voltage that the speed at which the turbine is operating has a high influence on the voltage of the PMSM.

### 5.4.5 Phase RMS Current vs Water Velocity

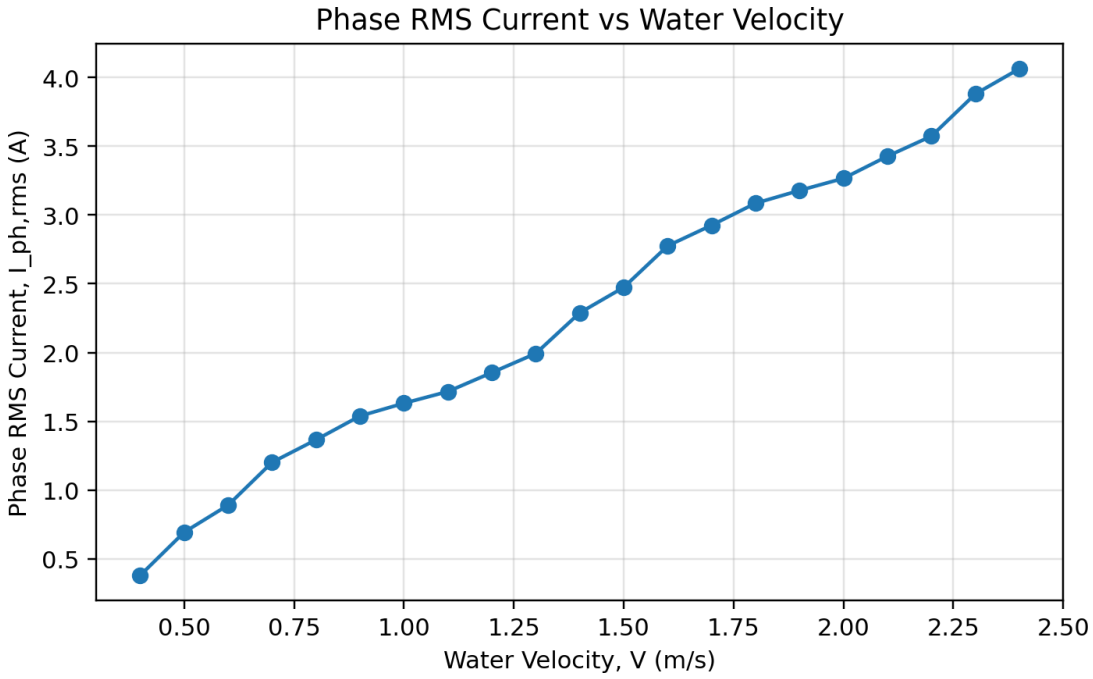



Fig. 5.11. Phase RMS current vs water velocity for the PMSM generator connected to a balanced 15Ω load.

The phase RMS current delivered to the balanced three-phase resistive load versus water velocity is shown in figure 5.11. When the velocity of the water increases the current will increase as the voltage generated will increase, but the load resistance will be constant at 15Ω per phase. When the velocity is lowered, the generator will generate less voltage which will lead to less load current. The magnitude of the voltage and current generated by the PMSM will increase with the increase in speed of the turbine. The RMS current rises from approximately 0.379 A at a speed of 0.4 m/s to approximately 4.064 A at a speed of 2.4 m/s. The load current is determined by Ohm's law, and a higher phase voltage leads to a higher load current for a balanced resistive load. The growing current trend has a direct impact on the increase in three-phase load power with increase in tidal velocity. Hence, as the flow of the tide increases, both RMS voltage and RMS current increase.

### 5.4.6 Mechanical to Load Efficiency

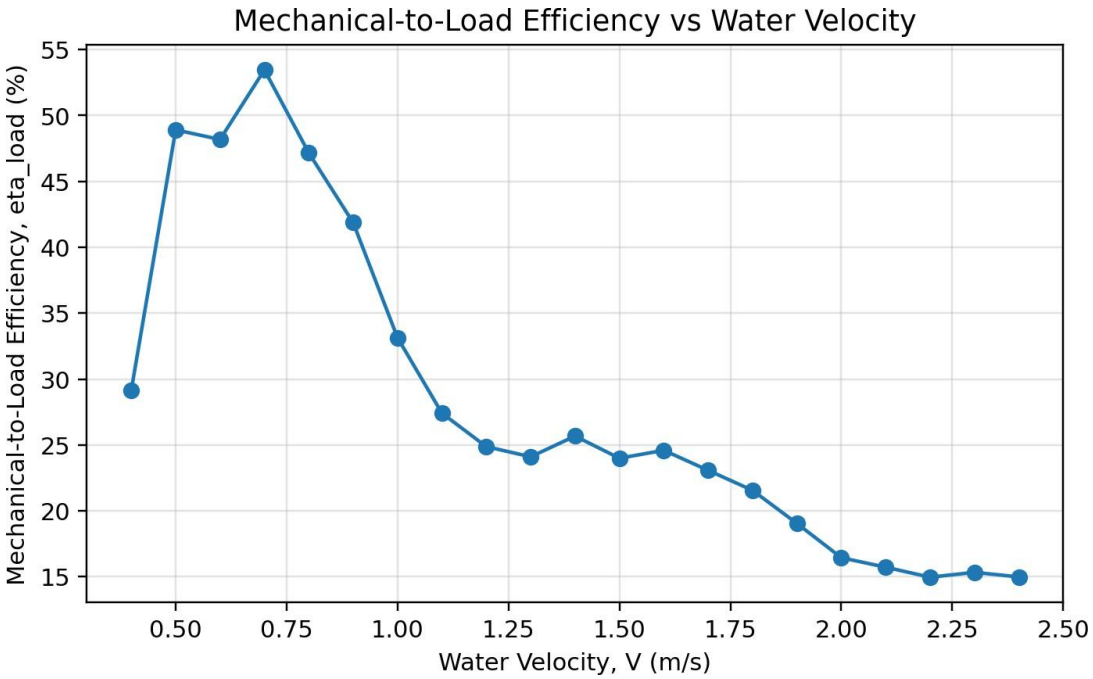



Fig. 5.12. Mechanical-to-load efficiency vs water velocity for the PMSM generator load system.

The mechanical-to-load efficiency of simplified PMSM load system is shown in figure 5.12 The efficiency is the ratio of the three-phase load power to turbine mechanical shaft power. It can be seen from the graph that the best efficiency is achieved at low to moderate velocities of water and the maximum water velocity at which efficiency is the best is approximately 0.7 m/s. Following this, efficiency drops gently with speed, reaching some 15% at 2.4 m/s. This reduction is due to the fact that the mechanical power of the generator rises at a greater rate than the electrical power of the fixed load (15 Ω). So, the graph shows that the load resistance chosen is more suitable for lower operating velocity; load matching/power conditioning may be required at higher velocities to optimize energy conversion. This is because, when a fixed load of 15 Ω resistance is used, the mechanical shaft power changes much more rapidly than the electrical load power. Hence, the fixed load is not optimized for all modes of operation. This outcome suggests that load matching or power electronic control including a rectifier, DC bus, DC-DC converter and MPPT control can be employed to enhance power extraction and overall efficiency.

### 5.4.7 Electrical Frequency

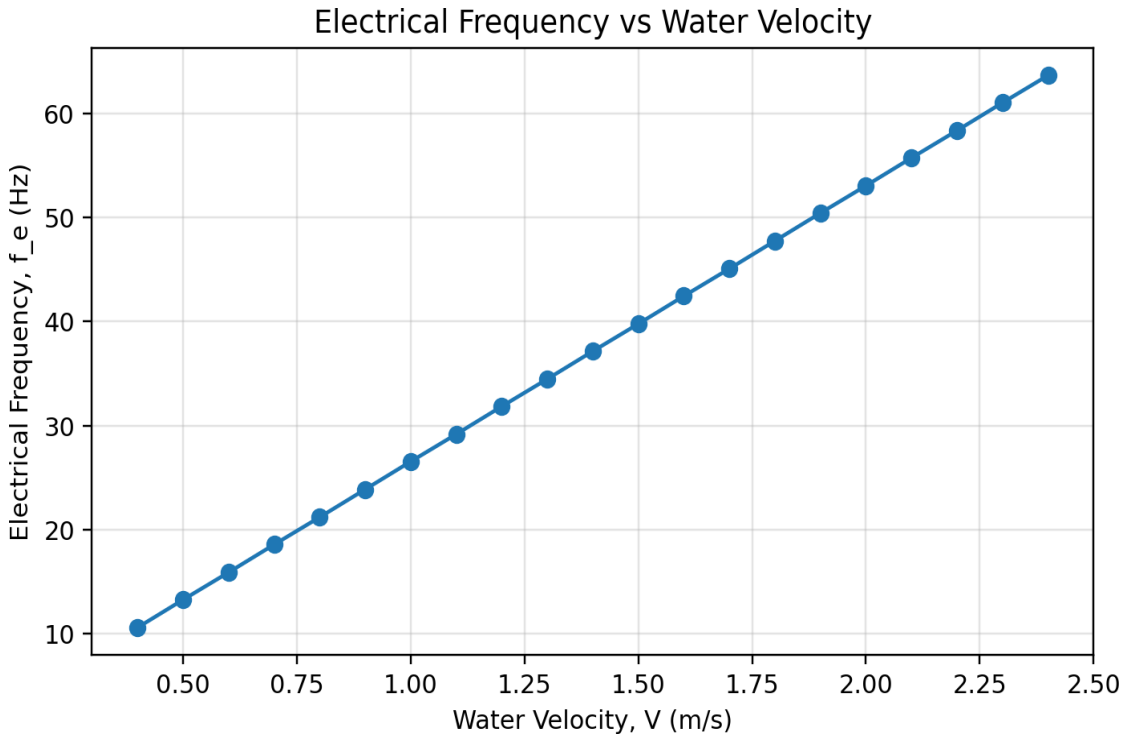



Fig. 5.13. Electrical frequency vs water velocity for the PMSM generator.

Figure 5.13 shown the relationship of electrical frequency to water velocity is represented by X. As the mechanical rotational speed of the PMSM generator is directly proportional to the electrical frequency, the frequency will increase linearly. With the turbine operating at a constant TSR, increasing the water velocity will result in an increase in the angular speed and therefore RPM. If PMSM is designed with 30 pole pairs the electrical frequency changes from around 10.6Hz at 0.4m/s to around 63.65Hz at 2.4m/s. This finding validates the fact that the generator frequency fluctuates as per the velocity of the tidal flow as it is the characteristic of any variable speed tidal energy conversion system. This verifies that the generator frequency is controlled by the speed of rotation of the turbine and hence the velocity of the tidal flow. The linear trend also confirms the relationship between mechanical speed and electrical frequency of PMSM generator as expected. In practical use in a grid or domestic application, the output frequency and voltage would need to be controlled by using power electronics or control systems.

## 5.5 Three Representative Operating Points

To find a comparison, the performance of the PMSM generator is extracted from the entire range of the simulation results and three typical operating points (tidal velocity) are selected to compare. The flow rates at those operating points are 0.7 m/s, 1.4 m/s and 2.1 m/s tidal velocity at low, medium and high flow respectively. This comparison is made to see the electrical output of the generator varies with the change in tidal flow velocity. Selected results are the angular speed, torque, mechanical shaft power, phase RMS voltage, phase RMS current, three-phase load power, load energy, efficiency and electrical frequency.

**Table 5.3** Simulated Comparison of PMSM-load performance at selected operating points.

| Tidal Velocity (m/s) | Angular speed (rad/s) | Torque, (N.m) | Mechanical Shaft Power (W) | Phase RMS Voltage (V) | Phase RMS Current (A) | Three-Phase Load Power (W) | Mechanical -to-load Efficiency (%) | Three-Phase Load Energy (J) | Three-Phase Energy (kWh) | Electrical Frequency, fe (Hz) |
|---|---|---|---|---|---|---|---|---|---|---|
| 0.7 | 3.89 | 31.1886 | 121.32 | 18.01 | 1.201 | 64.86 | 53.46 | 2106 | 5.8510e-4 | 18.57 |
| 1.4 | 7.78 | 118.092 | 918.76 | 34.34 | 2.289 | 235.8 | 25.67 | 5835.2 | 1.6209e-3 | 37.15 |
| 2.1 | 11.67 | 288.16 | 3362.83 | 51.42 | 3.428 | 528.7 | 15.72 | 12049.76 | 3.3472e-3 | 55.72 |

As can be seen from Table 5.3, the mechanical input which is supplied to the PMSM generator is increased considerably when the tidal velocity is increased. At 0.7 m/s the mechanical shaft power shows 121.32W, while at 1.4 m/s it increases at 918.76W, and at 2.1 m/s it reaches 3362.83W. This increase occurs because the velocity of the tide would be higher, which would give a higher torque and rotation speed of the turbine. Therefore, the output voltage and the current of the generator can be increased with the increase of the tidal velocity.

### 5.5.1 Load Power Comparison

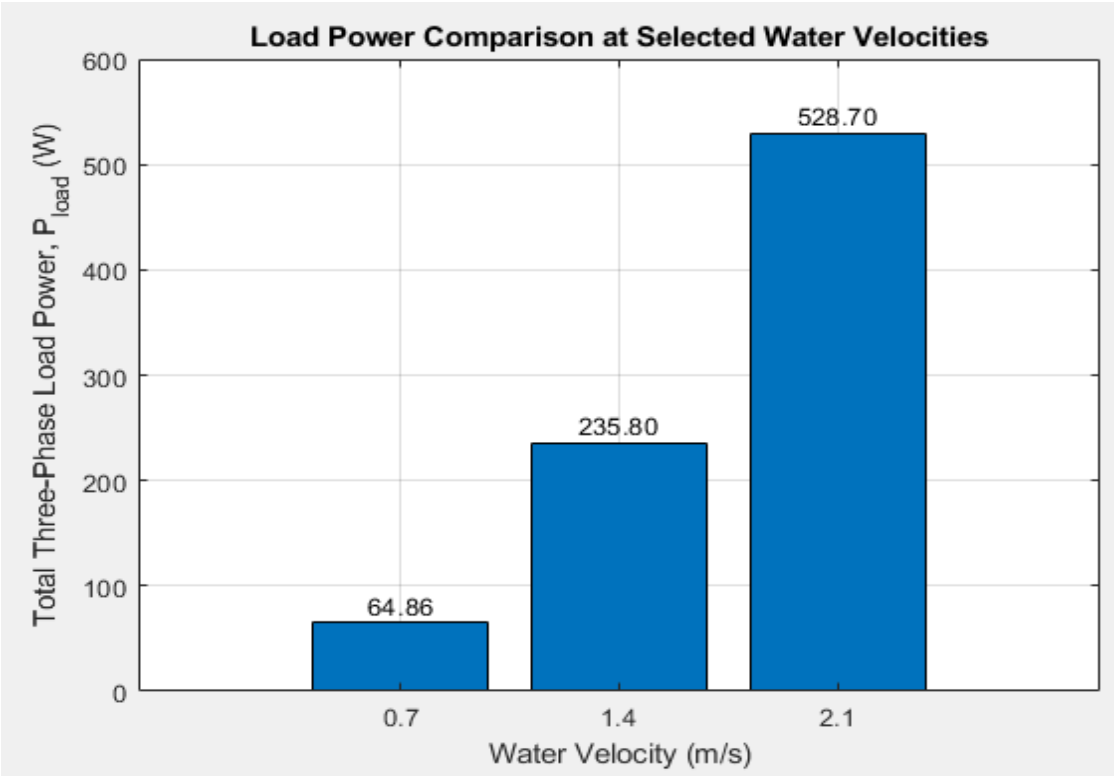



Fig. 5.14. Three-phase load Power comparison at selected operating points.

The power of the three-phase load also increases with speed of the tide. When the velocity is 0.7 m/s the load is receiving 64.86W, and at 1.4 m/s the load power is 235.8W; at 2.1 m/s the load power is 528.7W, the high-flow condition. This means that the speed of tide increases the more electrical power generated by PMSM generator. This increase trend can be seen very clearly in the bar graph as shown in figure 5.14, it can be observed that the load power at the high flow operating point is at the maximum power.

### 5.5.2 Mechanical to Load Efficiency

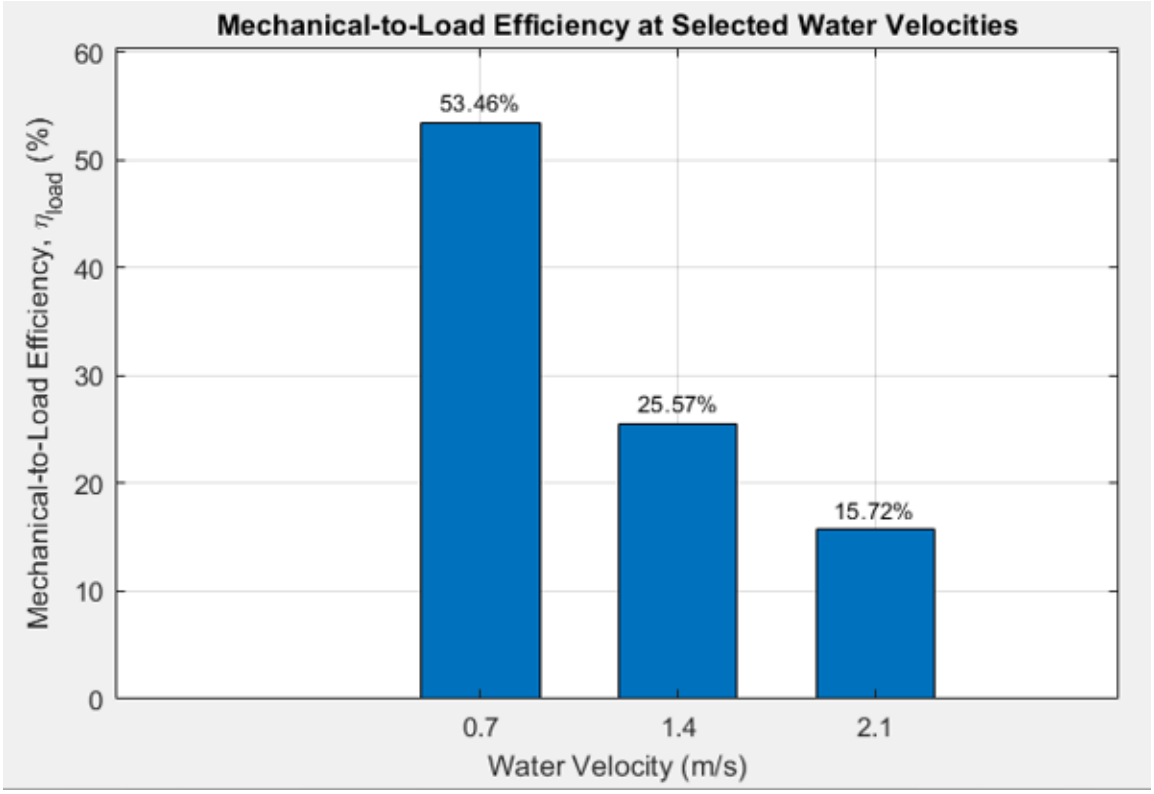



Fig. 5.15. Mechanical-to-load efficiency comparison at selected operating points.

But as the tide velocity rises the mechanical to load efficiency declines. The efficiency is at 53.46 0.7 m/s, 25.67% 1.4 m/s, and 15.72% at 2.1 m/s. This does not necessarily mean that the velocity higher the output of the system is lower. Rather, it implies that the mechanical power is much greater than the electrical power supplied to the constant 15Ω load. Therefore, it is not suitable for all operating conditions for fixed load. This indicates that there is scope for better conversion efficiency with load matching or with a power electronic interface, especially at higher velocities [Fig. shown as 5.15]

### 5.5.3 Estimated Seasonal Variation of Monthly Delivered Load Energy

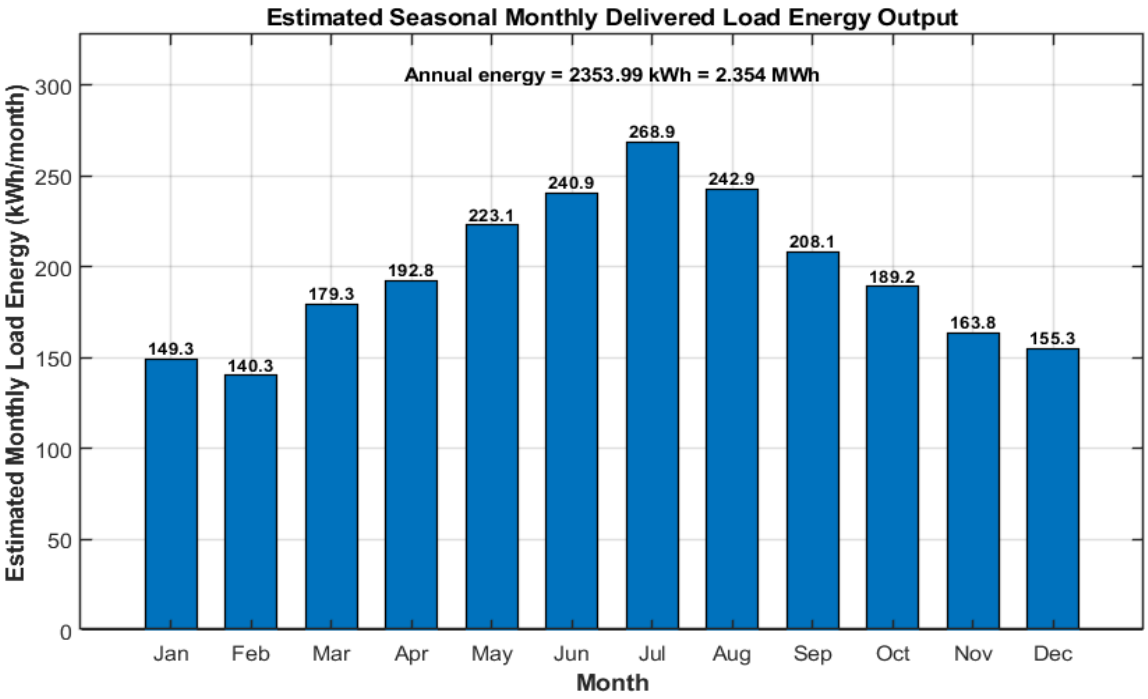



Fig. 5.16. Estimated Seasonal monthly delivered load energy output from the PMSM tidal turbine generator system.

**Table 5.4** Seasonal summary of estimated delivered load energy output

| Season | Months | Energy Output |
|---|---|---|
| Winter | Dec–Feb | **444.9 kWh** |
| Pre-monsoon | Mar–May | **595.2 kWh** |
| Monsoon | Jun–Sep | **960.8 kWh** |
| Post-monsoon | Oct–Nov | **353.0 kWh** |

The estimated load energy output of the PMSM generator system for the different months of the season is presented in figure 5.16 and Table 5.4. The annual energy output for the latest 21 operating point interpolation method was obtained, which was about 2353.99 kWh/year or (2.354 MWh/year). This annual value was allocated to the months by the

seasonal monthly weighting pattern. The peak estimated monthly energy production is 268.9 kWh/month in July, and the lowest is 140.3 kWh/month in February.

Table 5.4 shows a summary of the estimated delivered energy output based on four seasons. It is found that the monsoon season (June to September) produces the highest energy output of around 960.8 kWh during the season as the flow conditions for the tide are assumed to be higher during this season. In March-May the pre-monsoon season generates approximately 595.2 kWh and the winter season (December-February) generates approximately 444.9 kWh. The minimum seasonal contribution is acquired during the post-monsoon period (October – November) with an approximately 353.0 kWh. When combined, the seasonal values equal the energy estimated for the year (around 2353.99 kWh), which shows that the monthly distribution fairly matches the yearly energy estimated.

## 5.6 Simulated Scope Waveform Results

The waveforms of Simulink scope which has been obtained from the PMSM generator model for the representative operating point is shown in this section for the tidal velocity of 1.4m/s. In this condition, the rotational speed generated by the turbine was approximately 74.29 rpm with the produced angular speed of 7.78 rad/s. A balanced three phase resistive load of 15Ω per phase was used with the generator. In order to observe the time-domain behavior of the generator-load system, the voltage, current and load power waveforms were observed.

The results are accurate and precise as they are taken from the scope component inside the Simulink software. The configuration has been dialed to the correct standards for measuring the continuous and uninterrupted sine wave signals from the model. It shows that continuous power is being transmitted from the turbine to the load as well as from the load to the turbine.

### 5.6.1 Phase-A Voltage Waveform from Scope

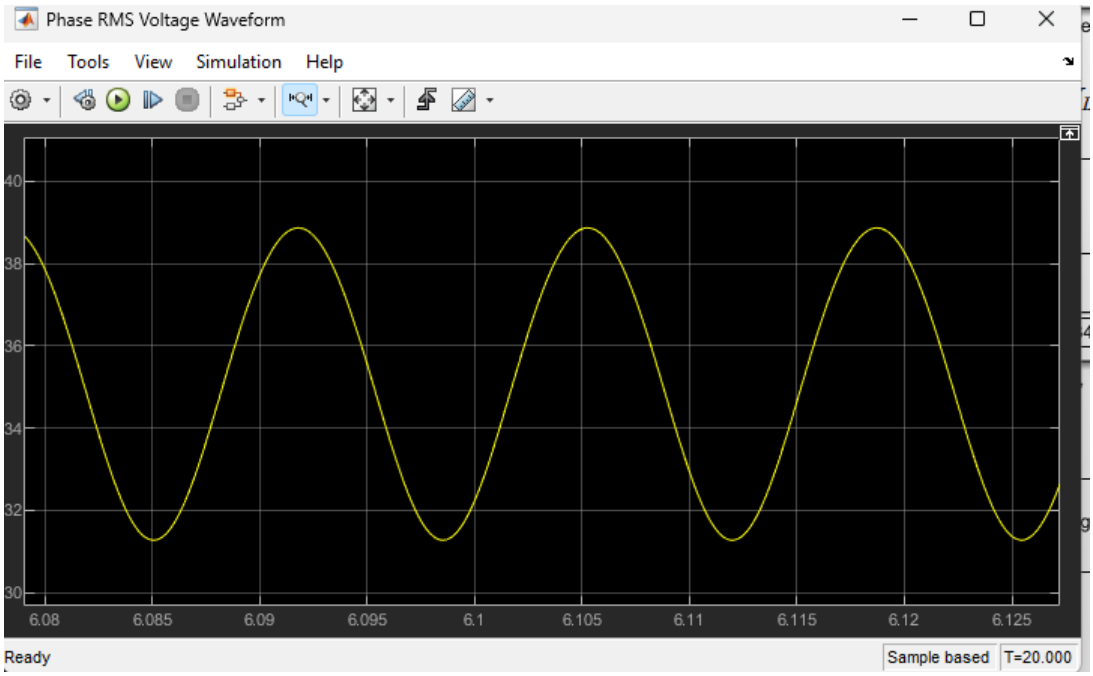



Fig. 5.17. Phase-A RMS voltage Waveform at 1.4 m/s tidal velocity and 74.29 rpm rotor speed.

Figure 5.17 shows the Phase-A RMS voltage waveform of the PMSM generator at the representative operating point of 1.4 m/s. The waveform shows small periodic variation because the generator output is produced from rotating magnetic flux, and the RMS block calculates the effective value over a moving time window. After the initial transient response, the voltage remains within a stable operating range. At this operating condition, the measured phase RMS voltage is approximately 34.34 V. This RMS voltage is the effective voltage supplied to one phase of the balanced resistive load and is used for calculating the electrical load power. This sinusoidal wave shows that the turbine is producing uninterrupted power to the load and so the power is consistent all the time during the simulation period.

### 5.6.2 Phase-A Current Waveform from Scope

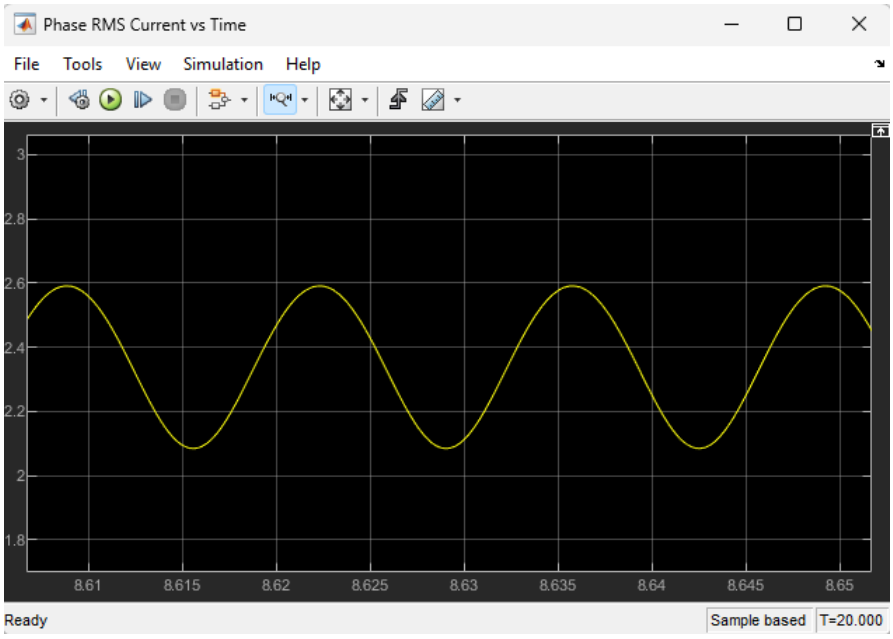



Fig. 5.18. Phase-A RMS current Waveform at 1.4 m/s tidal velocity and 74.29 rpm rotor speed.

The same operating point of 1.4 m/s is now shown in figure 5.18 in which the Phase-A RMS current waveform is plotted. As the PMSM generator is connected to a balanced resistive load, the current is behaving in the same manner as the voltage as per Ohm's law. Beyond the transient, the RMS current is stable and periodic, as indicated by the waveform. At this condition, the measured RMS current of the phase is about 2.289 A. This demonstrates that the generator is continuously supplying current to the electrical load and that the current load is the same as in the case of the generated voltage, varying in direct proportion to the generated phase voltage. This sinusoidal wave shows that the turbine is producing uninterrupted power to the load and so the power is consistent all the time during the simulation period.

### 5.6.3 Three-Phase Load Power Waveform

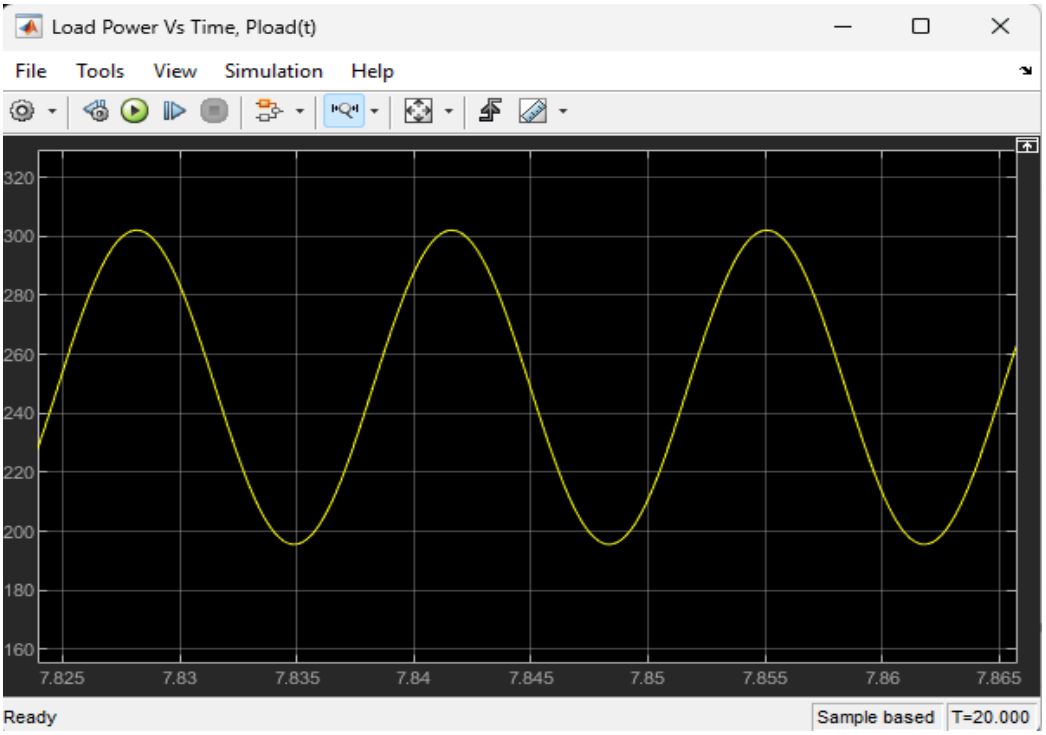



Fig. 5.19. Three-phase load power Waveform at 1.4 m/s tidal velocity and 74.29 rpm rotor speed.

In Figure 5.19 at the Representative Operating Point of 1.4 m/s tidal velocity, the turbine could be spinning at the speed of approximately 74.29 rpm or an angular speed of 7.78 rad/s. At this condition, the PMSM generator was reconnected to a three-phase equal resistive loads of 15Ω/phase. The voltage sensor and current sensor have been used to measure the phase voltage and phase current respectively and the obtained instantaneous AC signals were fed to RMS blocks to obtain the RMS value of each phase.

From the per-phase RMS voltage waveform, it is seen that the generator output voltage is in stable operation range after the initial transient time, while the first transient time, the output voltage of the generator is transient. The measured value of the phase RMS voltage for this operating point was approximately: Vph,rms = 34.34 V.

The reason for the small fluctuation in the RMS voltage waveform is related to the output of the AC generator being time varying, and the RMS calculation window taken in Simulink. The RMS value is a constant value, and it is the voltage that is supplied to each

phase of the load; the instantaneous voltage is continually changing in value with time. So, RMS voltage should be used to calculate the power for the load and not the instantaneous voltage.

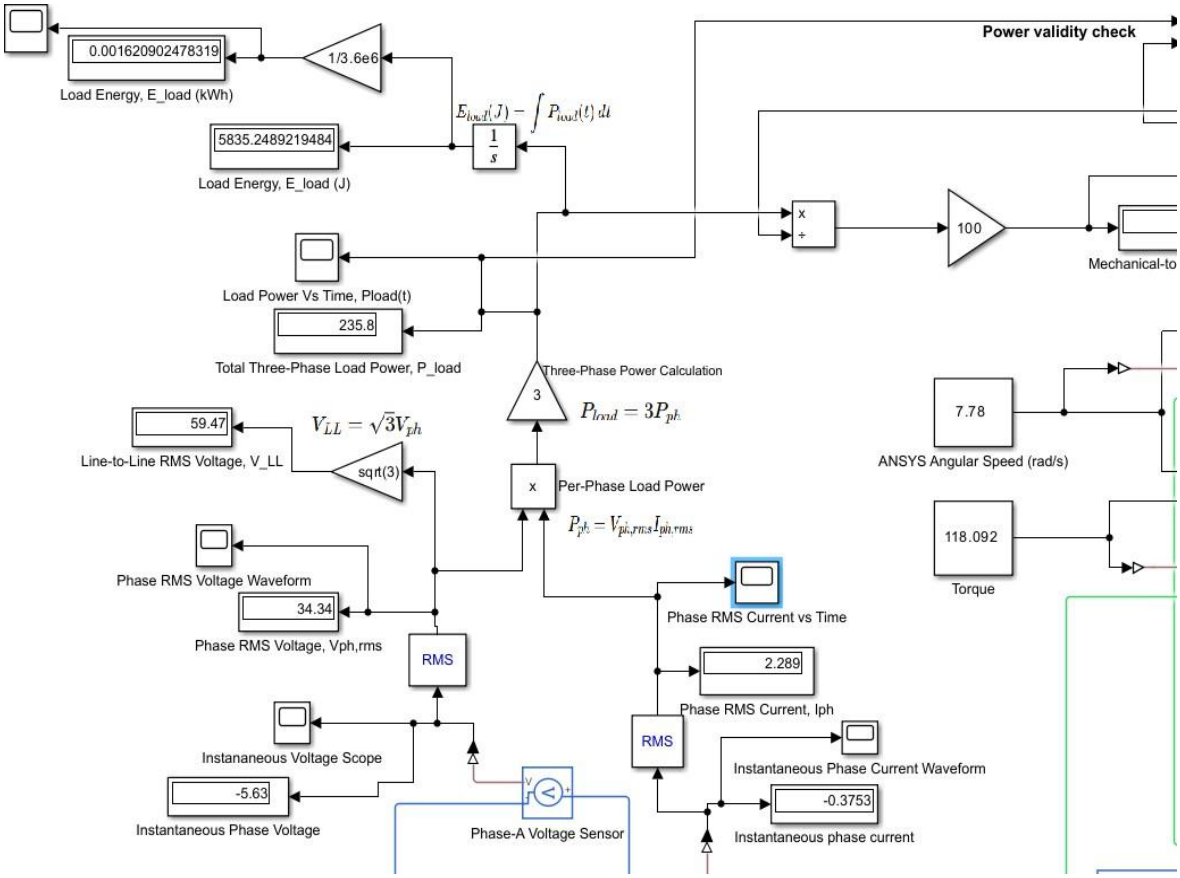



Fig. 5.20. Three-phase power calculation in MATLAB/Simulink.

Effective current through one of the phases of the balanced 3-phase load is also per phase RMS current wave form. When operating in the same condition, the measured phase RMS current was about: Iph,rms = 2.289 A Also, there are small fluctuations in the RMS current waveform, due to the fact that the output of the generator is AC and the RMS block calculates the RMS value over a time window. But, once the transient has passed, the RMS current is near steady operating current. Load is resistive and is balanced; therefore, the increase in the current in each phase is as per the increase in the phase voltage & load resistance [Fig shown as 5.20]

Using the obtained RMS voltage and current values, the total three-phase load power was calculated as:

$$P_{load} = 3\, V_{ph}, rms \times I_{ph}, rms$$

$$P_{load} = 3 \times 34.4 \times 2.298$$

$$P_{load} = 235.8W$$

## 5.7 Simulated Scope Waveform Results for Load resistance on Three-Phase

**Table 5.5** Effect of load resistance on three-phase Electrical output at a fixed turbine operating point.

| Load Resistance, R (Ohms) | Three-Phase Load Power (W) | Mechanical Shaft Power, (W) | Mechanical-to-Load Efficiency, $\eta_{load}$(%) | Power Validity Check if $P_{load} < P_{mech}$ |
|---|---|---|---|---|
| **1.5** | 3283 | 2387.86 | **137.5** (Invalid as load Demand is higher than mechanical power) | **0** (Invalid as load demand is higher than Mechanical power) |
| **5** | 1263 | 2387.86 | 52.9 | 1 |
| **10** | 668.9 | 2387.86 | 28.01 | 1 |
| **15** | 454.7 | 2387.86 | 19.04 | 1 |
| **20** | 344.4 | 2387.86 | 14.42 | 1 |
| **30** | 231.9 | 2387.86 | 9.71 | 1 |

The influence of load resistance on three phase electrical output of PMSM generator at fixed turbine operating point is shown in Table 5.5. The present study is done for different resistance of the load in three phase scenarios, with the same value of tidal velocity, angular speed, torque and mechanical shaft power. This analysis was to explore the effects of changing load resistance on voltage, current, load power, efficiency, and physics. It is noticed that the phase RMS current drops considerably and the phase RMS voltage rises

appreciably with increase in load resistance. Consequently, the power for the three-phase load decreases as the load resistance increases. This 1.5 Ω case would produce a high load power of 3283 W, which is greater than the mechanical shaft power of 2387.86 W, thus 137.5% efficiency. This operating point is considered as not valid, because efficiency cannot be higher than 100%. From the valid cases, it can be seen that 5 Ω load has the best load power and efficiency, which means load resistance has a great influence on the power extraction. This therefore proves that a fixed load is not necessarily going to be best for all operating conditions, and the matching of loads is important to enhance the performance of the system.

### 5.7.1 Efficiency vs Load Resistance

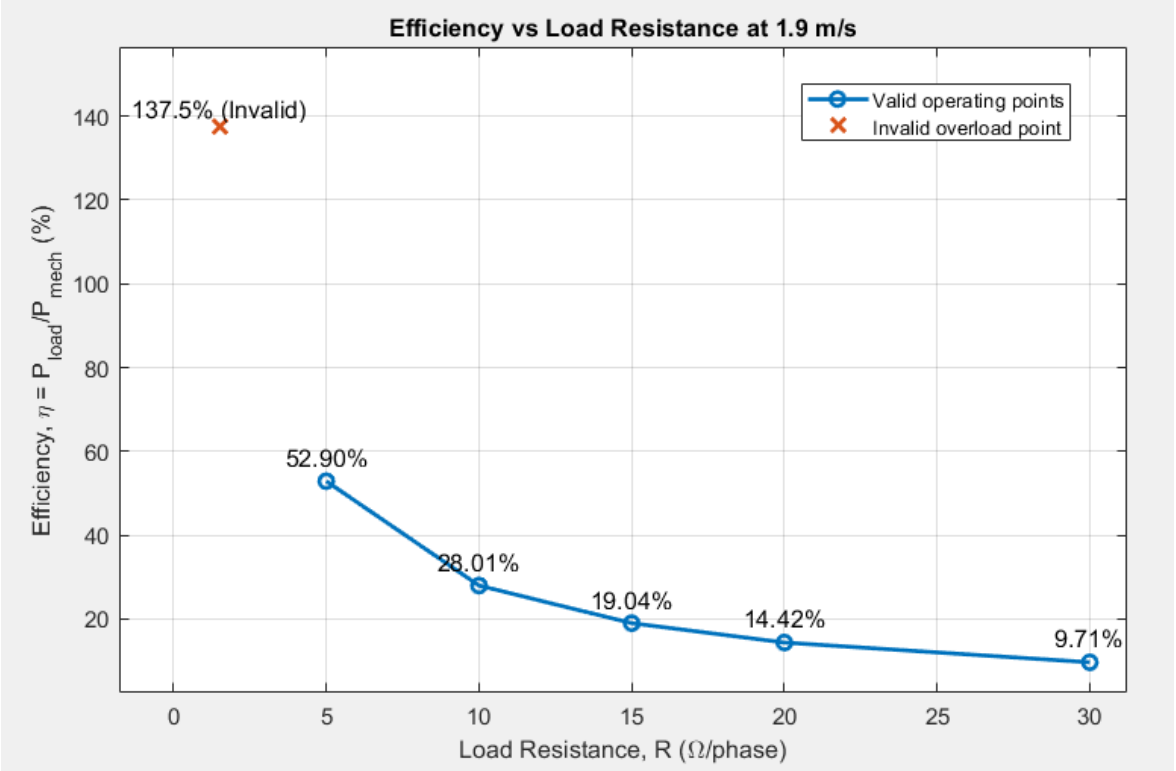



Fig. 5.21. Mechanical-to-load efficiency vs load resistance at 1.9 m/s tidal velocity.

The mechanical to load efficiency changes as load resistance changes at the operating point of 1.9 m/s tidal velocity in figure 5.21. The efficiency for the invalid case is 137.5%, which represents an efficiency that is larger than 100%, physically unacceptable as the load

is requesting more than the mechanical shaft can deliver. Hence this point is not considered in the valid operating range. In this section, the efficiency and resistance of the load are compared. The highest efficiency of 52.9% is obtained at 5Ω for the valid load resistances. If the load resistance is increased from 5Ω to 30Ω, the efficiency decreases from 52.9% to 9.71%. The graph shows that the electrical output is greatly affected by the load resistance, and that a proper matching of the load resistance to the electrical output is necessary for more efficient conversion of mechanical shaft power to useful electrical load power.

### 5.7.2 Three-Phase Load Power vs Load Resistance

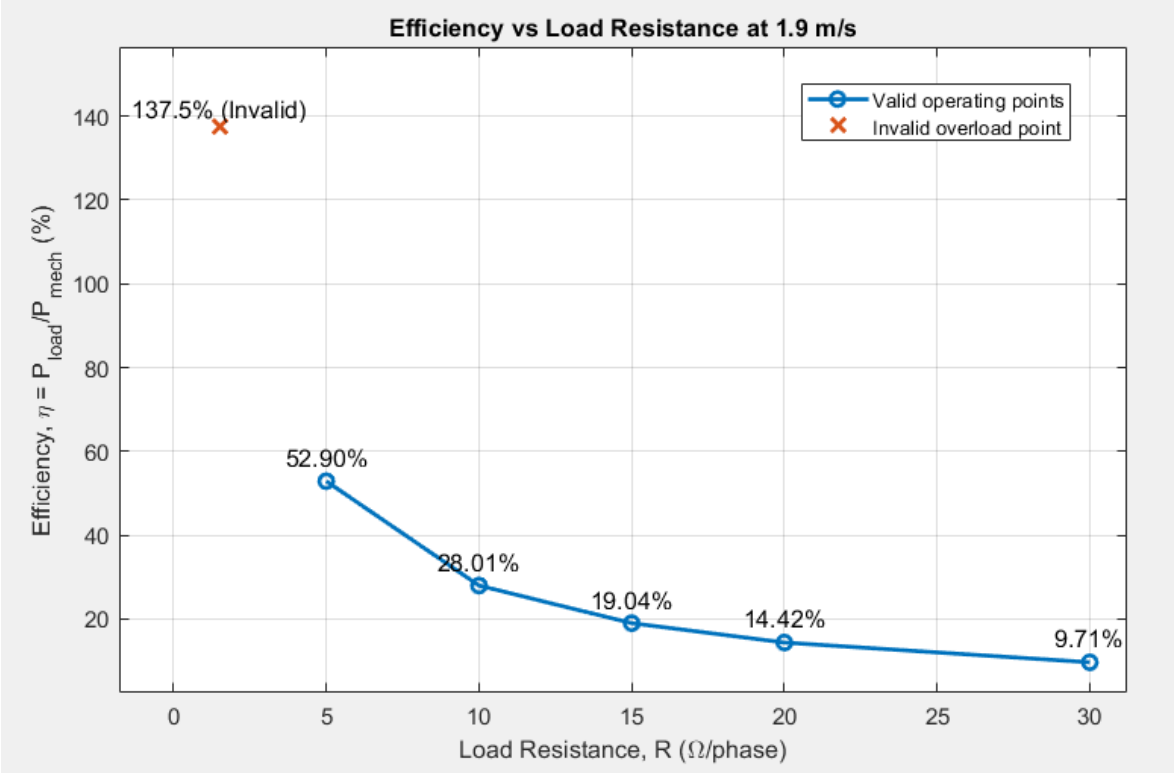



Fig. 5.22. Mechanical-to-load load power vs load resistance at 1.9 m/s tidal velocity.

Figure 5.22 illustrates the change of total load 3-phase power at the same fixed turbine operating point with respect to load resistance. The highest apparent load power of 3283 W occurs for the invalid 1.5 Ω case but this is physically an invalid point since the mechanical shaft power is exceeded. Of the valid operating points, a three-phase load power of 1263 W is achieved at 5 Ω, or maximum load power. As the load resistance increases

further, the load power decreases to 668.9 W at 10 Ω, 454.7 W at 15 Ω, 344.4 W at 20 Ω, and 231.9 W at 30 Ω. This reduction is due to the decrease of the current phase with an increase in the resistance. Thus, it is seen from the graph that the PMSM generator is not able to deliver maximum power to all load resistances. There is however an optimum load range that has a higher valid power extraction. This finding indicates the requirement of load matching or a power electronic interface for better power extraction in different tidal conditions including the use of rectifier, DC bus, DC-DC converter and MPPT controller.

The load-resistance study demonstrates that this is highly dependent on the load that is selected. The 1.5Ω load is drawing too much load current at 1.9 m/s, and gives an apparent efficiency of over 100%, which is physically impossible because the load power is greater than the mechanical shaft power. This row will thus be indicated as invalid. Valid tested resistances: 5 ohm provides the most load power at this operating point with the highest efficiency. But that doesn't mean that 5Ω is the ideal value for all velocities. It is not always best to use fixed 15 ohm and load matching is important.

This is an example that supports their argument and displays engineering judgment. A simple fixed load is convenient for testing purposes, but in the case of a real tidal system power electronics or an MPPT controller should be used, and the effective load, as viewed by the PMSM, should vary with tidal velocity. So, in the future, a rectifier, DC bus, DC-DC converter, battery and load matching control will be added.

## 5.8 Tidal Velocity Profile and Daily Energy Estimation

The 20 second Simulink simulations give value for the operating points. They are not a complete real day. All 21 simulation rows were then used as a power/velocity lookup table for estimating daily energy. This tidal velocity magnitude profile was made during one lunar tidal day (24.84 hours). MATLAB was used to interpolate the load power for each time point. Power was then integrated with respect to time.

The magnitude of the tidal velocity was used as the turbine was assumed to be bidirectional. At flood tide, the direction of flow is one direction. At ebb tide the flow turns around. For bidirectional turbines, the positive power can be generated in both directions, and the current velocity is used to estimate energy. Near high tide and near low tide, the power is low as these are slack-water times. At high and low tide, the current is usually near slack water, so velocity is low Maximum current occurs between high and low tide. This is

the reason why the cumulative energy curve steepens between the tide turning points, and levels off near slack-water times [Fig shown as 5.23]

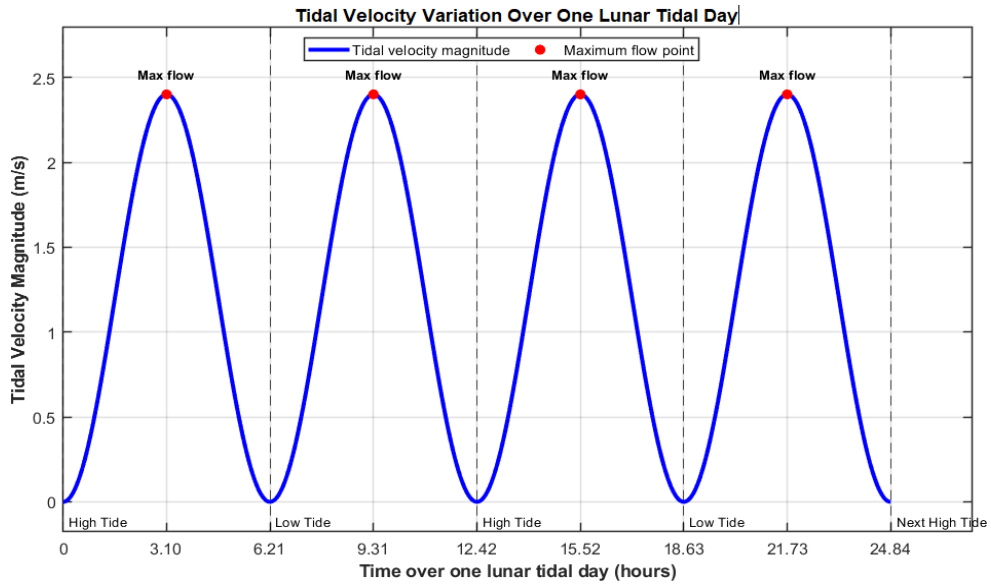



Fig. 5.23. Mechanical-to-load load power vs load resistance at 1.9 m/s tidal velocity for over one lunar day.

### 5.8.1 Cumulative Energy Graph

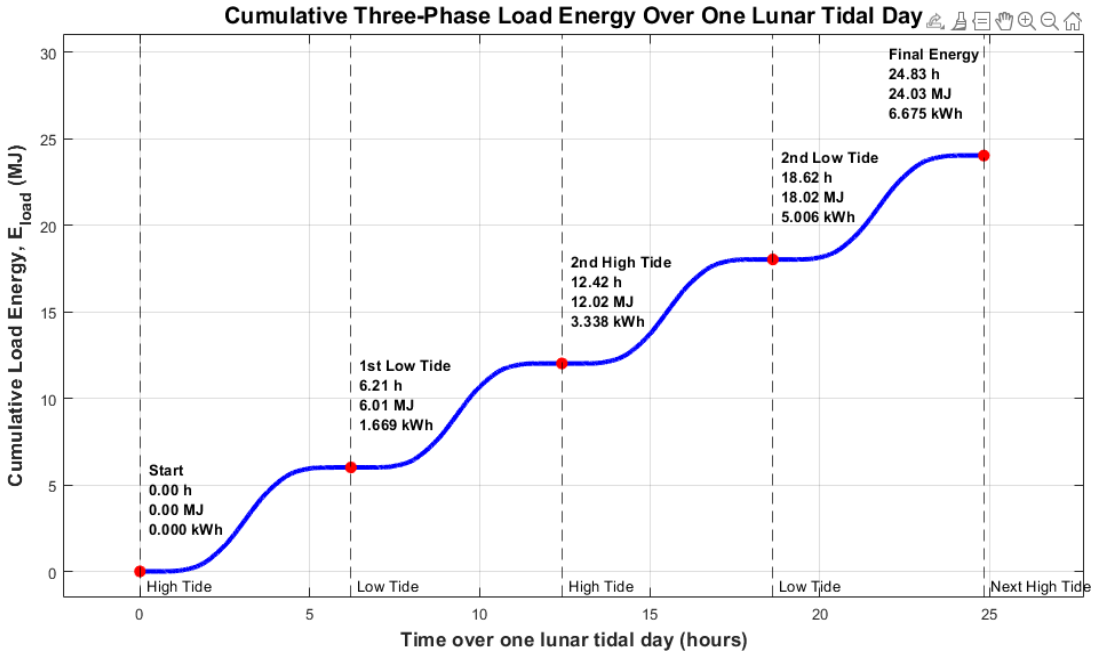



Fig. 5.24. Cumulative three-phase load energy over one lunar tidal day.

Figure 5.24 The load energy graph is the cumulative graph for the three phases which is obtained by the estimated electrical energy supplied by the PMSM generator over one complete lunar tidal day which is approximately 24.84 hours. To achieve this, the 21 MATLAB/Simulink operating point results were initially plotted to form a velocity-to-load-power look-up table with a simulated three-phase load power value for each tidal velocity. The measured value of tidal velocity profile was then smoothed for the entire tidal day and at each time step the load power was calculated through interpolation in the "table". The energy was determined by integrating the interpolated load-power curve with respect to time ($E_{load} = \int P_{load}\,(t)$). As the integration progressed, the energy accumulated over time, giving 1.669 kWh at 6.21 h, 3.338 kWh at 12.42 h, 5.006 kWh at 18.62 h, and finally 6.675 kWh at 24.84 h. This curve is steeper during high flow – periods, where the turbine is able to generate higher load power, and flatter nearer slack-water periods, where the tide velocity and load power generated are low. The final value of 6.675 kWh (24.03 MJ) is the estimated electrical energy output from one of the turbines for one lunar tidal day for the assumed tidal velocity profile.

## 5.9 Estimated Energy Output

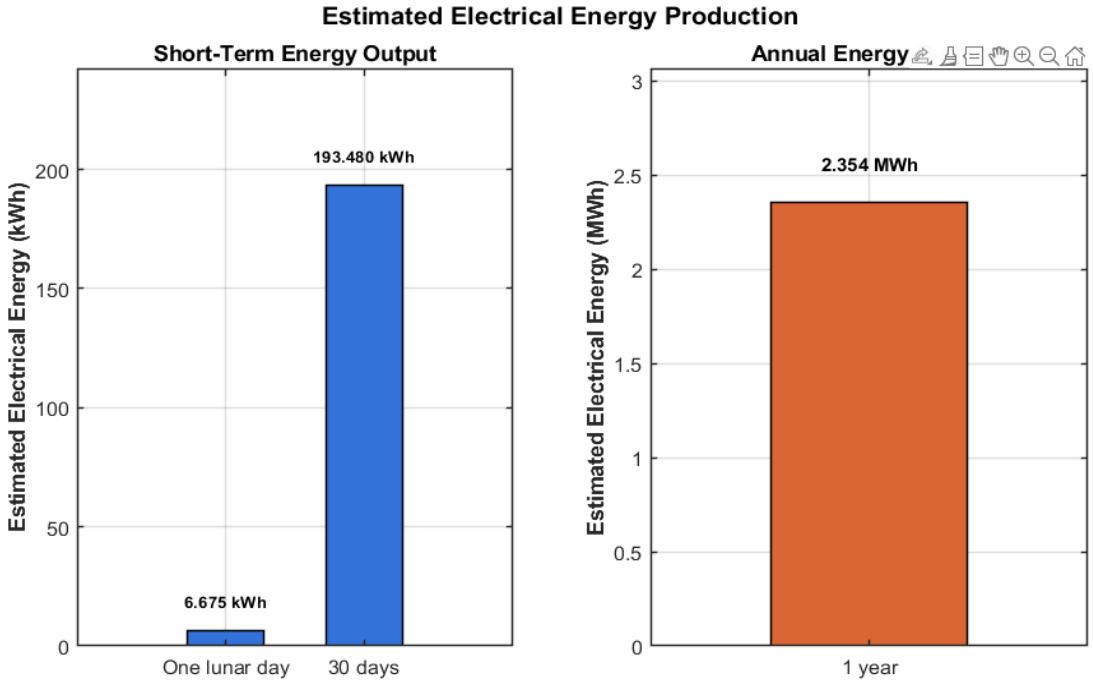



Fig. 5.25. Estimated electrical energy output for one lunar tidal day, 30 days and one year.

## 5.10 Energy Calculation

The length of the full lunar tidal day is T = 24.84 h. The final integrated value for energy from the tidal-cycle calculation is $E_{day} = 6.675\ kwh$. The average power over one lunar tidal day is $P_{avg} = E_{day} / T = 6.675 / 24.85 = 0.2687\ kW = 268.7W$

For a 30-day month, the number of lunar tidal days is approximately $N_{month} = \frac{(30 \times 24)}{24.84} = 28.99$ days. Therefore, $E_{month} = 6.675 \times 28.99 = 193.48\ kWh$.

For one year, the number of lunar tidal days is $N_{year} = \frac{(365 \times 24)}{24.84} = 352.66$ days. Therefore, $E_{year} = 6.675 \times 352.66 = 2353.99 \frac{kWh}{yaer} = 2.354\ MWh/year$.

The above values can be called estimated electrical load energy using the simulated power-velocity characteristic and assumed tidal velocity profile. They are not values measured in the field nor do they incorporate downtime, maintenance, biofouling, storms, battery losses, cable losses, or losses due to grid conversion [Table shown as 5.6]

**Table 5.6** Estimated energy outputs using 21-point interpolation and tidal-cycle integration.

| Quantity | Value |
|---|---|
| Energy per lunar tidal day | 6.675 kWh |
| Average load power over lunar tidal day | 268.7 W |
| Energy per 30 days | 193.48 kWh |
| Energy per year | 2353.99 kWh = 2.354 MWh |

## 5.11 Discussion of Accuracy and Defensibility

The final data set is internally consistent since the hydraulic power, mechanical power, electrical power and energy are all derived from well-defined equations. This corrected ANSYS table includes mass flow through Plane 1. The Simulink electrical table is

based on RMS values and three-phase power calculation. A simple average is not taken for the daily energy estimate but is calculated by an interpolation/integration method.

The most significant defensive item is that the study is an operating point simulation study. ANSYS gives the working conditions for the turbine for each velocity of the water. Then, MATLAB/Simulink checks the PMSM and loads response at those operating points. The 20-second simulation time is needed just to get stable electrical output values. The power-velocity look up table is used separately to determine the 24.84-hour energy estimate.

The load-resistance study also contributes to the work's strength. It clearly demonstrates fixed load resistance is not optimum for all velocities and that a future controlled electrical interface is required. This helps to avoid over-stating the thesis and demonstrates understanding of the limitations. The results are accurate and precise as whats calculated from the data obtained from the simulation. The configuration of the Solver has been set to precise tunings of 0.0001 time samples. Additionally, the settings have been selected for optimum range of results to be obtained.

Careful investigation of numerous simulation running’s have been made in order to validate the results and its accuracies. Each of the 21 observations have been done 5 times or more to understand that the pattern is consistent with the configuration of each model. Then furthermore, the results have been compared with the relevant data which was taken during each simulation. Important to note that each simulation is unique to its each different speed of the turbine.

The points of operation obtained from MATLAB/Simulink were used for the velocity to power look-up table for the energy-yield estimation. The lunar tidal velocity profile (24.84 hours) was then applied, and the load power was interpolated over the duration of the tide. The electrical energy output was estimated by integrating the interpolated load power over one lunar tidal day and was found to be 6.675 kWh/lunar tidal day. The number of cycles of the lunar tide in the month, and in the year, were used to scale the result to obtain these monthly and yearly energy values, since one lunar tidal day is 24.84 hours.

# CHAPTER 6

# SOCIO-ECONOMIC IMPACT AND SUSTAINABILITY

## 6.1 Impact of the project on societal, health, safety, legal and cultural issues

Bangladesh is a riverine and coastal country where many communities lie near the tidal channels, estuaries, coastal islands and offshore water routes [30]. Despite the tremendous progress towards improving national electricity access over the years, there are issues of electricity supply reliability, grid extension cost, cyclone vulnerability, and reliance on diesel-based back-up power for remote coastal and island communities [31]. In this context it is said that using the kinetic energy of the tidal current instead of using imported fuel, the micro tidal stream turbine can be considered as a locally available renewable energy source. Local energy systems are also crucial for long-term development as coastal regions in Bangladesh are very vulnerable to climate related hazards like flooding, cyclone effect, salinity intrusion and infrastructure disruption [32] .Recent research has also indicated that the access to services of infrastructure is also at risk due to climate hazards in the coastal zone of Bangladesh, particularly for poorer households [33].

The proposed project is of societal relevance as it aims to find out if a small open-centered bidirectional tidal stream turbine can produce useful electrical power from low velocity tidal flow. The project concentrates on one turbine unit, but it can be expanded to a microgrid or a turbine-array set-up in the future. This system can be used for small loads in rural areas like LED lights, mobile charging, emergency communication devices, fans, small DC/AC appliances, fishery loads or community lights. Based on the obtained MATLAB/Simulink result, it was concluded that the PMSM generator can generate electrical power when it is connected to a balanced three-phase resistive load when water velocity is present and the energy yield analysis indicated that the energy generated by the PMSM generator for a single turbine for one lunar tidal day based on the assumed profile of water velocity is approximately 6.675kWh. Hence, the project is socially relevant as it connects the hydrodynamic performance of a turbine to actual electrical output in terms of energy consumed by the community.

In health terms, local renewable energy can have indirect positive impacts on quality of life by providing lighting, communications, refrigeration of medicines, basic healthcare equipment, and safer night-time mobility in rural coastal communities [34]. Education, emergency response and home life and small businesses can be impacted by unreliable electricity in many isolated places [35]. A consistent supply of tidal energy can help to minimize reliance on diesel generators or kerosene lighting sources which can lead to smoke, noise and local pollution [36] .The project does not provide a panacea for health problems, but it helps to foster the broader concept of having clean energy sources in coastal settlements that are readily available for use and thus can help improve living conditions[37].

Safety is an important concern for this project since the turbine is underwater and is in contact with natural water flow. There is a need to carefully plan the design of the rotating blades, as well as the support structure, electrical generator, cables and connection to the load to minimize risks to users, fishermen, boats, aquatic animals and maintenance personnel [35]. The rotor speed is relatively low compared to many high-speed rotating machines and the proposed open centered turbine will be operated at low-speed tidal current. This helps to minimize mechanical risk but does not eliminate the need for safety measures [37]. In actual installation, the turbine must be equipped with protective duct, strong supporting structure, anchoring, warning marked, emergency shutdown mechanism, safe access procedure, etc. Electrical safety is also of crucial importance. The output of the generator shall be well insulated, earthed and protected by the use of fuses, breakers, waterproof connectors, corrosion resistant enclosures and appropriate cable routing [30].

Legal and regulatory aspects also apply to the project. The turbine to be installed in a tidal/coastal waterway would require consent from relevant local authorities, environmental agencies, marine or inland water transport authorities and perhaps fisheries related authorities in the future deployment. Location for installation shall not interfere with the navigation routes, fishing grounds, movement of the ferry, or access to the water by the community. Legal requirements would be more important if a turbine array were proposed in the future, as multiple turbines would impact the use of the waterway, sediment movement, aquatic habitat and local livelihoods. Hence, prior to implementation in the field, it would be required to conduct environmental impact assessments, a site survey, a stakeholder consultation and safety approval [31].

An important factor in Bangladesh is cultural acceptance. People living near the coast may rely on fishing, boat transport, salt production, aquaculture, as well as small trade and tourism related activities. These existing practices must be taken into account in any tidal turbine project. Local people may resist the project if they believe the turbine will affect their fishing routes, amount or types of fish, damage fishing nets, be dangerous for boats, or limit their access to water. Thus, it is essential that the design be communicated as an engineering system and also as a technology that will support the community. The participation of the local community, awareness campaigns, training and clear explanation of benefits and risks is essential. Involving the community or local maintenance participation has been found to help increase acceptance and reduce fear of new technology.

Technical/employment opportunities can also be generated by the project. Small scale local technical work can be generated around fabrication, installation, inspection and cleaning of micro tidal turbines as well as electrical wiring, maintenance and monitoring of the turbines. Developed to a greater extent, technology could promote skills in the areas of renewable energy, mechanical fabrication, marine maintenance, electrical systems and environmental monitoring. The project is also a good example for students and researchers about the application of mechanical design, CFD simulation, PMSM generator modelling and energy-yield estimation for solving a real coastal energy problem.

## 6.2 Impact of project on the environment and sustainability

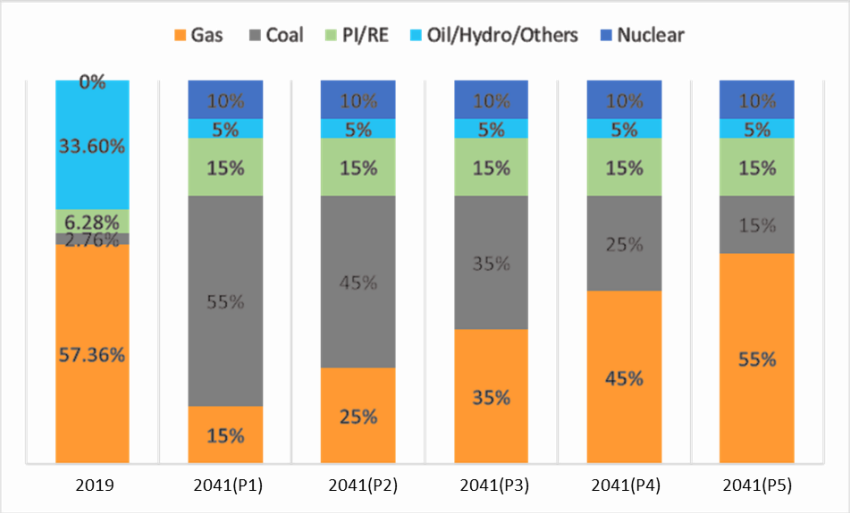



Fig. 6.1 Current (2019) and planned (2041) composition of fuel type for energy generation in Bangladesh.

The proposed bidirectional micro tidal stream turbine is an environmentally friendly as it utilizes the naturally available, renewable and predictable tidal-current energy in coastal areas. The turbine is not a fossil fuel turbine, which would be burning coal, diesel, furnace oil or natural gas while operating. Hence there is no direct combustion related $CO_2$ emissions, smoke, ash or fuel transport pollution in the operational stage. This is significant for Bangladesh, as its electricity generation still relies heavily on fossil fuels; for instance, in 2024, fossil fuels provided approximately 98% of the country's electricity generation, and low-carbon electricity generation was negligible [32]. This provides a compelling reason to investigate further renewable energy opportunities such as tidal Stream Energy where there are suitable coastal flow conditions [Fig. shown as 6.1]

Tidal stream technology also has a merit over large tidal barrage systems as it doesn't involve building a large dam across an estuary to get energy from the flowing water [33]. Significant alterations in tidal range, sediment transport, fish movement and estuarine ecology can occur as a result of the construction of large barrages [34]. By contrast a small tidal stream turbine (STT) has a smaller physical footprint, and water is able to flow through and around the turbine structure [35]. The proposed open-centered design is particularly appropriate for this concept, as the flow has a fraction of it passing through the device, and the power is useful mechanical power that can be extracted from the flow in the annular blade region [36]. This renders the design less obtrusive visually than many land based energy systems and more appropriate for local coastal or other island-based installations (with sufficient care in site selection).

While tidal stream power is a renewable energy source, it is not without its environmental issues. Marine renewable energy devices may cause potential hazards to fish through collision and disturbance to aquatic life, underwater noise, electromagnetic field from the cables, habitat alteration, local turbulence and sediment disturbance and/or navigational conflicts [37]. Fish collision, noise, electromagnetic field and habitat related impacts are potential environmental issues noted in marine renewable energy reviews [38]. Other studies have also pointed out that deployment of tidal energy has been delayed by uncertainty over risk of collision and environmental impacts, and more evidence is required in the field [39]. So, the proper environmental monitoring and mitigation measures need to be incorporated in this project later for the future roles.

There are a number of mitigation approaches that can be taken to minimize environmental impacts. The turbine should not be located in large fish breeding areas, protected areas or high fish traffic areas or traffic lanes [40]. The structure should be smooth, use corrosion-resistant materials and have a strong foundation to avoid accumulation of debris and damage [41]. The speed of the rotor as well as the duct or outer frame should be designed so that human contact with the blades is minimized, and the speed of the rotor is safe [42]. The proper sealing and routing of electrical cables are critical to avoid leakage or damage [43]. Regular checks must be made to assess biofouling, corrosion, sedimentation, vibration, noise and structural integrity [44].

The project is contributing towards sustainability due to the simple energy-conversion chain. The last MATLAB/Simulink model is designed where the torque and angular speed of the turbine obtained from ANSYS is fed to a PMSM generator which is directly connected to a balanced three phase resistive load. This eliminates the complication of a battery, inverter, rectifier and DC bus in the current simulation phase. A simplified model is useful to gain a clear understanding of the relationship between the tidal velocity, the shaft power of the turbine, the voltage and current of the generator, the load power and energy output. Power electronics and battery storage/grid interface can be incorporated in future, but the present study focuses on the basic conversion of tidal mechanical power to electrical load power.

Sustainability of the material is a factor as well. Because of the saline or brackish water in which the turbine will be working, corrosion resistant materials are required for the rotor, the stator support, the shaft, the fasteners, the electrical casing and mounting structure [45]. Low-cost materials (not properly coated) can cause the turbine to fail rapidly, leading to an increase in maintenance cost and environmental waste [46]. Hence, future fabrication should take into account the use of stainless steel, marine grade coatings, sealed electrical components, and use of structure materials that are easy to recycle and easy to disassemble for repair . Maintaining a design locally is more sustainable than having to replace the design often or import spare parts.

If the project shifts and/or reduces fossil fuel electricity use, it can be most environmentally beneficial. This type of turbine has low energy production in a year; however, it is important for small, decentralized loads. To achieve greater impacts, several turbines could be deployed in an array, but the deployment of arrays should be carefully investigated as energy extraction from the tidal currents can affect the behavior of the local flow [9] [10]. Various scales should be taken into account for tidal-energy research, including the device-level turbulence, and the array-level feedback on the resource. Hence, other future studies should be incorporated, such as array spacing, wake interaction, sediment impact, monitoring of marine-life and seasonal tidal variation.

The project is related to Sustainable Development Goal 7 (affordable and clean energy) and Sustainable Development Goal 13 (climate actions). Micro tidal energy could make a contribution towards decentralized renewable electricity generation in rural coastal communities. It could also contribute to Sustainable Development Goal 9 by providing innovations and local infrastructure development, and to Sustainable Development Goal 11 by increasing the resilience of coastal settlements. However, the turbine is in an aquatic environment so SDG 14 (Life below water) also applies in that environmental protection should be taken into account when the turbine is deployed in the future.

Overall, the project is moving in a positive direction towards sustainability as it is exploring a clean, predictable and readily available energy source for the coastal region of Bangladesh. It is not claiming to be a replacement to the national grid or large power plants just yet. It rather illustrates a small-scale renewable energy system, which can help rural coastal electrification and be applied to research and development, and future microgrid applications [46] [47]. If the installation location is properly selected, environmental assessment is performed, community is engaged and electrical design is safe and long-term monitoring is done, the bidirectional micro tidal stream turbine may emerge as a potential candidate for sustainable coastal energy development in Bangladesh.

The project is also good for sustainability as the energy-conversion chain is simple. In the final MATLAB/Simulink model, the torque and angular speed of the turbine obtained from ANSYS are fed to a PMSM generator and the generator is directly connected to a balanced three phase resistive load. This eliminates the complexity of a battery, inverter,

rectifier and DC bus in the current simulation phase. A simplified model is helpful in gaining clarity about the relationship between the tidal velocity, the shaft power of the turbine, the voltage and current of the generator, the power and the energy output of the load. For future development, power electronics, battery storage or grid interface can also be implemented, but for the present study, the basic conversion from the tidal mechanical power to the electrical load power is established.

The project also contributes to Sustainable Development Goal 7 Affordable also clean energy and Sustainable Development Goal 13 contributing Climate action. So, a much better option could be micro tidal turbine energy for decentralized electricity production for mainly rural coastal regions. It can also contribute to Sustainable Development Goal 9, through innovation, and Sustainable Development Goal 11, in terms of coastal settlements' resilience. As the turbine is in an aquatic environment, SDG14 (life below water) also applies as the environment should be a factor in future deployments.

Tidal Stream Energy, like all other renewable energy sources, is not entirely free of environmental concern. Marine renewable energy devices may pose potential risks of fish collision, disturbance of aquatic animals, underwater noise, electromagnetic properties of cables, habitat modification, local turbulence, sediment disturbance, and navigational conflicts [46]. Fish collision, noise and electromagnetic fields and habitat related effects have been cited as potential environmental issues to be monitored in marine renewable energy reviews [47]. Other research also indicates that uncertainty over risk of collision and environmental impacts can also retard the deployment of tidal energy, as additional evidence of actual experience is required. Therefore, future field installations of this project should include environmental monitoring and mitigation [48].

There are a number of mitigation measures that can be implemented to minimize environmental effects. The turbine needs to be located outside of critical fish breeding areas, protected areas, and busy fishing and navigation channels [49]. The design should be smooth, made of corrosion-resistant materials and provide a firm foundation to avoid debris buildup and accidental damage [50]. The rotor should be able to rotate at a safe speed, and the duct or outer frame should minimize the risk of direct human contact with the blades. The cables that run electricity should be sealed and directed correctly so that they won't leak

or break. It should periodically take place to monitor biofouling, corrosion, sediment deposition, vibration, noise and structural integrity [49].

Environmental impacts could be minimized greatly. If the turbine were located outside the fish breeding regions and also away from the navigational traffic areas, the environmental damage would be greatly minimized. For this, the very structural foundation of the turbine should be smooth surfaced and not edged, is made up of materials which do not corrode easily. Therefore, debris will not be accumulated, and so damage will be less. Also, the rotor should be spinning at a safe speed as to not introduce structural failure. The electric cables should be very properly sealed so direct contact will not be issued.

Sustainability of the material is also important. The turbine would be in contact with saline or brackish water, so corrosion resistant materials are required for the rotor, support for the stator, shaft, fasteners, electrical casing and mounting structure [50]. The use of low-cost materials may also result in the turbine wearing down rapidly, which leads to unnecessary maintenance and waste. Future fabrication should include stainless steel coatings, sealed electrical components, marine grade coating, disassembled and easy to repair and recyclable structural materials [50]. A locally maintainable design is more sustainable than a design that has to be replaced frequently or for which spares have to be brought in from outside.

The environmental gain of the project is highest if it displaces or decreases the use of fossil fuel generated electricity [50]. The annual energy production is modest but for a single turbine is still significant for small-scale, decentralized loads. Several turbines could be deployed in an array for greater impact [58]; however, the array deployment must be carefully considered as the extraction of energy from tidal currents would have an effect on the flow characteristics in the area. The study of tidal energy demonstrates that there are several levels of scales that should be accounted for in resource assessment and interaction with the environment, from the turbulence at the device level to feedback from the array on the resource [59]. Hence, in future, these should be incorporated: Array spacing, wake interaction, sediment impact, monitoring of marine-life and seasonal tidal variation.

# CHAPTER 7

# ADDRESSING COMPLEX ENGINEERING PROBLEMS AND ACTIVITIES

## 7.1 Addressing Complex Engineering Problems

Numerous complex engineering problems were associated with the present project due to its multidisciplinary nature, as shown in Table 7.1 The project required knowledge from fluid mechanics, renewable energy conversion, rotating electrical machines, computational fluid dynamics, CAD modelling and MATLAB/Simulink simulation. The main challenge was to connect the hydrodynamic performance of the open-centered bidirectional tidal turbine with its practical electrical output. Therefore, turbine torque, rotor speed, mass flow rate, available hydraulic power and turbine efficiency were first evaluated using ANSYS Fluent. These results were then used as input parameters for the MATLAB/Simulink PMSM generator model to estimate voltage, current, load power, electrical frequency and energy yield. The project also involved practical engineering issues such as low tidal velocity, reversing flow direction, variable turbine speed, load matching, fluctuating electrical frequency, mechanical durability and suitability for coastal application in Bangladesh.

**Table 7.1.** Complex engineering problems associated with the current project.

| **Problems** | | **Addressing the problems** |
|---|---|---|
| WP1 | Depth of knowledge required (WK3-WK5, WK8) | WK3–WK5 knowledge was required in fluid mechanics, tidal turbine theory, energy conversion, rotating machines, PMSM generation, CFD simulation, CAD modelling and MATLAB/Simulink analysis. |
| WP2 | Range of conflicting requirements | The project required trade-offs between maximizing power output, maintaining simple structure, limiting rotor speed, ensuring durability, achieving useful electrical output, and keeping the system suitable for low-cost coastal application. |

| | | |
|---|---|---|
| WP3 | Depth of analysis required | ANSYS Fluent results such as torque, RPM, mass flow rate, available hydraulic power and turbine efficiency were analyzed and linked with MATLAB/Simulink outputs such as voltage, current, load power, frequency and energy yield. |
| WP4 | Familiarity of issues | The project required awareness of real tidal-energy issues such as low-speed flow, reversing tidal direction, variable velocity, turbulence, CFD convergence, fluctuating electrical frequency, load matching, corrosion, sealing and maintenance. |
| WP5 | Extent of applicable codes | Relevant standards and guidelines include IEC TS 62600 series for marine energy systems, DNV-ST-0164 for tidal turbines, IEC 60034 for electrical machines, IEEE 519 for power quality, IEEE 1547 for future grid connection and local electrical safety rules. |
| WP6 | Extent of stakeholder involvement | Stakeholders include coastal communities, local households, government energy agencies, renewable energy organizations, utility/grid authorities, private investors, turbine manufacturers, researchers and environmental authorities. |
| WP7 | Interdependence | Blade geometry affects torque and RPM; torque and speed affect PMSM voltage, current and frequency; load resistance affects power and efficiency; tidal velocity variation affects daily, monthly and yearly energy output. |

## 7.2 Addressing Complex Engineering Activities

The complex engineering activities involved in the project are summarized in Table 7.2. A wide range of engineering resources was used, including SolidWorks for turbine modelling, ANSYS Fluent and CFD-Post for hydrodynamic simulation, MATLAB/Simulink for electrical output analysis, and MATLAB plotting for result interpretation. The activities included designing the open-centered turbine geometry, setting

tidal velocity boundary conditions, extracting torque and mass flow rate from CFD results, calculating mechanical shaft power and turbine efficiency, developing the PMSM generator model, and estimating load power and energy production from one lunar tidal day. The project also required interpretation of real tidal behavior for Sandwip, Bangladesh, where the turbine is expected to operate under low-speed and bidirectional flow. Although hardware fabrication was not performed in this stage, the project provides a strong simulation-based foundation for future prototype development, inverter-based frequency control, battery integration and practical field testing.

**Table 7.2.** Complex engineering activities associated with the current project.

| **Activities** | | **Addressing the activities** |
|---|---|---|
| EA1 | Range of resources | We used tools like ANSYS Fluent Excel, also needed local Knowledge, Design skills and real-world data to test our turbine's power efficiency. |
| EA2 | Level of interactions | The project combined mechanical design, fluid-flow simulation, electrical generation and energy-yield estimation. CFD torque and RPM were used as inputs for the PMSM electrical model. |
| EA3 | Innovation | The project uses an open-centered bidirectional micro tidal turbine concept with a direct-drive PMSM generator and a simplified balanced three-phase load model to evaluate usable electrical output. It uses no gearbox system, only magnets and coils simply and also cheaper. |
| EA4 | Consequences to society / environment | The system can support decentralized renewable electricity for coastal Bangladesh, reduce fossil-fuel dependence and help rural communities. Future testing must also consider aquatic safety, corrosion, maintenance and installation impact. |
| EA5 | Familiarity | The design applies known turbine and generator concepts to low speed reversing tidal flow. Since local users may be unfamiliar with this system, installation, operation, Safety and maintenance guidance will be required. |

# CHAPTER 8
# CONCLUSIONS, LIMITATIONS AND FUTURE WORKS

## 8.1 Conclusion

This thesis presented the design, hydrodynamic simulation and simplified electrical modelling of a bidirectional micro tidal stream turbine intended for coastal energy applications in Bangladesh. The turbine was designed as an open-centered ducted structure with six blades so that it can operate under low-speed tidal flow and allow flow passage through the center of the rotor. The torque and mechanical shaft power were found to be higher with higher tide velocity in the hydrodynamic results. Available hydraulic power ranged from 42.264 W at 0.4 m/s to 9033.520 W at 2.4 m/s and mechanical shaft power ranged from 22.13 W to 4960.53 W at the same velocities. Turbine efficiency was generally in the range of 50-56%, which shows a better and more reasonable turbine performance than the previous calculation method. The turbine output at the representative high flow velocity (2.1 m/s) was 288.16 N.m of torque and 3362.83 W of mechanical shaft power, with an efficiency of 55.62%, based on the available hydraulic power of 6046.264 W.

The MATLAB/Simulink model was used for the electrical part of work. In the final model the PMSM generator was directly connected with a balanced three-phase load. Mechanical inputs to the PMSM model were obtained from the ANSYS torque and angular velocity. For each of the 21 operating points, the phase RMS voltage, phase RMS current, three-phase load power, load energy and electrical frequency were measured or calculated. The turbine delivered 235.8 W power to the three-phase load at 1.4 m/s, 528.7 W at 2.1 m/s and 743.1 W at the maximum simulated velocity of 2.4 m/s. The points of operation obtained from MATLAB/Simulink were used for the velocity to power look-up table for the energy-yield estimation. The lunar tidal velocity profile (24.84 hours) was then applied, and the load power was interpolated over the duration of the tide. The electrical energy output was estimated by integrating the interpolated load power over one lunar tidal day and was found to be 6.675 kWh/lunar tidal day. It was estimated that each turbine would produce 193.48 kWh per month and 2.354 MWh per year. From these results, it can be concluded that the micro tidal turbine concept proposed in this study is capable of producing small scale

renewable energy, particularly when two or more turbines are deployed in an array for small scale applications such as for rural or coastal communities.

## 8.2 Limitation

The project drawback is the simulation-based study and physical prototype was not tested in water. Hence, there was no possibility to validate the CFD and MATLAB/Simulink results with real data measured torque, speed, voltage or current. The ANSYS Fluent results also vary based on the type of mesh used, the turbulence model, the time-step size, the length of the transient simulation, and the method used to extract the torque from the simulation. Hence, the effect of extra drag, wake disturbance and structural interaction due to the mounting frame was not considered. Selected steady operating points were also considered in the present simulation, without computing a fully coupled fluid-structure-electrical dynamic model.

Present Model does not contain Rectification, DC link control, Inverter control, Battery Storage, Protection Circuits, MPPT Control or Grid Synchronization. Hence, at this stage the output is not regarded as a full supply system to the household. The PMSM model is simplified as well. These were not fully included: detailed thermal effects, magnetic saturation, iron losses, mechanical losses, manufacturing constraints, long-term generator reliability. The electrical frequency is dependent on the speed of the rotor, and a power electronic conversion stage would be necessary in the future for regulated 50 Hz AC output for domestic use. Lastly, there is the assumed tide velocity profile and interpolation technique used in the energy yield estimation. It provides a good approximation of the amount of energy produced each day, month and year; however, long term measurements would have to be taken at the site to get a more realistic prediction for the real world.

## 8.3 Future Works

The torque, force and power results should be compared for different mesh densities, and a mesh independence study should be performed. The transient simulation should also be carried out to ensure that each case is simulated for not less than one full revolution of the rotor and the torque should be averaged over the steady part of the simulation. This would enhance confidence in the results of hydrodynamic performance. This should include the

practical support base which can be assessed for its contribution to drug, wake behavior and turbine performance.

The next big milestone is the development of physical prototypes. A scaled model should be built and tested in a water channel or towing tank. Comparisons should be made between experimental measurements of rotor speed, torque, voltage, current and load power. The results of the ANSYS and Simulink simulations are compared with. This would help to validate the simulation approach and to find the difference between the theoretical, numerical and experimental performance. Structural testing should also be conducted to assess blade strength, shaft loading, vibration, fatigue and long-term durability of repeated tidal loading. A rectifier, DC link capacitor, charge controller, battery storage system and inverter should be connected to the PMSM output. This would enable the output from the variable-frequency generator to be converted to regulated 50 Hz AC for household or community loads. Other control strategies such as the MPPT and load matching control should also be studied to achieve maximum power extraction from the different tides' velocities.

Additional research should also be conducted on the deployment of arrays. With an estimated energy output of 6.675 kWh per lunar tidal day and 2.354 MWh per year from one turbine, it was possible to install several turbines together to generate more energy for a rural coastal community. Future investigations should focus on the spacing of turbines, the wake interaction, array efficiency, anchoring method, maintenance access and environmental effects. The design should also be tested for corrosion, anti-biofouling, fish safety, sediment effects and storm/strong current survivability. Finally, a Techno-economic analysis should be conducted to estimate the manufacturing cost, installation cost, payback period and feasibility for coastal areas of Bangladesh.

# REFERENCES


[1] Dhaka Tribune, "Bangladesh ranks as fastest-growing economy in region," **Dhaka Tribune*,* 2023. Accessed: June 15, 2026 [Online]. Available:https://www.dhakatribune.com/business/economy/319804/bangladesh-ranks-as-fastest-growing-economy-in

[2] Energy IDEAS, "Energy transition indicators and pathways: Bangladesh 2024," **Energy IDEAS**, Accessed: May 2024 [Online]. Available: https://ideas.energy/bangladesh-2024. Accessed: May 2024.

[3] Centre for Policy Dialogue (CPD), "We have gas reserve for 10 years only—then what? Power and energy sector study," **CPD Power & Energy Policy Brief**, 2024. Accessed: April 18, 2025 [Online]. Available: https://cpd-power-energy-study.com/we-have-gas-reserve-for-10-years-only-then-what/. Accessed: Apr. 18, 2025.

[4] Moeve Global, "Tidal energy: What is it and how is it obtained?" **Moeve Global*,* 2023. Accessed: April 18, 2023 [Online]. Available: https://www.moeveglobal.com/en/planet-energy/green-energy/tidal-energy-what-is-how-is-it-obtained

[5] MIT Climate Portal, "Why don't we use tidal power more?" 2022. Accessed: February 2026 [Online]. Available: https://climate.mit.edu/ask-mit/why-dont-we-use-tidal-power-more

[6] Savree, "Tidal Stream Turbine," **Savree**, 2022. Accessed: February 2026 [Online]. Available: https://savree.com/en/encyclopedia/tidal-stream-turbine

[7] ScienceDirect Topics, "Tidal Stream Generator," **Elsevier Topics**. Accessed: December 2024 [Online]. Available: https://www.sciencedirect.com/topics/engineering/tidal-stream-generator

[8] S. P. Neill, K. A. Haas, J. Thiébot, and Z. Yang, "A review of tidal energy—Resource, feedbacks, and environmental interactions," **Journal of Renewable and Sustainable Energy**, vol. 13, no. 6, Art. no. 062702, 2021. doi: 10.1063/5.0069452.

[9] Global Bioenergy, "Advantages and Disadvantages of Tidal Power Generation," 2021. Accessed: July 2025 [Online]. Available: https://www.globalbioenergy.org/advantages-and-disadvantage-of-tidal-power/

[10] The Daily Star, "Tidal energy prospects along coastal belts," *The Daily Star*, July 12, 2010. Accessed: April 2024 [Online]. Available: https://www.thedailystar.net/news-detail-146470

[11] Consulate General of the People's Republic of Bangladesh, Sydney, "Bangladesh at a Glance." Accessed: February 2024 [Online]. Available: https://cgbdsydney.gov.bd/about-bangladesh/bangladesh-at-a-glance/

[12] World Population Review, "Bangladesh Location." Accessed: May 2024 [Online].Available:https://worldpopulationreview.com/countries/bangladesh/location

[13] Quader, "Country Report: Bangladesh," Asian Disaster Reduction Center (ADRC), 2020. Accessed: October 2025 [Online]. Available: https://www.adrc.asia/

[14] Power Development Board (BPDB), *Annual Report 2019–2020*, Ministry of Power, Energy and Mineral Resources, Government of the People's Republic of Bangladesh,2024. Accessed: December 2023 [Online]. Available:https://bpdb.gov.bd/pages/static-pages/6922dee6933eb65569e3c

[15] B. Imam, "Is Bangladesh Running Out of Gas Resources?," *The Daily Star*, May 20, 2021. Accessed: December 2023 [Online]. Available: https://www.thedailystar.net/opinion/news/bangladesh-running-out-gas-resources-2095805

[16] The Business Standard, "Dhaka's Air Quality World's Worst Today," Dec. 6, 2024. Accessed: January 2024 [Online]. Available: https://www.tbsnews.net/bangladesh/environment/dhakas-air-quality-worlds-worst-today-1011641

[17] Banglapedia, "Coastal Erosion," *Banglapedia: National Encyclopedia of Bangladesh*, 2021. Accessed: August 2024 [Online]. Available: https://en.banglapedia.org/index.php/Coastal_Erosion

[18] U. M. Misbah, M. J. Bin, Z. Huq, G. M. J. Hasan, and T. Rahman, "Two-Dimensional Hydrodynamic Modelling of Northern Bay of Bengal Coastal Waters," *Journal of Water Resource and Protection*, vol. 6, no. 14, pp. 1293–1305, 2014. doi: 10.4236/jwarp.2014.614119.

[19] M. A. Haque and M. S. Khatun, "Tidal Energy: Perspective of Bangladesh," *Journal of Bangladesh Academy of Sciences*, vol. 41, no. 2, pp. 201–215, 2017. doi: 10.3329/jbas.v41i2.35498.

[20] ScienceDirect Topics, "Tidal Stream Generator," *Elsevier Engineering Encyclopedia*. Accessed: February 2025 [Online]. Available: https://www.sciencedirect.com/topics/engineering/tidal-stream-generator

[21] European Marine Energy Centre (EMEC), "Tidal energy," *European Marine Energy Centre*, Accessed: July 2024 [Online]. Available: https://www.emec.org.uk/marine-energy/tidal-energy/

[22] ScienceDirect Topics, "Stream turbine," *Elsevier Topics*. Accessed: June 2024[Online].Available:https://www.sciencedirect.com/topics/engineering/stream-turbine

[23] A. K. Sikder, M. T. Rahman, M. Islam, N. A. Khan, and A. Hoque, "Possibility of a tidal power plant in Sandwip Island of Bangladesh," in *Proc. 3rd Int. Conf. Developments in Renewable Energy Technology (ICDRET)*, 2014. doi: 10.1109/ICDRET.2014.6861730.

[24] G. Lo Zupone, S. Barbarelli, C. Liu, J. Yan, and B. Liang, "Open center tidal turbine: How a new mooring system concept affects the performances," *International Journal of Energy Research*, vol. 45, no. 5, pp. 6727–6744, 2021. doi: 10.1002/er.6266.

[25] Encyclopaedia Britannica, "Bangladesh," *Encyclopaedia Britannica*. Accessed: January 2026 [Online]. Available: https://www.britannica.com/place/Bangladesh

[26] OPSIS, "Climate-resilient infrastructure in Bangladesh," *Oxford Policy Management*, Oct. 19, 2022. Accessed: March 2025 [Online]. Available: https://opsis.eci.ox.ac.uk/post/2022-10-19-climate-resilient-bangladesh/

[27] D. Adshead, A. Paszkowski, S. S. Gallet, *et al*., "Climate threats to coastal infrastructure and sustainable development outcomes," *Nature Climate Change*, vol. 14, pp. 45–56, 2024. doi: 10.1038/s41558-023-01887-6.

[28] Energy 4 Impact, "Sustainable cities and localized clean grids," *Mercy Corps Powering Development*. Accessed: March 2025 [Online]. Available: https://www.energy4impact.org/powering-development/sustainable-cities

[29] Capilano University, "Lights Out: An Analysis of the Daily Effects of Energy Inaccessibility in Bangladesh," *Capilano University Student Research Repository*, Feb. 11, 2024. Accessed: April 2024 [Online]. Available: https://capstone.capilanou.ca/2024/02/11/lights-out-an-analysis-of-the-daily-effects-of-energy-inaccessibility-in-bangladesh/

[30] Indian Ocean Rim Association (IORA), "Harnessing salinity gradient power for sustainable electricity generation in coastal Bangladesh," *IORA Blue Economy*

*Brief*, 2022. Accessed: June 2024 [Online]. Available: https://iora.int/harnessing-salinity-gradient-power-sustainable-electricity-generation-coastal-bangladesh

[31] M. Z. H. Majumder, M. T. A. Shampa, M. A. Islam, S. A. Deowan, and F. Hafiz, "Marine renewable energy harnessing for sustainable development in Bangladesh: A technological review," *Energy Reports*, vol. 11, pp. 1342–1362, 2024. doi: 10.1016/j.egyr.2024.01.001.

[32] T. Yoshida, et al., "Use of a model turbine to investigate the high striking risk of fish with tidal and oceanic current turbine blades under slow rotational speed," *Sustainable Energy Technologies and Assessments*, vol. 37, Art. no. 100586, 2020. doi: 10.1016/j.seta.2019.100586.

[33] Hakai Magazine, "Measuring the ecological risks of coastal tidal power deployments," Feb. 22, 2018. Accessed: October 2024 [Online]. Available: https://hakaimagazine.com/news/measuring-the-risks-of-tidal-power/

[34] DNV, *DNV-ST-0164: Tidal Turbines*, 2021. Accessed: September 2024 [Online]. Available: https://www.dnv.com/energy/standards-guidelines/dnv-st-0164-tidal-turbines/

[35] S. Momtaz, "Environmental impact assessment in Bangladesh: A critical review," *Environmental Impact Assessment Review*, vol. 22, no. 2, pp. 163–179, 2002. doi: 10.1016/S0195-9255(01)00106-8.

[36] Ember, "Bangladesh," *Ember*. Accessed: March 2026 [Online]. Available: https://ember-energy.org/countries-and-regions/bangladesh/

[37] T. Hooper, P. Cooper, A. Hunt, M. Austen, and N. Beaumont, "Tidal barrages in the UK: Ecological and social impacts, potential mitigation, and tools to support barrage planning," *Renewable and Sustainable Energy Reviews*, vol. 23, pp. 289–298, 2013. doi: 10.1016/j.rser.2013.02.016.

[38] S. Allsop, C. Peyrard, P. Bousseau, and P. Thies, "Adapting conventional tools to analyse ducted and open centre tidal stream turbines," *International Marine Energy Journal*, vol. 1, no. 2, pp. 91–99, 2018. doi: 10.36688/imej.1.91-99.

[39] G. Lo Zupone, M. Amelio, S. Barbarelli, G. Florio, and N. M. Scornaienchi, "Understanding the development and interaction of wake induced by an open centre turbine and its array design implications," *Applied Ocean Research*, vol. 128, Art. no. 103352, 2022. doi: 10.1016/j.apor.2022.103352.

[40] A. E. Copping and L. G. Hemery, Eds., *OES-Environmental 2020 State of the Science Report: Environmental Effects of Marine Renewable Energy*

*Development Around the World*, Ocean Energy Systems (OES), Tech. Rep., 2020. doi: 10.2172/1632878.

[41] J. Lossent, M. Lejart, T. Folegot, D. Clorennec, L. Di Iorio, and C. Gervaise, "Underwater operational noise level emitted by a tidal current turbine and its potential impact on marine fauna," *Marine Pollution Bulletin*, vol. 131, pp. 323–334, 2018. doi: 10.1016/j.marpolbul.2018.03.024.

[42] Pacific Northwest National Laboratory (PNNL), "Tidal Stream Energy Project: Collision Risk Data and Evidence Summary," *Tethys Knowledge Base*, 2023. Accessed: October 2024 [Online]. Available: https://tethys.pnnl.gov/publications/tidal-stream-energy-project-collision-risk-data-evidence-summary

[43] A. B. Gill and M. Bartlett, *Literature Review on the Potential Effects of Electromagnetic Fields and Subsea Noise from Marine Renewable Energy Developments on Atlantic Salmon, Sea Trout and European Eel*, Scottish Natural Heritage Commissioned Report No. 401, 2010. [Online]. Available: https://tethys.pnnl.gov/sites/default/files/publications/Gill_and_Bartlett_2010.pdf

[44] F. Zhu, L. Ding, B. Huang, M. Bao, and J. Liu, "Blade design and optimization of a horizontal axis tidal turbine," *Ocean Engineering*, vol. 195, Art. no. 106652, 2020. doi: 10.1016/j.oceaneng.2019.106652.

[45] T. Yoshida, et al., "Use of a model turbine to investigate the high striking risk of fish with tidal and oceanic current turbine blades under slow rotational speed," *Sustainable Energy Technologies and Assessments*, vol. 37, Art. no. 100586, 2020. doi: 10.1016/j.seta.2019.100586.

[46] S. Musabikha, I. K. A. P. Utama, and Mukhtasor, "State of the art in protection of erosion-corrosion on vertical axis tidal current turbine," in *IOP Conference Series: Materials Science and Engineering*, vol. 105, 2016.

[47] H. Rashid, M. Benbouzid, H. Titah-Benbouzid, Y. Amirat, and A. Mamoune, "Tidal stream turbine biofouling detection and estimation: A review-based roadmap," *Journal of Marine Science and Engineering*, vol. 11, no. 5, Art. no. 908, 2023. doi: 10.3390/jmse11050908.

[48] A. A. Nazeer, F. Al-Sagheer, and A. Bumajdad, "Marine corrosion protection using advanced nanomaterials: A review," *Frontiers in Chemistry*, vol. 8, Art. no. 391, 2020. doi: 10.3389/fchem.2020.00391.

[49] Massachusetts Institute of Technology (MIT) Climate Portal, "Why Don't We Use Tidal Power More?," 2022. Accessed: September 2025 [Online]. Available: https://climate.mit.edu/ask-mit/why-dont-we-use-tidal-power-more

[50] Pacific Northwest National Laboratory (PNNL), "SEASTAR: Enhancing Tidal Stream Environmental Monitoring and Sustainability," *Tethys Knowledge Base*, 2023. Accessed: October 2025 [Online]. Available: https://tethys.pnnl.gov/stories/seastar-enhancing-tidal-stream-environmental-monitoring-sustainability

[51] A. E. Copping and L. G. Hemery, Eds., *OES-Environmental 2024 State of the Science Report: Environmental Effects of Marine Renewable Energy Development Around the World*, Ocean Energy Systems (OES-Environmental), Tech. Rep., 2024. Accessed: December 2025 [Online]. Available: https://tethys.pnnl.gov/publications/oes-environmental-2024-state-science-report-environmental-effects-marine-renewable

[52] A. E. Copping, L. G. Hemery, H. Viehman, A. C. Seitz, G. J. Staines, and D. J. Hasselman, "Are fish in danger? A review of environmental effects of marine renewable energy on fishes," *Biological Conservation*, vol. 262, Art. no. 109297, 2021. doi: 10.1016/j.biocon.2021.109297.

[53] S. Ascher, I. M. Gray, and C. M. Collins, "Misplaced fears? What the evidence reveals of the ecological effects of tidal power generation," *Ecological Solutions and Evidence*, vol. 6, no. 1, p. e70124, 2025. doi: 10.1002/2688-8319.70124.

[54] International Association for Impact Assessment (IAIA), *Strategic Environmental Assessment Guidance—Chapter 10: Tidal Power*, IAIA Technical Training Manual, 2024. Accessed: March 2025 [Online]. Available: https://training.iaia.org/wp-content/uploads/2024/10/SEA-Guidance-CHAPTER-10.pdf

[55] M. Nachtane, M. Tarfaoui, M. Ait Mohammed, D. Saifaoui, and A. El Moumen, "Effects of environmental exposure on the mechanical properties of composite tidal current turbines," *Renewable Energy*, vol. 156, pp. 1132–1145, 2020. doi: 10.1016/j.renene.2020.05.020.

[56] P. Habibi, F. Abad, S. Dai, A. Mehmanparast, and S. Lotfian, "Failure analysis of tidal turbine blades: Understanding erosion mechanisms and their impact on structural integrity," *Engineering Failure Analysis*, vol. 168, Art. no. 109658, 2025. doi: 10.1016/j.engfailanal.2025.109658.

[57] D. Sarode, U. Saharkar, H. H. Ahire, M. M. Darade, S. M. Chougule, S. A. Dalvi, and A. S. Kurhade, "Corrosion-Resistant Materials for Ocean Structures:

Innovations, Mechanisms, and Applications," *Sustainable Marine Structures*, vol. 7, no. 3, pp. 63–87, 2025. doi: 10.36956/sms.v7i3.2335.

[58] F. Du, R. Mo, Z. Guo, S. Zhang, Y. Yang, and J. Wang, "Overview of wear-resistant coatings in marine environments: Structural review," *Journal of Marine Science and Engineering*, vol. 13, no. 11, Art. no. 2121, 2025. doi: 10.3390/jmse13112121.

[59] S. P. Neill, K. A. Haas, J. Thiébot, and Z. Yang, "A review of tidal energy—Resource, feedbacks, and environmental interactions," *Journal of Renewable and Sustainable Energy*, vol. 13, no. 6, Art. no. 062702, 2021. doi: 10.1063/5.0069452.